BIND

JET PROPULSION

A publication of the

AMERICAN ROCKET SOCIETY

Research and Development

VOLUME 28 MAY 1958 SCIENCE & TECHNOLOGY NUMBER 5

SURVEY ARTICLE

Artificial Satellites—A Bibliography of Recent Literature. Part One—1956 . . . . . *Mildred Benton* 301

CONTRIBUTED ARTICLES

Testing Air-Breathing Supersonic Powerplants . . *G. A. Sears and J. J. Bajek* 303
Techniques of Flight Simulation for Ramjet Engines . . . *Raymond Greenberg* 308
Ramjet Test Facility Planning . . *Robert O. Dietz Jr. and Arthur H. Hinners Jr.* 315
Spreading of Supersonic Jets From Axially Symmetric Nozzles . . . . . *C. J. Wang and J. B. Peterson* 321

TECHNICAL NOTES

Vertical Re-entry into the Earth's Atmosphere for Both Light and Heavy Bodies . . *R. D. Linnell* 329
Air Density Determination by Observation of a Satellite . . . . . *Robert E. Roberson* 330
Lifetimes of Artificial Satellites . . . . . *Robert R. Newton* 331
Vertical Ballistic Trajectories Over an Oblate Earth . . . . . *Robert E. Roberson* 333
Evaluation of Flame Stability at High Reynolds Numbers . . . . . *Loren E. Bollinger* 334
Effect of High Altitude Conditions on Atomization Phenomena . . . . . *C. C. Miesse* 335
Celestial Ionospherics, the Ultimate Astronomy . . . . . *William J. Berger* 337
Computation of Rocket Step Weights to Minimize Initial Gross Weight . . *Richard P. Ten Dyke* 338
Surface Combustion in Dissociated Air . . . . . *Sinclaire M. Scala* 340

TECHNICAL COMMENTS

Comment on 'Stresses in Rocket Grains' . . . . . *W. T. Cox* 342
Corrections to 'Comments on the Powered Flight Trajectory of a Satellite' . . . *B. D. Fried* 342

DEPARTMENTS

New Patents 344 Technical Literature Digest 348

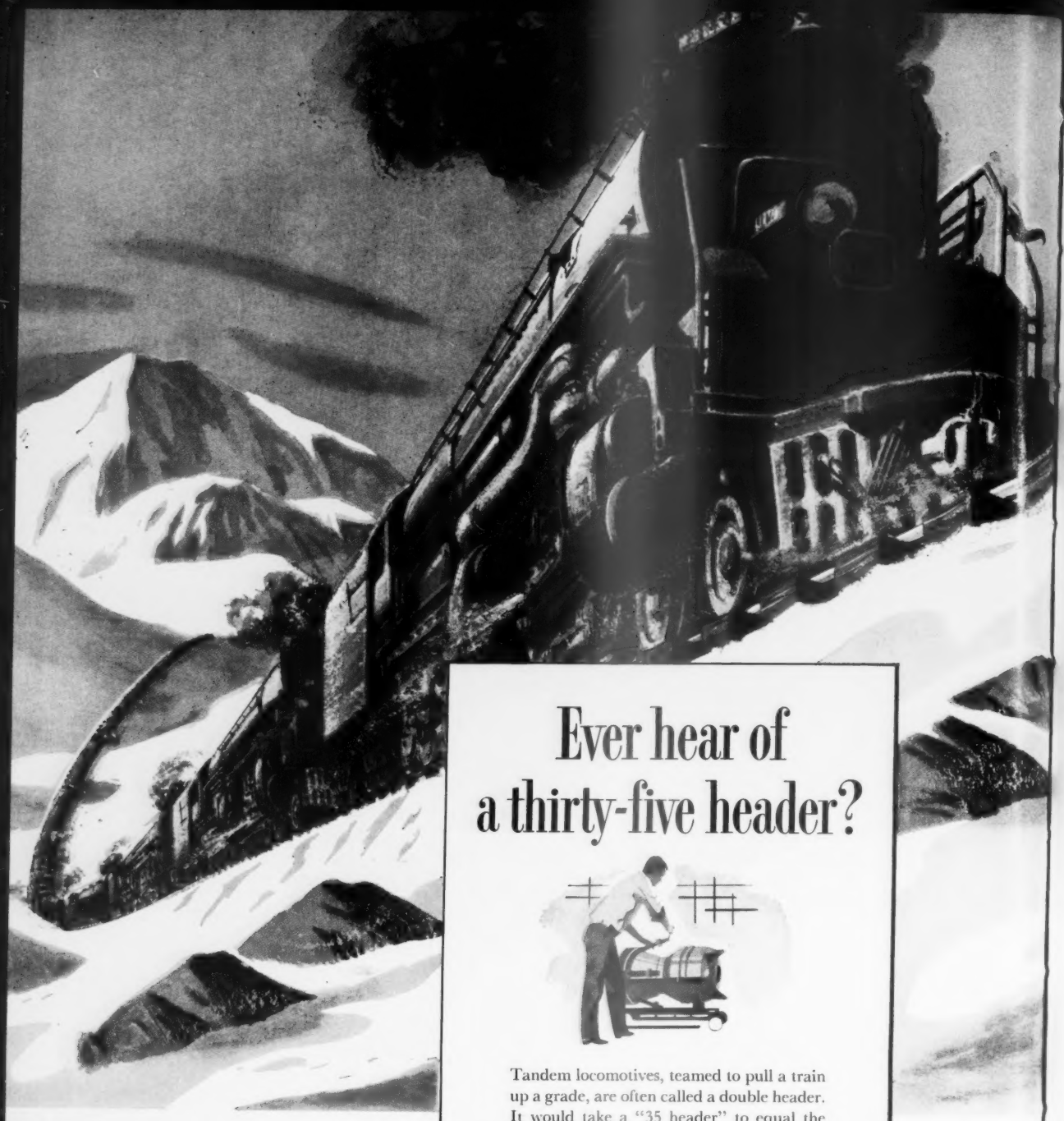

Ever hear of a thirty-five header?

Tandem locomotives, teamed to pull a train up a grade, are often called a double header. It would take a "35 header" to equal the power of the RMI rocket engine shown here.

RMI propulsion systems are now being perfected for use in ballistic and guided missiles as well as in the manned aircraft of the future. These advanced propulsion systems incorporate the principle which has guided RMI since 1941 . . . *reliability in application.*

Another reason why RMI's program of advanced research and engineering continues to be a good investment for taxpayers, government and industry!

RMI **REACTION MOTORS, INC.**

DENVILLE, NEW JERSEY

Now combined for the first time...

HYDROSPINNING AND CONTOUR FINISH MACHINING

As the technology of missile machining progressed missilemen looked forward to the many advantages of combining hydrospinning and contour finish machining. But the technical obstacles were great and no one dared the expensive risk of this research.

Diversey tackled this technical research and now after many months of experimentation Diversey has solved this problem. Above you see the successful production line results. You are looking at a Diversey hydrospun nose section for an IRBM being contour finish machined to extremely close tolerances.

This advance of Diversey is important to the missile industry because of its flexibility, because it saves valuable metal, and because it sharply reduces cost.

At Diversey you have the LARGEST FACILITIES for your missile metal machining and hydrospinning problems. You have a team of alert, experienced, and progressive technical people. Bring your tough jobs to Diversey.

SEND FOR FREE BOOKLET

LEADERS IN CONTOUR MACHINING

Diversey ENGINEERING COMPANY

10550 WEST ANDERSON PLACE
FRANKLIN PARK, ILLINOIS • *A Suburb of Chicago*

FROM NOSE TO NOZZLE, FROM FIN TO FIN, CONTOUR TURNED PARTS—WITH PRECISION BUILT IN

JET PROPULSION

A publication of the

AMERICAN ROCKET SOCIETY

Research and Development

IRWIN HERSEY—DIRECTOR OF PUBLICATIONS

EDITOR MARTIN SUMMERFIELD

ASSISTANT EDITOR LARKIN JOYNER

ART EDITOR JOHN CULIN

ASSOCIATE EDITORS

ALI BULENT CAMBEL, *Northwestern University*
IRVIN GLASSMAN, *Princeton University*
M. H. SMITH, *Princeton University*

CONTRIBUTORS

MARSHAL FISHER, *Princeton University*
GEORGE F. McLAUGHLIN

ADVERTISING PRODUCTION MANAGER

WALTER BRUNKE

ADVERTISING & PROMOTION MANAGER

WILLIAM CHENOWETH

ADVERTISING REPRESENTATIVES

D. C. Emery & Associates
155 East 42 St., New York, N. Y.
Telephone: Yukon 6-6855

James C. Galloway & Co.
6535 Wilshire Blvd., Los Angeles, Calif.
Telephone: Olive 3-3223

Jim Summers & Associates
35 E. Wacker Dr., Chicago, Ill.
Telephone: Andover 3-1154

R. F. and Larry Pickrell
318 Stephenson Bldg., Detroit, Mich.
Telephone: Trinity 1-0790

Louis J. Bresnick
304 Washington Ave., Chelsea 50, Mass.
Telephone: Chelsea 3-3335

John W. Foster
239 4th Ave., Pittsburgh, Pa.
Telephone: Atlantic 1-2977

AMERICAN ROCKET SOCIETY

Founded 1930

OFFICERS

President	George P. Sutton
Vice-President	John P. Stapp
Executive Secretary	James J. Harford
Secretary	A. C. Slade
Treasurer	Robert M. Lawrence
General Counsel	Andrew G. Haley

BOARD OF DIRECTORS

Terms expiring on dates indicated

Krafft Ehricke, 1959	H. S. Seifert, 1958
S. K. Hoffman, 1958	K. R. Stehling, 1958
Simon Ramo, 1960	Martin Summerfield, 1959
H. W. Ritchey, 1959	Wernher von Braun, 1960

Maurice J. Zucrow, 1960

TECHNICAL DIVISION CHAIRMEN

David G. Simons, Human Factors	John F. Tormey, Propellants and Combustion
Lawrence S. Brown, Instrumentation and Guidance	Brooks T. Morris, Ramjet
Edward N. Hall, Liquid Rocket	William L. Rogers, Solid Rocket

Krafft A. Ehricke, Space Flight

Scope of JET PROPULSION

This Journal is a publication of the American Rocket Society devoted to the advancement of the field of jet propulsion through the dissemination of original papers disclosing new knowledge or new developments. As used herein, the term "jet propulsion" embraces all engines that develop thrust by rearward discharge of a jet through a nozzle or duct; and thus it includes air-consuming engines and underwater systems as well as rockets. JET PROPULSION is open to contributions dealing not only with propulsion but with other aspects of jet-propelled flight, such as flight mechanics, guidance, telemetering, and research instrumentation. Increasing emphasis will be given to the scientific problems of extraterrestrial flight.

Information for Authors

Manuscripts must be as brief as the proper presentation of the ideas will allow. Exclusion of dispensable material and conciseness of expression will influence the Editors' acceptance of a manuscript. In terms of standard-size double-spaced typed pages, a typical maximum length is 22 pages of text (including equations), 1 page of references, 1 page of abstract, and 12 illustrations. Fewer illustrations permit more text, and vice versa. Greater length will be acceptable only in exceptional cases.

Short manuscripts, not more than one quarter of the maximum length stated for full articles, may qualify for publication as Technical Notes or Technical Comments. They may be devoted to new developments requiring prompt disclosure or to comments on previously published papers. Such manuscripts are usually published within two months of the date of receipt.

Sponsored manuscripts are published occasionally as an ARS service to the industry. A manuscript that does not qualify for publication according to the above-stated requirements as to subject scope or length, but which nevertheless deserves widespread distribution among jet propulsion engineers, may be printed as an extra part of the Journal or as a special supplement, if the author or his sponsor will reimburse the Society for actual publication costs. Estimates are available on request. Acknowledgment of such financial sponsorship appears as a footnote on the first page of the article. Publication is prompt since such papers are not in the ordinary backlog.

Manuscripts must be double spaced on one side of paper only with wide margins to allow for instructions to printer. Include a 100 to 200 word abstract. State the authors' positions and affiliations in a footnote on the first page. Equations should be typewritten. Identify *all handwritten* symbols and Greek letters for the printer. References are to be grouped at the end of the manuscript and are to be given as follows: for journal articles: authors first, then title, journal, volume, year, page numbers; for books: authors first, then title, publisher, city, edition, and page or chapter numbers. Line drawings must be clear and sharp to make clear engravings. Use black ink on white paper or tracing cloth. Lettering should be large enough to be legible after reduction. Photographs should be glossy prints, not matte or semi-matte. Each illustration must have a legend; legends should be listed in order on a separate sheet.

Manuscripts must be accomplished by written assurance as to security clearance in the event the subject matter lies in a classified area or if the paper originates under government sponsorship. Full responsibility rests with the author.

Submit manuscripts in duplicate (original plus first carbon, with two sets of illustrations) to the Editor, Martin Summerfield, Professor of Aeronautical Engineering, Princeton University, Princeton, N. J. Preprints of papers presented at ARS national meetings are automatically considered for publication.

JET PROPULSION is published monthly by the American Rocket Society, Inc., and the American Interplanetary Society at 20th & Northampton Sts., Easton, Pa., U. S. A. Editorial offices: 500 Fifth Ave., New York 36, N. Y. Price: $12.50 per year, $2.00 per single copy. Second-class mail privileges authorized at Easton, Pa. Notice of change of address should be sent to the Secretary, ARS, at least 30 days prior to publication. Opinions expressed herein are the authors' and do not necessarily reflect the views of the Editors or of the Society.

© Copyright 1958 by the American Rocket Society, Inc.

Artificial Satellites—A Bibliography of Recent Literature Part One—1956[1]

MILDRED BENTON[2]

U. S. Naval Research Laboratory, Washington, D. C.

THIS annotated listing of about 340 references,[1] alphabetical by author, brings up to date the bibliography on "A History of the Artificial Satellite" by Alan R. Krull, published in JET PROPULSION, May 1956, pages 369–383.

Since, with the exception of one or two 1956 entries, the Krull bibliography covered the literature through 1955, this listing purposely includes references selected from books, unclassified research reports and technical periodical articles published during 1956, 1957 and January-February 1958.

Much has been written since 1955, for much has transpired to make the artificial satellite one of the chief topics of the times. Instead of theorizing, man has actually launched artifical satellites, so this bibliography is really a recorded reference story of Vanguard, Sputnik and Explorer, their progress, development and scientific uses.

The same guide lines mentioned by Mr. Krull in his earlier bibliography have been followed in this one; that is, fiction, juvenile literature and news items are omitted. There are a few entries connected with space law, but no attempt has been made to include everything; also, there is nothing on space medicine, manned flight, interplanetary flight, trips to the moon or to Mars or space stations. The following bibliographies are suggested for further information on these phases:

Benton, Mildred. "Earth Satellites, Guided Missiles, Rockets and Space Flight," Wilson Lib. Bull. 32: 412–419, Feb. 1958.

Department of the Army Library. "Guided Missiles, Rockets and Artificial Satellites (Including Project Vanguard)," 153 pp., Jan. 1957 (Spec. Bib. 11).

Hogan, J. C. "Space Law Bibliography," J. Air Law & Commerce 23: 317–325, Summer 1956.

Krzywoblocki, M. Z. "The Forces Acting on an Air Vehicle. A Review of the Literature," 112 pp., Chicago University, June 1955 (Aerodynamic Studies, Suppl. 10).

Ley, Willy. "Rockets, Missiles and Space Travel," 528 pp., New York, Viking, 1957 (Bibliography, pp. 489–520).

"Missiles and Myths," Missiles and Rockets 2: 74, Aug. 1957.

National Science Foundation. "A Bibliography for the International Geophysical Year," 51 pp., Washington, D. C., July 1, 1957 (NSF-57-25).

Rosen, M. W. "Twenty-Five Years of Progress Toward Space Flight" (includes literature review). JET PROPULSION 25: 623–626, Nov. 1955.

Anderton, D. A.

Gas Dynamics, Part I—Key Tool for ICBM, Satellite Studies. Part II—Hypersonic Quest Yields New Techniques. Missile Eng. 1: 4–11, illus., Sept. 1956. A discussion of the two extremes of aerodynamic flow problems—hypersonics (ICBM) and superaerodynamics (IGY satellite).

Vanguard Depends on Tools and Gages. Aviat. Wk. 65: 50–52, Nov. 5, 1956. Tools and gages will determine whether the Vanguard will be a satellite or a meteor.

Army Signal Corps Engineering Laboratories, Fort Monmouth, N. J.

The Environment of an Earth Satellite, by R. Griffith, W. Norberg and W. G. Stroud. 41 pp., diags., 1956. (Tech. Memo. 1747). Graphs, tables and other data summarizing what is known of the composition and properties of the upper atmosphere and the presence of radiation, gravity, geomagnetism and meteorities at high altitudes.

Baum, W. A.

A Fundamental Cosmological Experiment for the Artificial Satellite. Astron. Soc. Pac. Publ. 68: 118–120, Apr. 1956. Information to be sought by means of instruments is brightness and color of the extragalactic sky.

Bennett, W. H.

Proposed Measurement of Solar Stream Protons. In Van Allen, J. A., ed., *Scientific Uses of Earth Satellites,* pp. 194–197, Ann Arbor, University of Michigan Press, 1956. The solar protons in their initial approach in free orbits and any protons traveling later in captive orbits can be detected and measured only in the vicinity of the auroral zones of magnetic latitude, and an artificial satellite which passes approximately over the two poles of the earth will be needed for this purpose.

Bergaust, Erik

Satellite Science Not So Simple. U. S. Satellite Designs Copied? Missiles and Rockets 1: 18–19, Nov. 1956. Includes illustration from a Russian magazine which indicates what the Russian public think their IGY satellite will look like. It is an exact copy of S. F. Singer's early MOUSE (1954).

Bergaust, Erik, and Beller, William

Satellite. 287 pp., illus., New York, Hanover House, 1956. A general nontechnical discussion of the projected program for the launching of earth satellites—their operation, their possible uses and their likely effects on earth.

Berning, W. W.

Ionospheric Structure as Determined by a Minimal Artificial Satellite. In Van Allen, J. A., ed. *Scientific Uses of Earth Satellites,* pp. 253–262, Ann Arbor, University of Michigan Press, 1956. Discusses the problems and develops the analytical methods necessary for determining ionospheric electron densities from trajectory measurements.

Blitzer, Leon, Weisfeld, M., and Wheelon, A. D.

Perturbations of a Satellite's Orbit Due to Earth's Oblateness. J. Appl. Phys. 27: 1141–1149, Oct. 1956. Points up possible use of the US-IGY satellites for determining the earth's oblateness to a new precision. (For extension of this paper, see Blitzer entry in Part Two, 1957.[1])

Chubb, T. A., Friedman, H., and Kupperian, J.

A Lyman Alpha Experiment for the Vanguard Satellite. In Van Allen, J. A., ed. *Scientific Uses of Earth Satellites,* pp. 147–151, Ann Arbor, University of Michigan Press, 1956. A satellite experiment offers the possibility of monitoring the sun in Lyman alpha almost continuously for many days, and would be worth hundreds of individual rockets for the same purpose.

A Satellite Experiment to Determine the Distribution of Hydrogen in Space. In Van Allen, J. A., ed. *Scientific Uses of Earth Satellites,* pp. 152–156, Ann Arbor, University of Michigan Press, 1956. Proposed use of a photon counter to measure simultaneously the intensity of hydrogen Lyman alpha radiation (1215.7 A) received directly from the sun and the resonance radiation of the same wave length produced by sunlit hydrogen atoms in space.

Cornig, R.

Economics of Rocket Propelled Aeroplanes. II. Aero. Eng. Rev. 15: 49–58, Oct. 1956. An appendix is included which indicates costs for placing material in a satellite orbit.

Cushman, Robert

Next Satellite Problem: Data Descent. Aviat. Wk. 64: 53, 56–57, May 14, 1956. Discusses satellite data recovery and mentions proposal by R. W. Porter to recover data from a future earth satellite by a stainless steel balloon. Article with same title appears in Missile Eng. 1: 48–49, illus., Sept. 1956.

Daniels, F. B.

Electromagnetic Propagation Studies with a Satellite Vehicle. In Van Allen, J. A., ed. *Scientific Uses of Earth Satellites,* pp. 276–282, Ann Arbor, University of Michigan Press, 1956. The proposed experiment is a determination of the integrated value of the ionization from the earth's surface to the satellite, by measuring the rotation of the plane of polarization of a radio wave transmitted from the satellite.

Davis, R. J., Whipple, F. L., and Zirker, J. B.

The Orbit of a Small Earth Satellite. In Van Allen, J. A., ed. *Scientific Uses of Earth Satellites,* pp. 1–22, Ann Arbor, University of Michigan Press, 1956. Considers motion of a satellite launched into an inclined, moderately eccentric orbit from a point approximately 500 km above sea level. Discusses effects on desired initial orbit produced by

Received March 11, 1958.

[1] Part Two of this Bibliography covering the period from January 1957 through February 1958 will appear in a subsequent issue of JET PROPULSION.

[2] Consultant in Research Information.

deviations from desired launching conditions and atmospheric drag. Additional perturbations are discussed, such as action of the sun and moon, and variations of the density of the upper atmosphere with time and latitude, Bernoulli forces acting on a spinning object, and effect of upper-atmospheric winds.

Davis, R. J.

Ultraviolet Stellar Magnitudes. In Van Allen, J. A., ed. *Scientific Uses of Earth Satellites*, pp. 157–165, Ann Arbor, University of Michigan Press, 1956. Computations are performed from which it is possible to construct a tentative map of the sky at 1249 A. Results of this survey should prove valuable in the selection of the most interesting regions for study when extraterrestrial photometry of high resolution from artificial satellites becomes possible.

deBey, L. G.

Systems Design Considerations for Satellite Instrumentation. In Van Allen, J. A., ed. *Scientific Uses of Earth Satellites*, pp. 49–54, Ann Arbor, University of Michigan Press, 1956. Discusses some of the factors which must be considered in establishing sound objectives and adequate observing methods.

de Nike, John

The Effect of the Earth's Oblateness and Atmosphere on a Satellite Orbit. In Franklin Institute. *Earth Satellites as Research Vehicles.* Proceedings of a Symposium, Philadelphia, Franklin Institute, April 18, 1956, pp. 79–86, Lancaster, Pa., Journal of the Franklin Institute, June 1956. (Monograph 2.) A member of The Martin Company, designers and builders of the rocket vehicle for the Vanguard satellite, relates some of the problems.

Summary of article with same title, Brit. Interplan. Soc. J. 16: 29–30, Jan.-Mar. 1957.

Dubin, Maurice

Meteoric Bombardment. In Van Allen, J. A., ed. *Scientific Uses of Earth Satellites*, pp. 292–300, Ann Arbor, University of Michigan Press, 1956. An experiment for the detection of meteoric particles entering the earth's atmosphere is proposed for an earth satellite.

Easton, R. L.

Radio Tracking of the Earth Satellite. An Opportunity for Amateur Collaboration. QST 40: 38–41, 134, illus., July 1956. Describes simplified tracking system for amateur use.

Ehricke, K. A.

Aero-Thermodynamics of Descending Orbital Vehicles. Astronautica Acta 2: 1–19, 1956. The theory of laminar and turbulent friction and heat transfer in the compressible boundary layer with and without dissociation is discussed with respect to the descent of orbital vehicles through the atmosphere.

Ascent of Orbital Vehicles. Astronautica Acta 2: 175–190, 1956. Ascent into a satellite orbit along a minimum energy ellipse (elliptic ascent) is compared with ascent along an arc of an elliptic trajectory (ballistic ascent) where the satellite stage is transferred into the oribit at or near the summit. Discussed are basic energy requirements (other than losses during powered ascent), thrust program, effect on the size of stages, visibility during ascent, and flight time.

Astronautical and Space-Medical Research with Automatic Satellites. In Franklin Institute. *Earth Satellites as Research Vehicles.* Proceedings of a Symposium, Philadelphia, Franklin Institute, April 18, 1956, pp. 25–62, Lancaster, Pa., Journal of the Franklin Institute, June 1956. (Monograph 2.) Technical and scientific research aspects in conjunction with technological satellites are outlined and their correlation with various phases of manned astronautics is shown. The survey of the space-medical research by means of bio-satellites also considers the relevant technical and scientific aspects.

Instrumental Satellites and Instrumental Comets. Interavia 11: 960–962, Dec. 1956. Discussion of future developments in satellites and their scientific applications concerns flight performance and accuracy, tracking and data transmission.

Solar Power for Space Craft. Missiles and Rockets 1: 44–46, illus., Nov. 1956. Hydrogen-manufacturing satellites could rely on concentration of solar power in power collectors. The manufacturing process could be completely automatic, requiring only occasional human supervision and maintenance.

Findlay, D. A.

Electronics in the IGY Program. Electron. 29: 138–142, Dec. 1956. Projects planned for the IGY will use electronic instrumentation to sense, record and telemeter data. Earth satellite program will use transistorized oscillators for tracking and telemetering of data to ground from subminiature measuring equipment.

Franklin Institute

Earth Satellites as Research Vehicles. Proceedings of a Symposium held April 18, 1956. 115 pp., illus., The Institute, June 1956. (Monograph 2.) In a conference on rockets for peace, the discussion was devoted to different kinds of research that we may hope to accomplish with transistors and rocketry. See also entries under de Nike, Ehricke, Lawrence, Newell, Porter, Spitzer.

Furth, F. R.

Project Vanguard—The International Geophysical Year Earth Satellite. Aero. Eng. Rev. 15: 55–59, Mar. 1956. Survey of problems, trends and practical progress in techniques of very-high-altitude research under the USAF-Army-Navy sponsorship in terms of the design and construction requirements of the launching rocket and the satellite, selection of the launching site and tracking stations, and the determination of the satellite orbit.

Also in Eng. J. (Canada) 39: 1531–1536, Nov. 1956, and Shell Aviation News 215: 6–9, May 1956.

Gast, P. R.

Insolation of the Upper Atmosphere and of a Satellite. In Van Allen, J. A., ed. *Scientific Uses of Earth Satellites*, pp. 73–84, Ann Arbor, University of Michigan Press, 1956. A consideration of temperatures.

Gatland, K. W.

The Vanguard Project. Spaceflight 1: 15–28, Oct. 1956. Vehicle design, launching and tracking problems, with a review of rocket development.

Ginzburg, V. L.

Eksperimental' Naya Proverka Obshchei Teorii Otnositel'nosti i Iskusstvennye Sputniki Zemli (Experimental Verification of the General Theory of Relativity and Artificial Earth Satellites). Priroda 45: 30–39, Sept. 1956. In Russian. In a suggestion for measuring the gravitational displacement of frequency it is proposed that one measures not the frequency but the difference between the readings on clocks on earth and the readings on clocks on the satellite. Also in Usp. Fiz. Nauk 63: 119–122, Sept. 1957.

Possibility of Using Artificial Earth Satellites for the Experimental Verification of the Theory of General Relativity. Soviet Phys. JETP 3: 136–138, Aug. 1956. The reception of the radio signals on earth from the satellite can be used to determine the gravitational shift of frequency in the earth's field. The second effect that may be verified with the help of the satellite is the precession of the perihelion of the orbit. Translation of article appearing in Zh. Eksper. Teor. Fiz. 30: 213–214, 1956.

Great Britain, Royal Aircraft Establishment, Farnborough

The Descent of an Earth-Satellite Through the Upper Atmosphere, by D. G. King-Hele. 9 pp., figs., Aug. 1956. (Tech. Memo GW-277) A theoretical study is made of the flight path of an uncontrolled but aerodynamically stable satellite as it spirals down through the earth's atmosphere from an initially circular orbit under the action of air drag. The earth and its atmosphere are taken as spherically symmetrical. For altitudes above about 125 n. miles a simple solution is found; the velocity of the satellite is independent of its size, shape, weight and initial altitude and equal to the oribital velocity appropriate to its current altitude; while its angle of descent, in radians, is twice its drag/weight ratio. Estimates of lifetime are also made.

Haber, Heinz

Space Satellites, Tools of Earth Research. Natl. Geog. Mag. 109: 487–509, illus., Apr., 1956. A general and lucid explanation of plans for a true space vehicle.

Hagen, J. P.

The Exploration of Outer Space with an Earth Satellite. Inst. Radio Engrs. Proc. 44: 744–747, June 1956. A brief account of the beginnings of Project Vanguard: Why it is important to launch an earth satellite, some of the problems involved, and what is to be gained, research-wise.

Haley, A. G.

Basic Concepts of Space Law. JET PROPULSION 26: 951–957, 968, Nov. 1956. The unmanned earth satellite, pp. 955–957.

Happner, J. P.

Satellite Geomagnetic Measurements. In Van Allen, J. A., ed. *Scientific Uses of Earth Satellites.*, pp. 234–246, Ann Arbor University of Michigan Press, 1956. Practical requirements and techniques for obtaining useful data concerning magnetic storms and other disturbances.

Hartman, L. M., and Haviland, R. P.

A Satellite Propagation Experiment. In Van Allen, J. A., ed. *Scientific Uses of Earth Satellites*, pp. 268–275, Ann Arbor, University of Michigan Press, 1956. A satellite ionosphere and propagation experiment is proposed which will enlist the aid of operators in the Radio Amateur Service. Particular measurements to be made at specially equipped stations are reviewed.

Haviland, R. P.

On Applications of the Satellite Vehicle. JET PROPULSION 26: 360–363, illus., May 1956. An introduction to the possibilities and problems of the inward-looking fields of mapping and cartography, communications, and weather charting and forecasting.

Hinteregger, H. E.

Quantitative Intensity Measurements in the Extreme Ultraviolet. In Van Allen, J. A., ed. *Scientific Uses of Earth Satellites*, pp. 166–170, Ann Arbor, University of Michigan Press, 1956. Calls attention to the weak position of E. U. V. (extreme ultraviolet) as to its scientific exploration, and points out possible experiments which would indicate its interactions with matter.

Hok, Gunnar, Sicinski, H. S., and Spencer, N. W.

Temperature and Electron-Density Measurements in the Ionosphere by a Langmuir Probe. In Van Allen, J. A., ed. *Scientific Uses of Earth Satellites*, pp. 263–267, Ann Arbor, University of Michigan Press, 1956. Directs attention to the Langmuir probe technique as a means for collecting important data from a satellite in the ionosphere.

Hudson, D. E.

Possibility of Visual Tracking of a Satellite. In Van Allen, J. A., ed. *Scientific Uses of Earth Satellites*, pp. 39–43, Ann Arbor, University of Michigan Press, 1956. It is suggested that visual tracking may be feasible by means of short flashes of light.

Jensen, Jorgen

Satellite Ascent Guidance Requirements. J.

(*Continued on page 352*)

Testing Air-Breathing Supersonic Powerplants

G. A. SEARS[1] and J. J. BAJEK[2]

Marquardt Aircraft Co., Van Nuys, Calif.

Basic information concerning the free jet method of supersonic development testing is presented. Parameters necessary to specify test hardware, define test facility capabilities, and optimize facilities for this type of testing are discussed. The substantial gains obtainable in a facility's testable range by separately exhausting engine gas flow and free jet air spilled around the engine are defined, as are performance levels of various free jet diffuser types. A nomograph is included which permits rapid estimation of facility requirements and/or capabilities.

Introduction

THE development of supersonic powerplants of ever-increasing power to higher operating speeds has created demand for more powerful ground test facilities. The expense of such facilities makes necessary the optimization of the various components which indirectly or directly affect the power requirements.

Three principal methods of engine development currently in use are wind tunnel, free jet and connected pipe (or bell mouth) inlet testing. The free jet method of engine development testing is discussed herein. Performance levels obtainable with the components which comprise a free jet test arrangement are presented and parameters necessary to define test hardware, testability of an engine in a facility and optimization of a facility for this type of test are discussed.

General Considerations

It is considered essential in the development testing of air-breathing powerplants to simulate as closely as possible those conditions which would exist in flight. Full-scale development of a complete engine is desirable, if not imperative, because of inadequate scaling criteria for the combustion processes, structural components and possible coupling effects between diffuser and compressor or diffuser and combustor.

It is desirable, of course, to provide exact flight simulation of all internal and external flow conditions. However, this can be accomplished only by flight testing or by use of a wind tunnel. Development by flight testing can be dangerous as well as expensive. Although wind tunnel testing probably costs less than flight testing, it is still prohibitively expensive for testing all but small powerplants. This can be attributed to the large tunnel size and power requirements to provide complete flight simulation. Generally, a nonreturn type wind tunnel is necessary because the engine exhaust products contaminate the tunnel air, thereby necessitating large-capacity driers and heaters for the continual inflow of atmospheric air, or an elaborate scavenging system.

To date, the simplest and most economical engine development testing method available is considered to be the direct-connect or bell mouth inlet system. This system requires the least facility power because only that air flow required by the engine in flight must be supplied; however, no external simulation is provided and internal simulation is limited. Such factors as boundary layer shock wave interactions and their resultant effects upon diffuser velocity profiles, angle-of-attack effects on diffuser performance and diffuser-combustor (or diffuser-compressor) coupling effects cannot be evaluated.

A suitable compromise between the aforementioned methods can be obtained by use of the free jet test arrangement where exact flight conditions of Mach number, pressure, temperature and angle-of-attack are simulated at the diffuser inlet. This provides flight simulation of all flow parameters inside the engine, provided the engine exit flow is sonic. Consequently, all internal components and the aerothermodynamic system can be evaluated with much less power than a closed test section wind tunnel and a much larger degree of flight simulation than that offered by the direct-connect type test.

The expression "free jet" as used in this article refers to a nozzle with no constant area test section downstream as compared to a wind tunnel.

Flight Simulation Requirements

Inlet Flow Field

Free jet nozzle configurations which have either rectangular or circular exit cross sections are most common. Generally, the rectangular end section is used when optical instrumentation is desired since it is readily adaptable for such a purpose. In addition, variable Mach number free jets are more easily developed in rectangular dimensions. However, nacelle type engines are usually circular and, for a given inlet diameter, a circular free jet of smaller size than a square one can be used, thus reducing facility air flow requirements. Also, as noted in (1),[3] better free jet diffuser performance is obtained if the diffusing passage is geometrically similar to the entering air flow. Generally, the free jet and diffuser parameters discussed herein are for the circular type, although the same general considerations prevail regardless of shape.

Minimum free jet sizes are desirable in order to minimize facility air supply power requirements or, conversely, to permit tests of larger engines in a particular facility. The

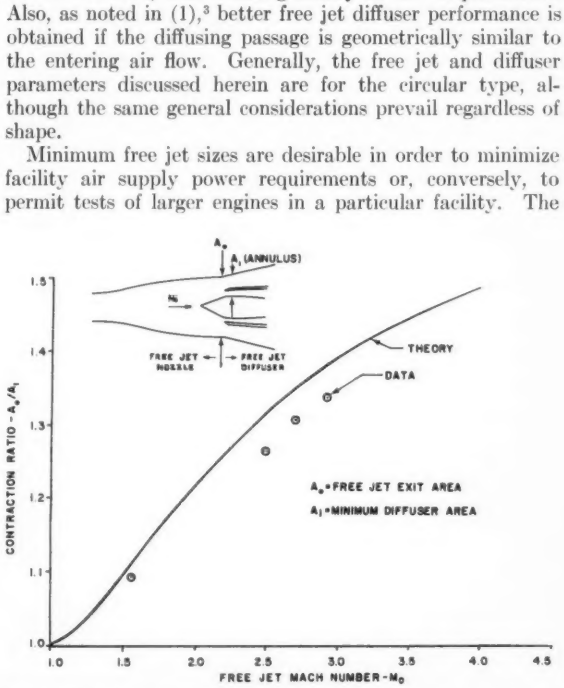

Fig. 1 Maximum contraction ratio that permits starting of supersonic flow in a diffuser

Presented at the ARS Semi-Annual Meeting, San Francisco, Calif., June 10–13, 1957.

[1] Project Engineer.

[2] Group Engineer.

[3] Numbers in parentheses indicate References at end of paper.

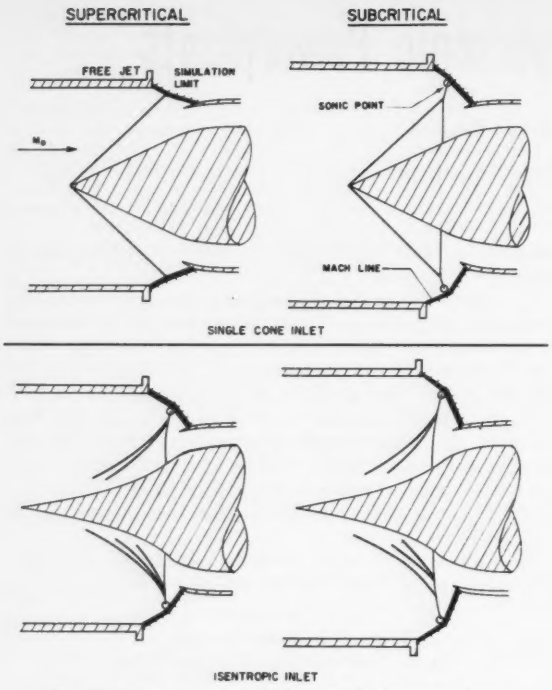

Fig. 2 Flow patterns required for inlet simulation

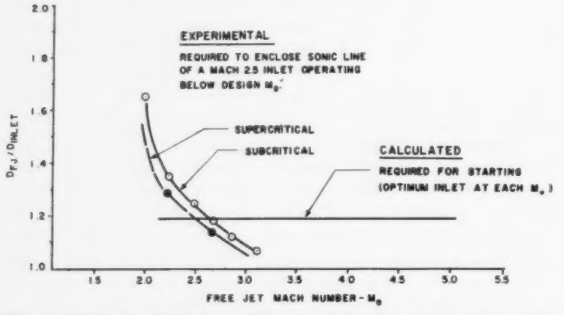
EXPERIMENTAL
REQUIRED TO ENCLOSE SONIC LINE OF A MACH 2.5 INLET OPERATING BELOW DESIGN M_0
SUPERCRITICAL
SUBCRITICAL
CALCULATED
REQUIRED FOR STARTING (OPTIMUM INLET AT EACH M_0)
D_{FJ}/D_{INLET}
FREE JET MACH NUMBER - M_0

Fig. 3 Typical minimum ratios of free jet nozzle exit diameter to engine inlet diameter

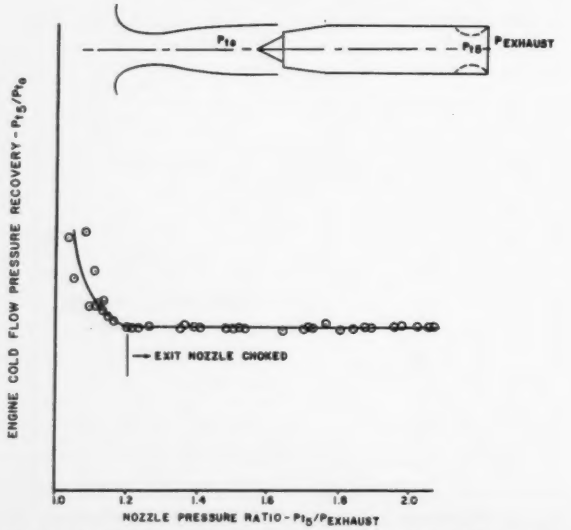

Fig. 4 Exhaust diffuser performance obtainable with engine divergent exit

minimum size is defined as that which will permit starting of supersonic flow into the engine and free jet diffusers, and which will contain the engine inlet flow field within the test rhombus.

The requirement for starting supersonic flow into the free jet and engine diffusers is shown in Fig. 1. As shown, this theoretical curve can be approached very closely in practice. The flow area which must start (A_0) is the free jet exit area and the contracted area (A_1) is the sum of the minimum areas of the engine and free jet diffusers.

The requirement for simulation of the inlet flow field after starting is accomplished is somewhat more complex since it is a function of engine inlet type, engine operating condition and free jet nozzle operation. For example, it is postulated that for proper inlet flow field simulation, the Mach or shock wave emanating from the free jet nozzle must intersect the engine inlet somewhat downstream of the cowl lip and enclose the inlet subsonic flow region (if one exists). However, shock systems for external compression inlets and particularly isentropic spikes, operating below design Mach number, are sometimes impossible to predict theoretically. Fig. 2 depicts typical shock systems which would be encountered with two different inlet types. These may be obtained experimentally by model scale tests utilizing conventional optical methods. The definition of minimum size free jet requirements is in many instances made only by analysis of shadowgraph or schlieren pictures.

Fig. 3 presents the experimentally determined free jet diameter requirements for an isentropic spike inlet designed for Mach 2.50. For comparison, the analytically determined requirements for an isentropic spike inlet or design at each Mach number are also included. The calculations were based upon design information presented by J. Conners and R. Meyer (2) with the assumption that the minimum annulus area required for starting occurred at the inlet plane. Consequently, it can be seen that the governing requirements for above design Mach number are those which can be attributed to starting supersonic flow and those below design Mach number to the enclosure of the inlet subsonic flow region in the test rhombus. The latter requirements require quite large free jet nozzles, as shown.

Exhaust Flow Simulation

Proper simulation of inlet flow conditions described above would be of small value in free jet testing unless provisions were also made for obtaining exhaust flow simulation. This can be accomplished by choking the engine exit nozzle throat. Hence, with inlet flow established and a sonic condition existing at the exit nozzle throat, complete internal flight simulation (with the exception of the divergent portion of the exit nozzle, if such exists) is obtained. Therefore, the maximum altitude that can be simulated (as far as the exit is concerned) is a function of the efficiency with which the sonic exit flow is diffused to external cell pressure according to the relationship

$$P_{t_0} = \frac{(P_{exh})\ (P_{t_5}/P_{exh})}{P_{t_5}/P_{t_0}}$$

where

P_{exh} = minimum facility exhaust pressure available (atmospheric pressure for pure blowdown operation)

P_{t_5}/P_{exh} = engine exit nozzle minimum pressure ratio required for choking

P_{t_5}/P_{t_0} = engine operating total pressure ratio

P_{t_0} = minimum total pressure which will maintain a choked exit; defines maximum test altitude at a given Mach number

This relationship reveals the importance of efficient exhaust flow diffusion (minimum P_{t_5}/P_{exh}) which directly affects

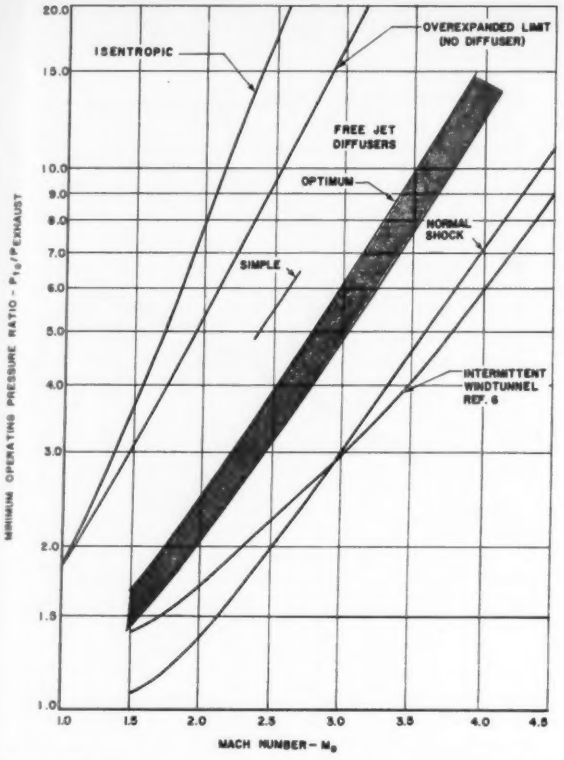

Fig. 5 Minimum supersonic diffuser operating pressure ratios

maximum test altitude and/or exhauster power requirements.

A simple exhaust diffuser such as that formed by a divergent exit nozzle will yield a good pressure recovery. Fig. 4 shows that a value $P_{t5}/P_{exh} = 1.2$ is obtainable. For simplification, this is obtained by plotting the engine cold flow (no burning) pressure recovery vs. exit nozzle pressure ratio. At values of P_{t5}/P_{exh} above which the exit is choked, the internal engine pressure recovery P_{t5}/P_{te} is fixed as shown by the horizontal portion of the curve. The break point in the curve defines the minimum value of P_{t5}/P_{exh} which will maintain choked exit conditions. Although these data are for air, data for burning conditions show only slight variation from this minimum pressure ratio.

Free Jet Diffusers

The free jet nozzle which has no physically bounded test section (hence the name free jet) may be operated over a wide range of operating pressure ratios depending upon the degree of efficiency with which the free jet kinetic energy is converted into pressure energy.

In a simple stored air blowdown facility, where P_{exh} equals atmospheric pressure, high efficiencies are mandatory since the maximum test altitude and test duration are directly a function of operating pressure ratio. These are generally much higher than the pressure ratios required for choking the engine exit. This importance is further evidenced in an altitude facility where exhausters are required to evacuate the test cell. Reference (1) notes that starting pressure ratios for free jet nozzle diffusers may be slightly higher than the minimum operating pressure ratio, particularly at higher Mach numbers. However, this is relatively unimportant in all but extremely marginal facilities. Generally, if any range of testable altitudes is available, sufficient pressure ratio will exist for starting at the lower altitudes.

As shown in Fig. 5, the efficiency to be expected from a free

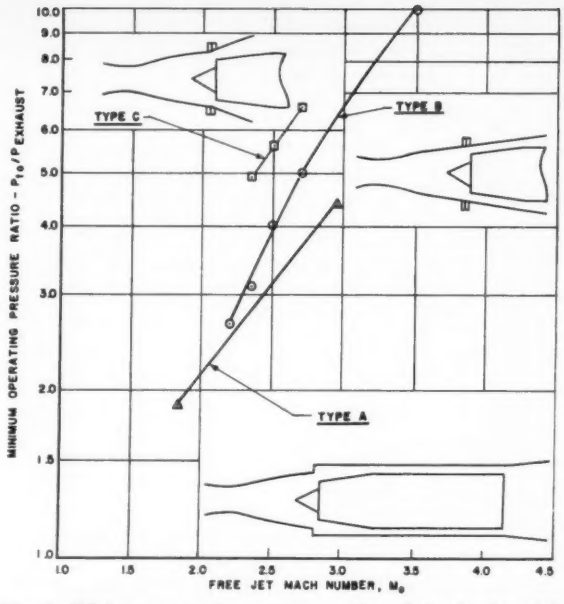

Fig. 6 Minimum operating pressure ratios of circular free jet diffusers and nozzles; angle-of-attack = 0 deg; free jet exit to engine inlet diameter = approx. 1.3

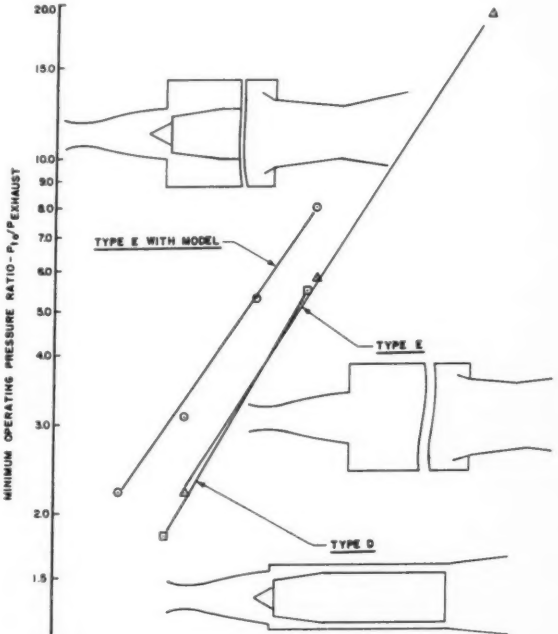

Fig. 7 Minimum operating pressure ratios of square free jet diffusers and nozzles; angle-of-attack = 0 deg; free jet width to engine inlet diameter = approx. 1.3

jet arrangement will vary between the limit of free jet nozzle overexpansion and that of wind tunnel diffusers. The band of optimum free jet diffusers serves as a guide to show the relative performance level that can be currently achieved. Due to the numerous arrangements that can be evolved with free jet systems, a complete survey of free jet diffuser minimum pressure ratio performance would be difficult to present.

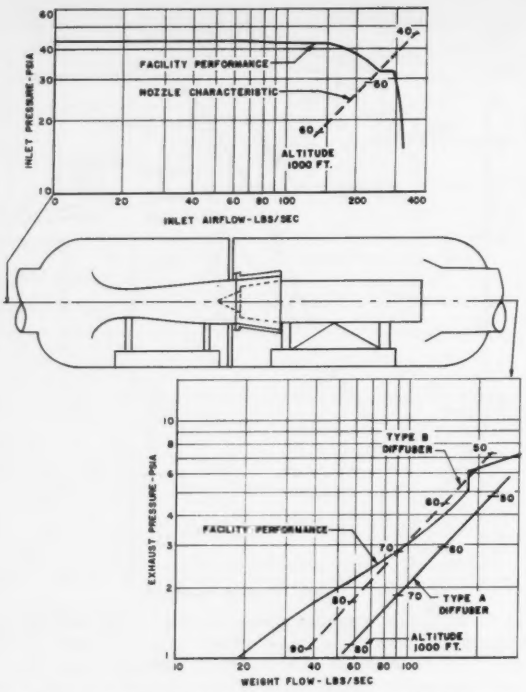

Fig. 8 Typical altitude free jet test facility and its test capabilities; Mach 2.50, ramjet at minimum power

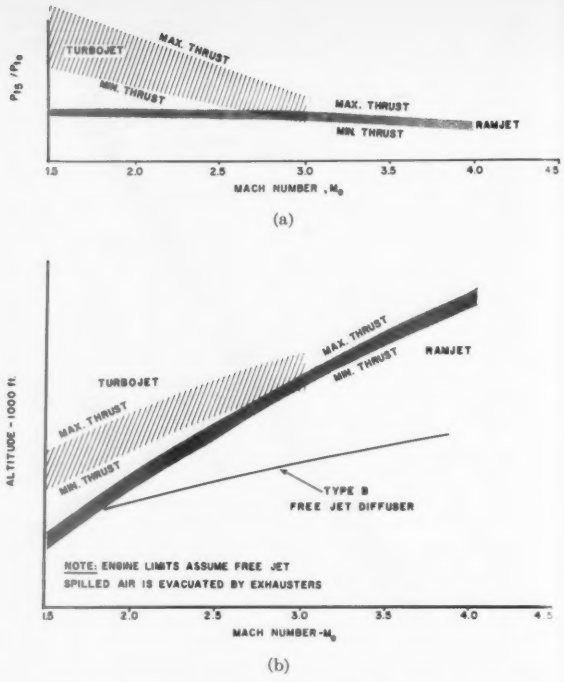

Fig. 9 (a) Supersonic engine total pressure ratios. (b) Maximum blowdown test altitudes for supersonic ramjet, turbojet and typical free jet diffuser

Since the engine itself forms part of the free jet diffuser passage, some compromise has to be made between good diffuser performance and engine accessibility and viewability. The extent of the compromise is dictated by the free jet nozzle size required and the ability of the facility to operate these nozzles.

A comparison of free jet diffuser operating pressure ratios is shown in Figs. 6 and 7 for circular and square geometrical arrangements. The optimum pressure ratio can be obtained from a configuration such as type A, where the diffuser passage is geometrically similar to the pattern of inflowing air and a long constant area section is followed by a gradual subsonic diffuser. This makes the engine quite inaccessible, however, for repair, modification and instrumentation. Tests with this type are reported in (1).

Two types of free jet diffusers that are used by Marquardt Aircraft Co. for full-scale ramjet engine testing are the "tailored diffuser" and the "alternate diffuser." The performance of both are shown in Fig. 6 as types B and C, respectively. The tailored diffuser is comprised of a relatively long circular diffuser which, together with the engine cowl, forms the annular duct passage. Some flexibility and accessibility is sacrificed, but good minimum operating pressure ratios are obtained.

The alternate diffuser is a design compromised in favor of flexibility. This short segment which is added to the free jet nozzle markedly improves overexpanded nozzle performance and makes the engine more accessible for inspection, repair and modification. In addition, remotely controlled transient angle of attack may be accomplished without altering the test setup.

A square free jet diffuser, similar to the circular version (type A), performs as shown in Fig. 7, type D. Slightly poorer performance is shown (1), probably due to the circular engine and square diffuser forming a less efficient diffusing passage.

An arrangement commonly called a "pressure box" system which permits shadowgraph or schlieren coverage of the inlet flow field is shown in Fig. 7 as type E. Good performance without an engine installed has been shown by Ohio State University (3), while the University of Minnesota (4) shows somewhat poorer performance with a model installed, the inlet area of which was 50 per cent that of the free jet nozzle. This is to be expected considering the less favorable turning angles and diffusion passages associated with a model installed in the pressure box.

It can be seen that various arrangements of free jets and diffusers which fall into the optimum free jet diffuser band of Fig. 5 are possible. The selection is dictated by engine inlet size, desired test altitudes and facility capabilities.

Testability

Testing capabilities of an engine test facility may be most conveniently illustrated by presenting a facility operation curve. The capacity is set by the operating limit of the equipment which makes up the basic testing facility. For convenience, the AEDC engine test facility (Tullahoma, Tenn.) was chosen as a representative test facility which is capable of conducting development testing on a supersonic air-breathing powerplant (5). Fig. 8 presents an arrangement of an altitude free jet test cell and its operational capabilities. The inlet test air is supplied continuously through the supersonic free jet nozzle by a system of compressors, where part of this air passes through the engine and part is spilled around the engine. In the test cell downstream of the engine, the spilled air mixes with the hot gases being ejected by the engine, the mixture then being evacuated by a system of exhausters.

The effect of operating pressure ratios upon the range of test altitudes available from this particular facility for types B and C free jet diffusers at Mach 2.5 is also presented in Fig. 8. The free jet size was arbitrarily chosen to be limited to a 70,000 ft test altitude with a type B diffuser. The simpler type C diffuser does not permit free jet nozzle operation at any altitude, whereas the type B diffuser permits opera-

tion from 48,000 to 70,000 ft (with a small untestable region around 55,000 ft). Required operating pressure ratios are shown in Fig. 6. Only zero degrees angle of attack testing was considered and flight inlet temperature simulation was assumed to vary according to an NACA Standard Day. The high altitude limit can be attributed to the maximum capability of exhauster equipment to evacuate the total mass flow handled to the required cell pressure, while the inlet compressor limitations are responsible for the lower altitude limit. The determination of these limits is obtained from the intersections of the free jet nozzle characteristic lines with the facility operational curves. It is evident that choice of proper test hardware plays an important role in determining the testability of a given supersonic air-breathing powerplant in a particular facility. With improved efficiencies in free jet diffusers, exhaust diffusers and optimization of exhauster systems, significant increase in testable altitude can be made.

Facility Exhauster Optimization

Altitude free jet test cells have generally been designed to operate in the manner described above. Namely, the free jet spilled air is mixed with engine exhaust gases and both are evacuated to a pressure which is required to provide inlet flow simulation (operate the free jet diffuser). However, a much higher pressure ratio is generally required to permit inlet flow simulation than to provide engine exit simulation (choke the exit). Consequently, it follows that a more efficient utilization of test facility capabilities can be obtained by handling the diffusion of free jet spilled air and engine exhaust products separately. This type of "split cell" arrangement can be accomplished by having either the engine gases exhausting to atmosphere or to a system of exhausters separate from those exhausting free jet spilled air.

For the case where the engine exhausts to atmosphere (and assuming that sufficient facility exhaust capacity is available for the purpose of exhausting the free jet spilled air), engine operating pressure ratios can then be converted directly into lines of maximum altitude on a Mach number vs. altitude plot. This can be illustrated by considering two typical cases of supersonic air-breathing powerplants, the ramjet and the turbojet. Fig. 9(a) presents representative pressure ratios for each engine as a function of Mach number. The conversion of these pressure ratios into altitude limitations is also presented in Fig. 9(b) where they are compared with the pure blowdown limits for a type B free jet diffuser. As shown, much higher altitude simulation at high Mach numbers is possible by arranging the engine exhaust products and free jet diffuser spilled air to discharge to separate pressure levels.

For both cases a supersonic pressure recovery of an optimum axisymmetric isentropic spike inlet was obtained from (2), and a pressure ratio $P_{t5}/P_{exh} = 1.2$ was assumed for the exhaust diffuser.

For testing at altitudes above those shown in Fig. 9(b), exhausters must be used to reduce engine exit pressure as well as free jet diffuser discharge pressure. Significant gains can be made over the upper testable altitude shown in Fig. 8 by dividing the exhauster capacity such that a portion exhausts the engine gases and the remainder exhausts the free jet spilled air. For example, the maximum altitude testable at Mach 2.5 in Fig. 8 is 70,000 ft. This is determined by the intersection of the combined engine gases plus spilled free jet air characteristic with the facility exhauster operational curve. However, in Fig. 10 the free jet spilled air and engine gas flow characteristics are plotted separately. Consequently, if the total facility exhaust capacity is split such that half exhausts engine gases and the other half spilled air, then the maximum testable altitude becomes 90,000 ft. Conversely, for the same altitude limit of 70,000 ft a 40 per cent larger frontal area engine could be tested.

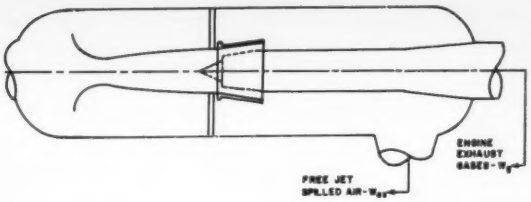

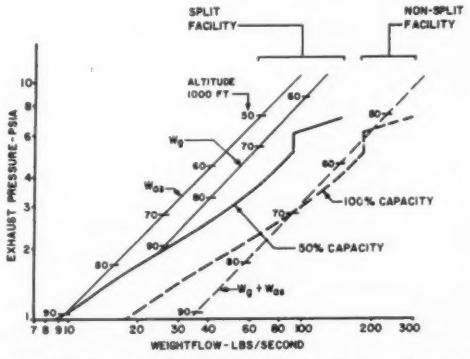

Fig. 10 Increase in maximum test altitude with split facility exhauster arrangement; Mach 2.50, ramjet at minimum power

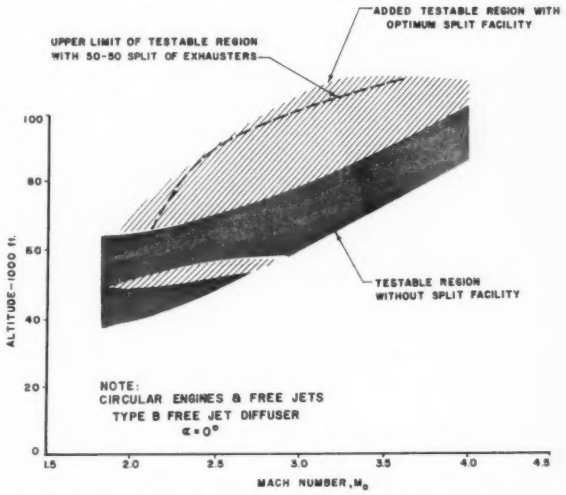
ADDED TESTABLE REGION WITH OPTIMUM SPLIT FACILITY
UPPER LIMIT OF TESTABLE REGION WITH 50-50 SPLIT OF EXHAUSTERS
TESTABLE REGION WITHOUT SPLIT FACILITY
NOTE:
CIRCULAR ENGINES & FREE JETS
TYPE B FREE JET DIFFUSER
$\alpha = 0°$
ALTITUDE - 1000 ft.
MACH NUMBER, M_0

Fig. 11 Comparison of testable altitude-Mach number regions with and without split facility exhauster arrangements; angle-of-attack = 0 deg

Complete optimization of an altitude exhaust facility would require very complex ducting to a large number of individual exhausters. The exhauster capacity would have to be divided between engine and free jet spilled air at different ratios, depending upon Mach number, free jet to inlet diameter ratio, and free jet diffuser type. The testable region gained for the example set forth would be as shown in Fig. 11. Much of this gain can be achieved, however, by providing for one splitting arrangement such as half for free jet spilled air and half for engine exhaust gases. The gain for this arrangement is also shown in Fig. 11.

Facility Nomograph

Rapid estimation of testing capabilities can be facilitated by the use of a nomograph such as that shown in Fig. 12. This may be best illustrated by considering a typical example of given conditions and solving for the limiting testable alti-

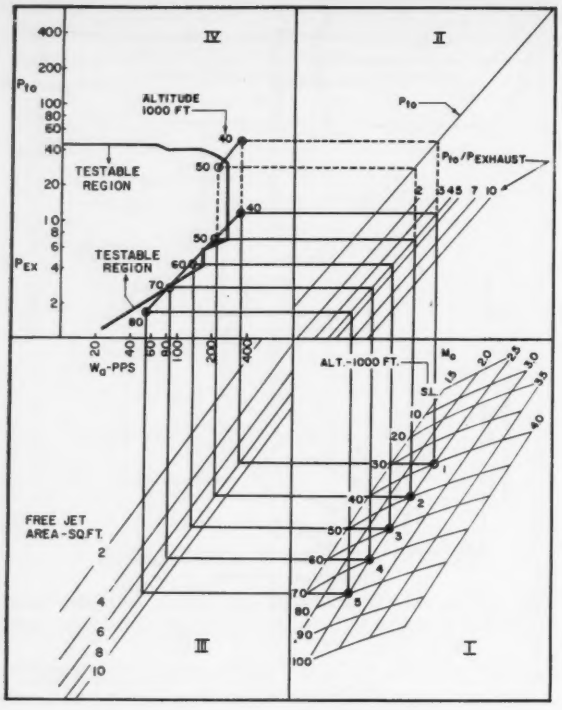

Fig. 12 Nomograph for rapid estimation of Mach number-altitude test limits

tudes. The problem can be resolved into two parts, one which will be determined by the facility exhauster limits and the other by the facility inlet pressure limits.

For a typical determination of high altitude boundaries on a Mach number vs. altitude plot (exhauster limits) enter chart I of Fig. 12 with starting points 1, 2, 3, 4 and 5 at Mach 2.50. Enter charts II and III to respective compression ratio and free jet area requirements. The intersection of these requirements in chart IV will yield a locus of altitude points relative to the available facility operational curve. The intersection of a line through these points with the facility operational curve determines the maximum testable altitude at the chosen Mach number.

Similarly, low altitude boundaries (inlet pressure limits) are determined by following the same procedure, except, when entering chart II, the P_{to} line is used instead of compression ratio.

For other Mach numbers, the same procedure may be employed provided requirements for charts II and III are known.

Conclusions

Free jet testing is perhaps the most efficient engine development testing method available. The test apparatus, however, should be optimized to minimize facility cost or, conversely, to permit testing over a much broader range of flight conditions. This optimization consists of defining minimum free jet nozzle sizes and providing efficient free jet diffusers. Further improvements of large magnitude can be obtained by utilizing facility exhausters to evacuate free jet spilled air and engine exhaust gases separately.

References

1 Feldman, F. K., Gafarian, A. V., and Bitondo, D., "Aerodynamic Research for the Design of Altitude Free Jet Test Sections for Ramjet Test Facilities," North American Aviation, Report AL-1265, May 1951.

2 Conners, James F., and Meyer, R. C., "Design Criteria for Axisymmetric and Two-Dimensional Supersonic Inlets and Exits," NACA TN 3589, Jan. 1956.

3 Lee, J. D., and Von Eschen, G. L., "Critical Performance Parameters of an Intermittent High-Pressure Free Jet Supersonic Wind Tunnel," Ohio State University, Final Report RF Project 344, July 1954.

4 Hermann, Rudolph, and Hsu, Cheng-Ting, "Free-Flight Simulation of the Testing of Supersonic Inlet Diffusers in a Free Jet Wind Tunnel with 50 Percent Area Ratio in the Mach Number Range from 1.5 to 3," University of Minnesota, Institute of Technology, Research Report 117, Aug. 1955.

5 Addison, W. E., "Operational Capabilities of the AEDC Engine Test Facilities," AEDC-TN-53-7, June 1955.

6 Lukasiewicz, J., "Development of Large Intermittent Wind Tunnels," *Journal of the Royal Aeronautical Society*, April 1955, pp. 259–278.

Techniques of Flight Simulation for Ramjet Engines

RAYMOND GREENBERG[1]

Curtiss-Wright Corp., Wright Aeronautical Division, Wood-Ridge, N. J.

Ground testing of ramjet engines must be accomplished under simulated flight conditions. Because the ramjet is an air-breathing engine that must operate at supersonic air speeds at high altitudes, the requirements for simulation demand extensive facilities. The Wright Aeronautical Division of Curtiss-Wright Corp. operates a blowdown-type facility capable of a wide range of simulation for testing large full-scale ramjet engines.

Presented at the ARS Semi-Annual Meeting, San Francisco, Calif., June 10–13, 1957.

[1] Manager, Ramjet Test Division.

THE development of ramjet engines as air-breathing propulsion devices in the supersonic range fostered the requirement for testing in ground facilities under flight conditions. By virtue of its inherent design, the ramjet requires speed and altitude before it can function. In flight, this is accomplished with the aid of an auxiliary booster. Consequently, in the interests of economy, time and reliability, the answer to ramjet testing lies in simulating flight conditions in a ground facility.

Creating the environment of the flight regime is in itself a technique that requires extensive facilities, equipment and ingenuity. It is first necessary to understand the requirements

of high altitude supersonic flight so that we may more fully appreciate the techniques involved.

The ramjet engine is air-breathing by design, and for optimum performance is sized to operate in the supersonic range at altitudes greater than 40,000 ft (as shown in Fig. 1). Under these conditions, high stagnation temperatures are encountered. Although operation is virtually all in the isothermal range, the temperature variation is considerable. For example, at Mach 3 the temperature is approximately 650 F, and at Mach 4 it becomes 1300 F. The ramjet is basically a simple power plant. It requires air and fuel as do conventional engines but is devoid of any major rotating parts. In flight, air for combustion is obtained from the ram-effect through a precisely designed supersonic inlet which, for practical purposes, can be considered comparable with a turbojet compressor. The inlet may or may not be a part of the engine, and, in the latter case, the inlet may be designed integrally with the air frame of the flight vehicle. Thrust for propulsion is obtained by virtue of the mass flow and the change of velocity of the gases going through the engine from the inlet to the exhaust. The component sections comprising a ramjet can be considered as follows: an inlet diffuser, combustion chamber, exhaust nozzle and a fuel control system. Fig. 2 describes a typical ramjet with respect to station locations.

As previously discussed, the inlet diffuser can be considered analogous to a compressor and, in addition, serves to reduce the air velocity from supersonic at the inlet entrance to subsonic at the face of the combustion chamber. With regard to ground testing, the inlet simulation poses one of the most exacting challenges because of the supersonic flow requirements and inlet velocity distribution.

Combustion takes place in the combustion chamber where the energy level is raised. This results in the pressure drop necessary to expel the gases through the exhaust nozzle where they are accelerated to the terminal velocity required to produce thrust.

The fuel control system consists of a control device, fuel pump and distribution system. Performance of the engine is controlled by the fuel system which requires considerable development under simulated flight conditions. The fuel system in supplying fuel to the engine senses the effect of engine combustion on the inlet diffuser and automatically compensates to maintain the desired fuel-air ratio. Hence, flight simulation of these conditions is necessary to study the inlet shock-positioning and buzz characteristics of a particular ramjet installation.

Performance of a ramjet at present is considered optimum in a region of approximately Mach 2 to Mach 3.5, and altitudes of 40,000 to 100,000 ft. The accompanying stagnation temperatures at the ram inlet, which are a function of speed and altitude, are on the order of 250 to 800 F. The weight flow of air, of course, is dependent upon the size of the engine, which at the present level of development has become quite large. Consequently, the ground facility necessary to provide the quantities and temperatures of air and fuel and, further, to depress the atmosphere to the required pressure altitudes, has become an extremely elaborate and intricate structure. The Phase IV facility at the Wood-Ridge plant of the Wright Aeronautical Division, Curtiss-Wright Corp. (illustrated in Fig. 3), is in altitude facility for accomplishing these aims.

The facility is basically a blowdown type that supplies air to the engine by utilizing high pressure air from storage bottles, coupled with low pressure air from continuously operated compressors. Large capacity heaters raise the air temperature to that required to simulate the desired flight condition. Pressure altitudes are achieved by exhausting the air through a series of steam-fed ejectors. The air supply system (shown schematically in Fig. 4) can be operated in either an intermittent fashion for blowdown, which is necessary for relatively low altitude testing in the neighborhood of 45,000 ft, or continuously from compressors which permit higher altitude operation. Air can be supplied to either of two test chambers through insulated ductwork and a surge chamber.

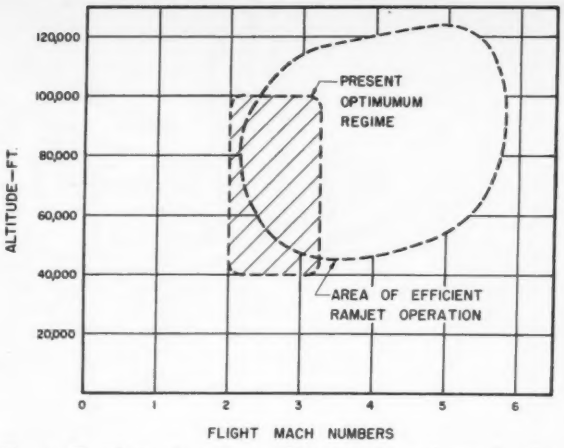

Fig. 1 Envelope of range considered to be optimum for the operation of ramjets

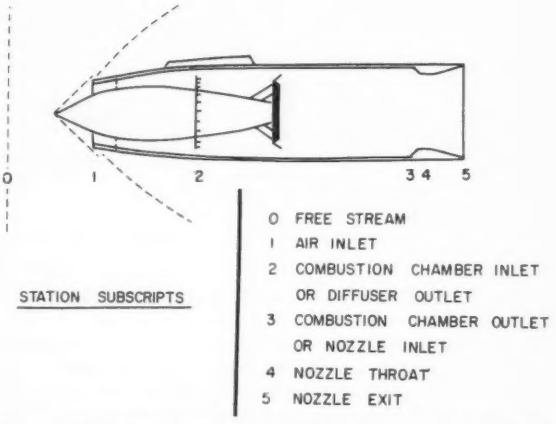

Fig. 2 Typical ramjet engine showing component locations

One chamber is 12 ft in diam and 60 ft long with a removable surge chamber to permit engine installation. The other is 14 ft in diam and 90 ft long with 36-ft side hatch for ease of engine handling. The surge chamber on the latter is also removable and, in addition, is provided with a nozzle chamber that may be included between the test chamber and the surge chamber. Both chambers are pressurized by incorporating hydraulic locks and water-inflated seals. Three modes of testing can be accomplished, namely, direct connect, free jet or ducted nozzle. Both chambers are operated from a common control room that features a schematic process control panel (shown in Fig. 5), an engine control panel, data recording equipment and periscopes for observing and recording combustion chamber flame conditions.

The primary or blowdown system consists of 240 storage bottles that contain 63,000 lb of air at 3200 psi. This air is expanded through a control valve which automatically programs for a selected surge chamber pressure. Air flows up to 700 lb per sec at 90 psia are obtained in this manner. The control system is operated either manually or automatically so as to give a 9-sec response with 3 per cent overshoot, maintaining $\pm\frac{1}{4}$ per cent stability. During this operation, secondary air is introduced and mixed with the high pressure air through an air-to-air ejector. Consequently, since the ramjet engine provides no motive power of its own, it must be boosted to a minimum altitude at a supersonic velocity before

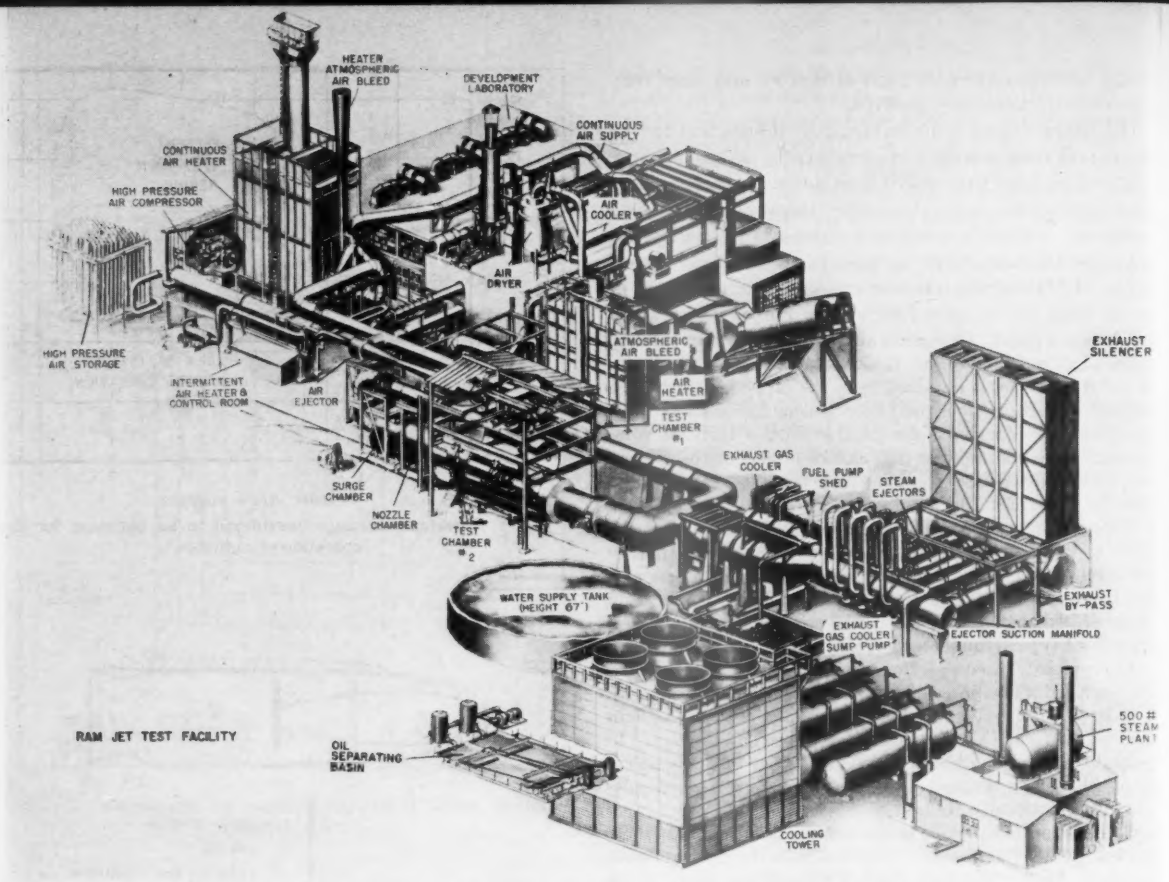

Fig. 3 Phase IV ramjet test facility located at the Wright Aeronautical Div. Wood-Ridge plant

ignition can be realized. Utilizing the blowdown air system, then, permits high mass flow to simulate the low altitude condition, and, once ignition is effected, the high pressure system is turned off and transition to a higher cruise altitude is maintained by a virtue of the secondary air from the compressor which is permitted to continue through the air-to-air ejector. This air flow is then controlled by regulating the compressor output.

The secondary air is supplied by turbojet aircraft compressors that are driven by a 15,000-hp prime mover. Various combinations of compressors are available that provide flows up to 215 lb per sec at 73.5" HgA or 130 lb per sec at 200" HgA. The compressor output is controlled by regulating the prime mover speed and through bleed valves in the compressor discharge ductwork. A comprehensive chart of available air is shown in Fig. 6.

Air heating is accomplished, in the case of intermittent supply, by passing the air through either a horizontal tube and shell heat exchanger which is 6 ft in diam by 70 ft long, or a metal fill type vertical heat exchanger that is 8 ft in diam by 80 ft long. The air within the shell is heated by forced air from direct-fired air heater that utilizes steam-atomized #2 fuel oil for combustion. The heat realized from the tube and shell heater is 4,400,000 Btu per hour and can raise the air temperature to 800 F, while the metal fill heater releases 7,000,000 Btu per hour and raises the air temperature to 1260 F. Continuous air is caused to flow through a 94-ft-high radiant, convection-type, natural-draft heater. Steam-atomized #2 fuel oil is likewise used for fueling the burners. A heat release of 299,000,000 Btu per hour is realized in raising the air temperature to 800 F. Air temperature is controlled by regulating the heater temperature and preheating the ductwork to the test chambers to assure stabilization. Air requirements for flight conditions up to Mach 3.25 and altitude range of 40,000 to 83,000 ft are achieved in this way.

Fig 7 is a schematic diagram of the exhaust system which serves to depress the test cells to the desired pressure altitude and utilizes the pumping action of eleven steam ejectors. The steam is used as the primary source and is controlled through remote-operated valving to each ejector. The secondary ports of the ejectors are similarly valved to the cell exhaust manifold. In this way the ejectors, which are sized from 24 to 48 in. in diam, can be selectively operated to produce test chamber pressures in accordance with the curves in Fig. 8. A total capacity of 3,400,000 lb per hour of steam is available through these ejectors to handle the 700 lb per sec air flow at 45,000 ft. Steam for the ejectors is supplied from six package boilers which produce 410,000 lb per hour of steam. The boilers charge seven partially water-filled accumulators with steam at 500 psi. The total storage capacity of these accumulators is 245,000 lb. This steam is released through control valves that regulate the pressure to approximately 156 psi.

The steam and exhaust products are exhausted to atmosphere through a 57-ft-high silencer fitted with "sound stream" sound treatment for noise attenuation.

Because of the high temperature (approximately 3500 F) gases emitted from the engine, an elaborate water cooling system is provided. Fig. 9 is a schematic diagram of the water system. The temperature at the exhaust gas cooler enters at 800 F after preliminary cooling in the test cell exhaust diffuser. Water sprays and exhaust gas cooler drop the temperature to 150 F, after which the water is separated from the exhaust gases through a separator section that removes 98 per cent of the moisture. This water is regenerated through a 33,000-gpm circulating pump that is driven by a 1000-hp synchronous motor. The circulating pump returns the water to a 67-ft storage tank that has a capacity of 2,100,000 gal of water. The warm and contaminated water is returned to the top of the tank from where it is drawn off by a 5600-gpm pump that

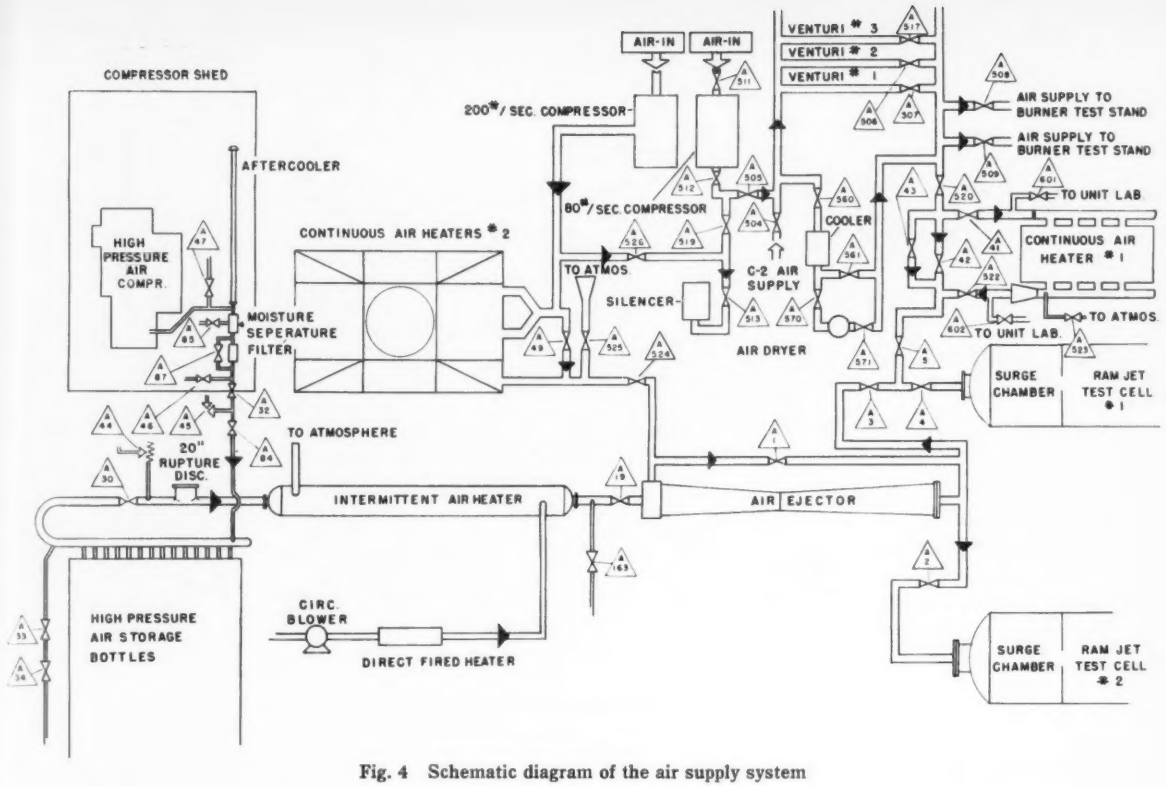

Fig. 4 Schematic diagram of the air supply system

pumps the water to an air-flotation, oil-separating system. The oil and contaminating matter are floated to the surface of the separating basin as a result of air entrainment that creates bubbles which adhere to the foreign matter. Skimming paddles that are operated on an endless conveyor belt skim the impurities over a weir and the remaining warm water is pumped to the top of either of two cooling water towers. The towers are equipped with four controllable fans that create air columns against which the water rains down. The temperature is dropped in the cooling towers from 140 to 80 F. This cleaned and cooled water is then returned to the bottom of the storage tank from which it is gravity-fed to the exhaust cooler system. The water regenerative cycle is applied continuously during the test operation.

The fuel requirements for a ramjet are very demanding in so far as mass flow and temperature are concerned. Therefore, a fuel system (shown schematically in Fig. 10), is provided that has a capacity of pumping 90,000 lb per hour through three centrifugal pumps that raise the pressure to 600 psi. The pumps can be operated selectively and can be caused to flow through any of the three systems to either test chamber. Each of the three systems is sized for a particular range and can be individually controlled by remote control valves and pressure regulators

High fuel temperatures are necessary to simulate the stagnation temperature effect in flight. This is accomplished by passing the fuel through heat exchangers that are heated with 500-psi steam. Three-way control valves are provided for by-passing and mixing hot and cold fuel and thereby regulating the temperature to a maximum of 350 F. Where addi-

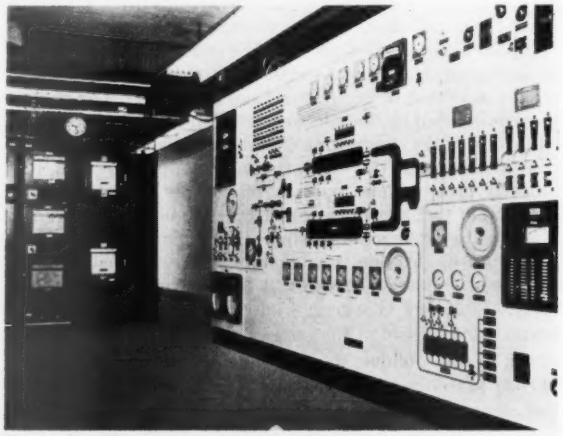

Fig. 5 Facility process control panel located in the central control room

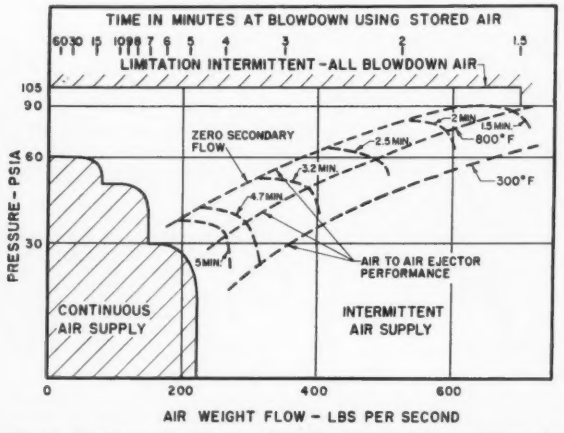

Fig. 6 Performance curves of continuous and intermittent air supply sources

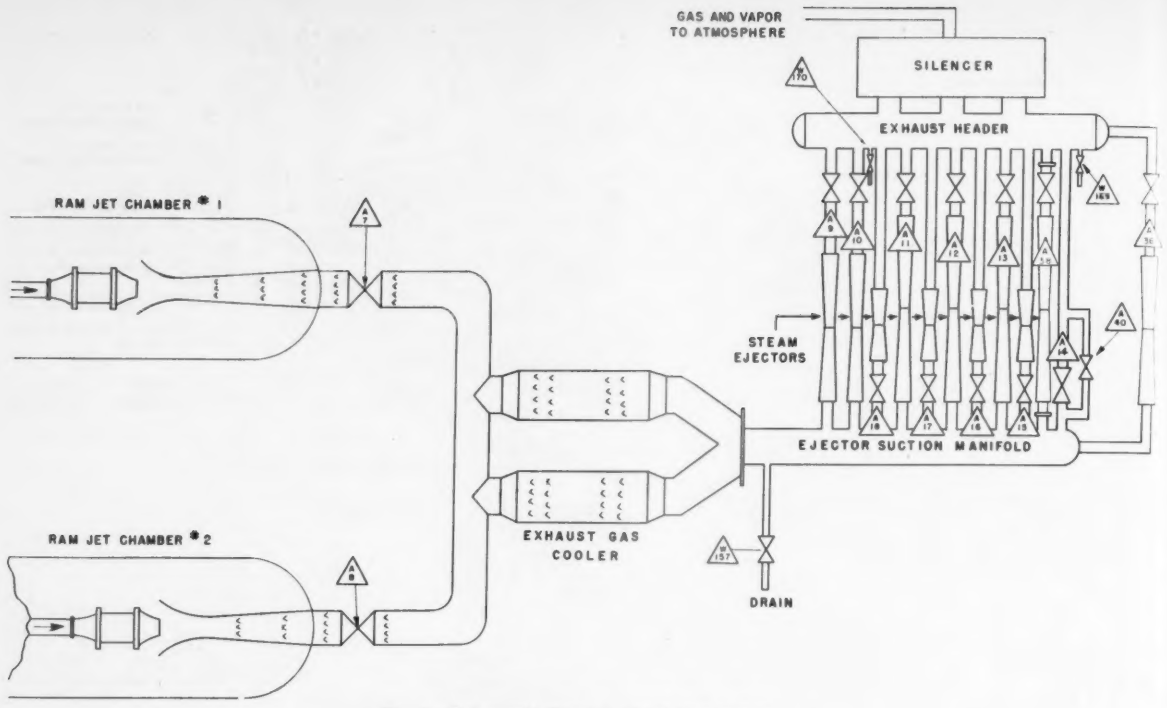

Fig. 7 Schematic diagram of exhaust system

tional temperature is required, the 350 F fuel is passed through a chemical heat exchanger that raises the temperature to 500 F.

Testing basically consists of investigating performance characteristics and durability of each system of the engine as well as determining acceptance of the complete engine. To accomplish these aims, conditions must be provided to accurately simulate the in-flight environment. Perhaps the most exacting are the requirements for inlet simulation. Because of unpredictable flight paths, studies of engine operation must be made both at design and off-design conditions. Hence the problem of inlet simulation.

The effect of off-design operation is a variation in the inlet air distribution at the engine face or combustion chamber entrance. Some characteristic profiles plotted for Mach number distribution in the subcritical region under varying conditions of speed and angles of attack are shown in Fig. 11. Of significance is the location of the high Mach number region observed in the center contours. The shifting of this high Mach number area, as noted in the diagrams, is reflected in

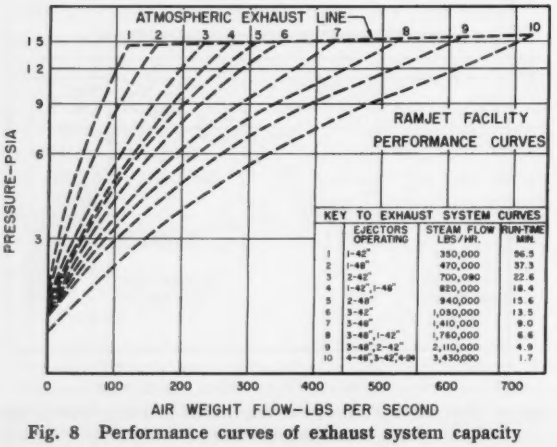

Fig. 8 Performance curves of exhaust system capacity

flame propagation in the combustion chamber. This may have a detrimental effect upon engine performance or durability. It is also interesting to note the contour rings which represent the low Mach number region and the positions they assume when the high Mach number area changes. Under adverse conditions, flow separation takes place in the peripheral contours and can seriously affect the boundary layer used for cooling air flow. The penalty for starving the cooling air obviously is lack of durability in the combustion chamber and exhaust nozzle.

For the particular cases illustrated, a side inlet was used but the problem is similar regardless of the inlet configuration. This study is of vital importance to the development engineer and, therefore, ground simulation of the in-flight inlet conditions must be conducted. A ducted nozzle is employed which provides the means to vary the inlet conditions necessary to affect the simulation of flight Mach numbers and angles of attack.

Inlet buzz phenomena studies are similarly important in the development of a ramjet—particularly as they affect the fuel control system. Buzz can be described as an objectionable pulsation of the air flow through the engine. It is controlled by positioning the oblique and normal shock waves in the inlet section indicated by the dotted lines on Fig. 2. The oblique shock is induced by the inlet geometry and the normal wave is a function of the combustion chamber pressure. The oblique wave emanates at the tip of the inlet center body and, in a properly designed and operated engine, is captured by the outer lip of the inlet diffuser cowl. The normal wave, which is normal to the direction of flow, is located in the inlet diffuser and, since its position is a function of the thermal blockage from the combustion chamber, it may move fore and aft as a result of fuel flow changes. Consequently, instability of the normal shock position that causes alternate spill and capture cycles of the oblique shock results in buzz. This can be likened to compressor surge, as it imposes a limitation on the fuel control system operating range.

Free jet testing is conducted to study the effects of the buzz cycle and determine the control system margin of perform-

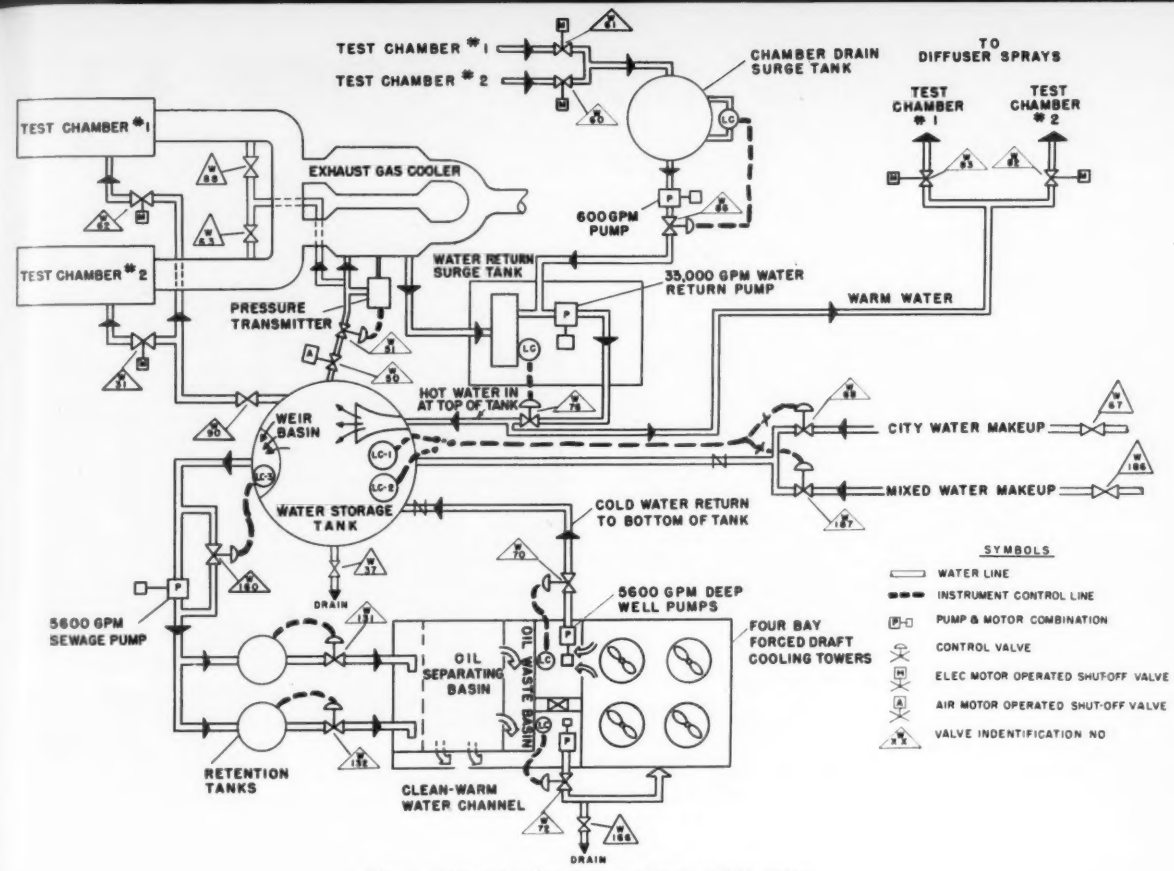

Fig. 9 Schematic diagram of exhaust cooling water

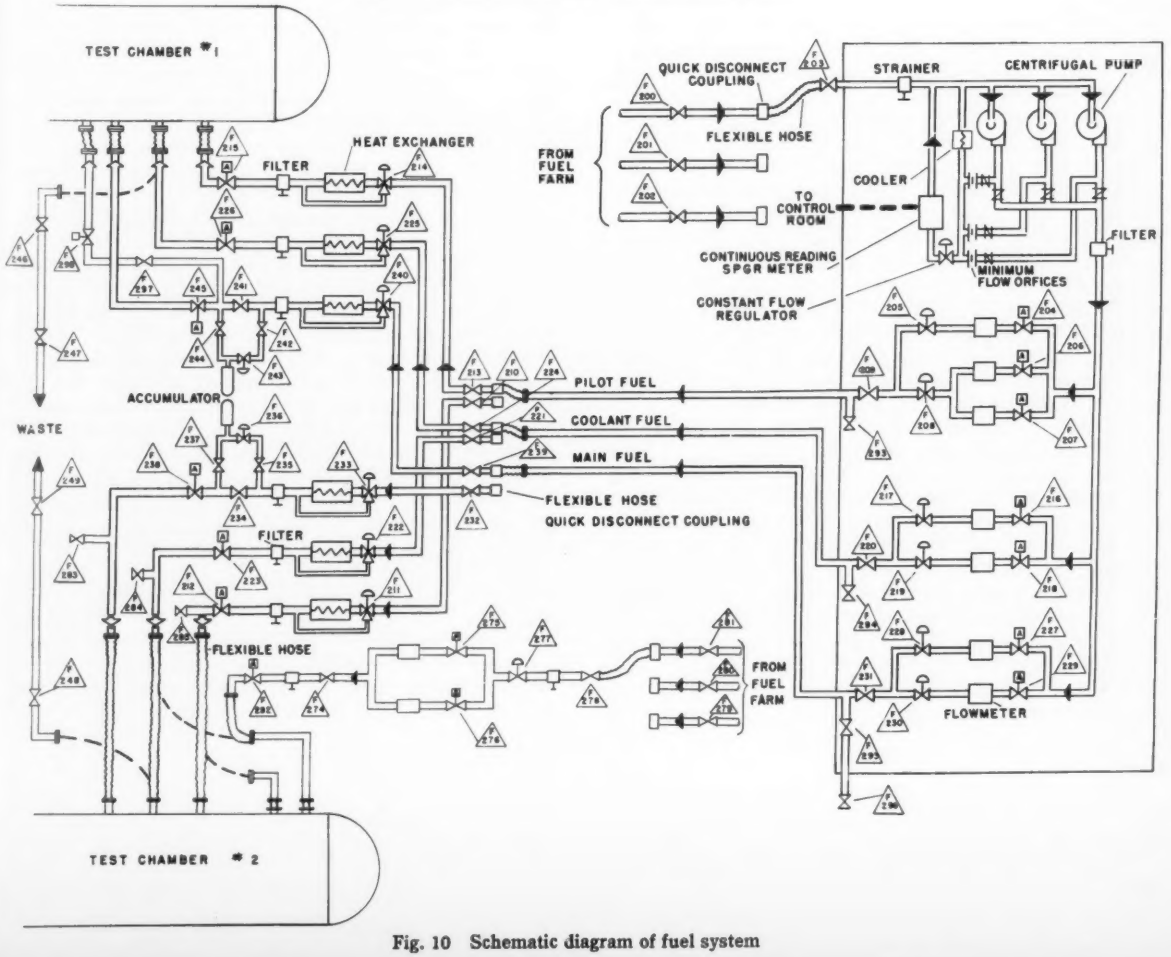

Fig. 10 Schematic diagram of fuel system

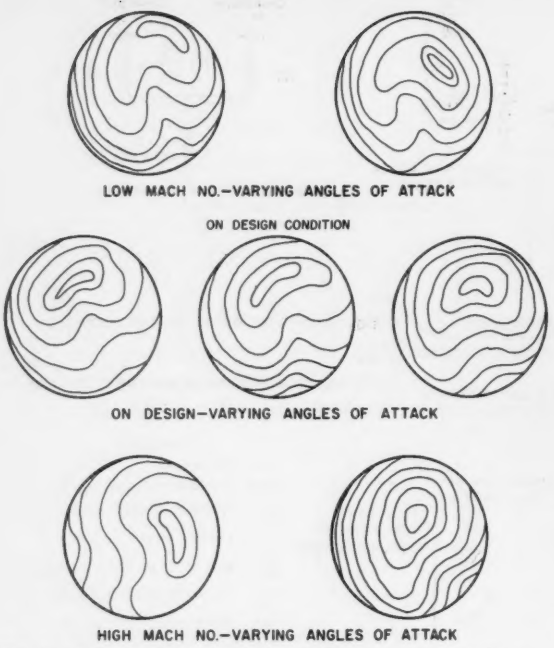
LOW MACH NO.—VARYING ANGLES OF ATTACK
ON DESIGN CONDITION
ON DESIGN—VARYING ANGLES OF ATTACK
HIGH MACH NO.—VARYING ANGLES OF ATTACK

Fig. 11 Inlet subcritical velocity profiles measured at the entrance to the combustion chamber for varying conditions of air speed and angle of attack

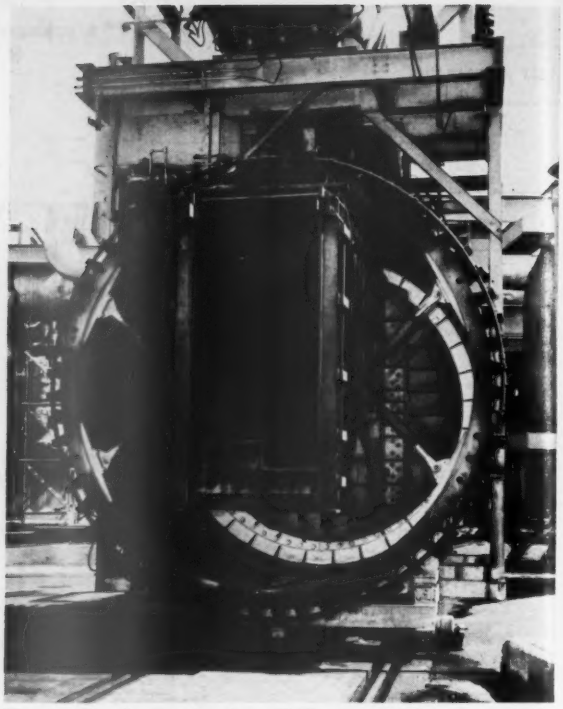

Fig. 12 Nozzle chamber for cell No. 2 containing the variable Mach number supersonic nozzle

ance. The testing technique involves using a supersonic nozzle in front of the inlet in conjunction with an exit diffuser to establish supersonic air flow simulating the in-flight condition. The positioning of the inlet cone with regard to the nozzle exit or test section is of extreme importance. This is significant in view of the fact that the region of the desired Mach number falls within an envelope commonly referred to as the test rhombus. The rhombus is formed by the resultant supersonic shock waves that emanate downstream of the nozzle throat as the flow expands to supersonic velocities. The shocks are confined within this diamond arrangement and it is, therefore, referred to as the test rhombus. In performing the test, oblique shock wave of the inlet must be located within this area to achieve accurate Mach number simulation. The positioning of the inlet within the test rhombus and the buzz cycle effects of the oblique shock wave are viewed with a shadowgraph or schlieren optical viewing system. The results are apparent on a screen surface that may be photographed for further analysis and record purposes.

For small-diameter engines having symmetrical, round inlets, relatively small nozzles are provided. However, for large engines, particularly where side inlets are concerned, much larger nozzles are required. A variable Mach number supersonic nozzle of the latter type permitting approximately 50 per cent secondary air flow is shown in Fig. 12. This nozzle incorporates two contoured blocks, the lower of which is stationary. The upper, movable block is remotely controlled and is operated by a hydraulic ram to produce variations that range from Mach 1.5 to Mach 3.25. The nozzle may be operated with fixed-geometry for on-design conditions and, further, has provisions for rapidly moving the sliding block to simulate the booster phase.

The three modes of testing, namely, direct connect, free jet and ducted nozzle, provide a broad variety of test simulation that covers all phases of testing necessary for ramjet development. Each has a particular advantage that is moderated by its limitations. Direct-connect testing is adequate for component evaluation and utilizes relatively simple equipment. However, although inlet velocity profiles may be varied with flow simulators, the actual recovery conditions in front of the engine inlet are not faithful reproductions because of the subsonic velocities in the straight inlet duct.

Free jet testing provides good inlet simulation; however, it imposes external drag forces on the engine that are not encountered in flight, as well as severe facility limitations because of the high pressure drops necessary to create supersonic flow. The high rate of flow necessary for free jet testing also requires prohibitive exhausting capacity.

The ducted nozzle provides a happy medium in that the inlet simulation for both on-design and off-design testing is feasible without taxing facility capacity. However, the equipment involved is rather complicated and requires a good deal more maintenance and service. Flight and wind tunnel tests provide the necessary reference profile data from which the ducted nozzle is oriented. Full-scale tests utilizing the ducted nozzle have demonstrated extremely close simulation of these supplied in-flight data.

It is apparent from this discussion that we have only begun in so far as flight simulation is concerned. Development of flight vehicles and powerplants is rapidly accelerating, and the requirements for people and technology to keep pace with the growth of the field of aviation offers a rigorous challenge for the future.

Ramjet Test Facility Planning

ROBERT O. DIETZ Jr.[1] and ARTHUR H. HINNERS Jr.[2]

Arnold Engineering Development Center, Tullahoma, Tenn.

A method of planning adequate test facilities to meet future ramjet test requirements is discussed. Data are presented to show that adequate planning with sufficient lead time can be accomplished most readily through careful review and analysis of ramjet component research results. The analysis shows that specification of ramjet test facility equipment requires careful consideration of the over-all operating envelope of ramjet engines since multiple use of air supply and exhauster equipment is possible. Potential effects of research in the field of test simulation methods upon facility performance requirements are discussed.

Introduction

FULL-SCALE ramjet test facilities are needed because the ramjet offers the most desirable aircraft propulsion performance over a broad range of flight conditions, and because methods of extrapolating performance and operational data procured from small-scale ramjet engines and components have not been evolved. Limited success has been achieved in scaling combustion chambers when fuel systems are properly scaled but the methods for scaling fuel systems are empirical and not completely reliable.

A method of planning adequate test facilities to meet future ramjet test needs is discussed in this paper. Data are presented to show that adequate planning with sufficient lead time can be accomplished most readily through careful review and analysis of ramjet component research results. The analysis also shows that specification of equipment for a ramjet test facility requires careful consideration of the over-all operating envelope of ramjets tested in that facility since multiple use of air supply and exhauster equipment is possible.

Discussion

A ramjet facility in which air is not recirculated is considered in this analysis. Inlet air is taken from atmosphere, raised to the proper pressure level in air supply compressors, and temperature conditioned by the use of heaters or coolers. Air then passes through the test installation, is cooled, and then exhausted to atmosphere through exhaust gas compressors. Effects of water spray cooling on exhaust gas volume have been neglected.

Operating envelopes to be simulated for ramjet engines were generated so that test facility performance required at each engine operating condition could be determined. Determination of test facility performance at each engine operating condition was necessary in order to show maximum performance limits for air heaters, air supply compressors and exhaust gas compressors. In addition, study of test facility equipment performance requirements over the complete range of operation for the engines provided information on the possibility of multiple use of air supply machines as exhausters at operating conditions at which exhaust requirements are at a maximum and air supply requirements are relatively low.

Presented at the ARS Semi-Annual Meeting, San Francisco, Calif., June 10–13, 1957.

[1] Chief, Advanced Analysis Division, USAF, Arnold Engineering Development Center.

[2] Engineer, Gas Dynamics Facility.

Ramjet Operating Envelope

A maximum Mach number (*C-D*) was chosen for the operating envelope shown in Fig. 1 on the basis of relative performance of ramjets, turbojets and rockets. A comparison of powerplants was made by the use of specific impulse, thrust per unit of frontal area and thrust per unit of weight. Fig. 2 (1)[3] shows specific impulse as a function of flight Mach number for the rocket, ramjet, turbojet and turbojet with afterburner. Specific impulse of the ramjet decreases above Mach 3 as shown in Fig. 6, but it appears that the ramjet offers attractive values of specific impulse at Mach 4. Thrust per unit of frontal area of a propulsion system is indicative of the drag of the powerplant installation and also indicates the variation of weight of a specific powerplant. Fig. 3 shows that on a thrust per unit frontal area basis the rocket will be superior to the ramjet at Mach 4. The rocket is lighter than the ramjet at the maximum Mach number studied.

A maximum sea level Mach number (*B*) was determined on the basis of the fact that it is possible and beneficial to accelerate ramjet-powered missiles to Mach numbers in the range of 2.5 at very low altitudes with the use of rocket engines. Maximum Mach number operation was limited to altitudes above 50,000 ft because dynamic pressure at that flight condition is approximately equal to dynamic pressure at Mach 2.5 at sea level.

Maximum Mach number for which the test facility should

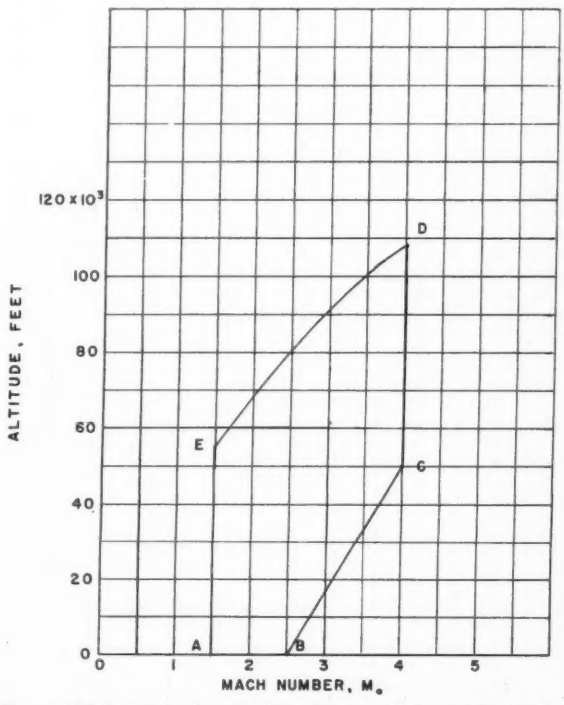

Fig. 1 Typical operating envelope for use in generating basic machinery requirements for ramjet test facility

[3] Numbers in parentheses indicate References at end of paper.

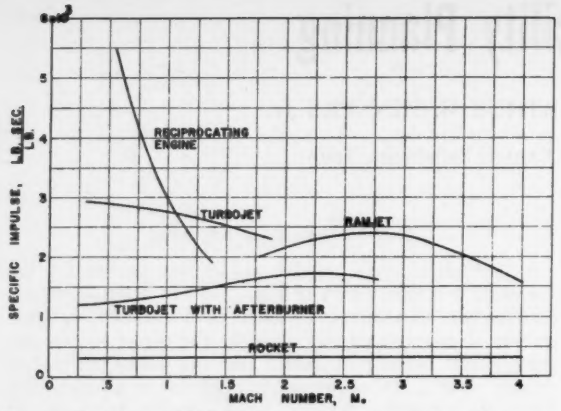

Fig. 2 Typical specific impulse of various types of engines as a function of Mach number

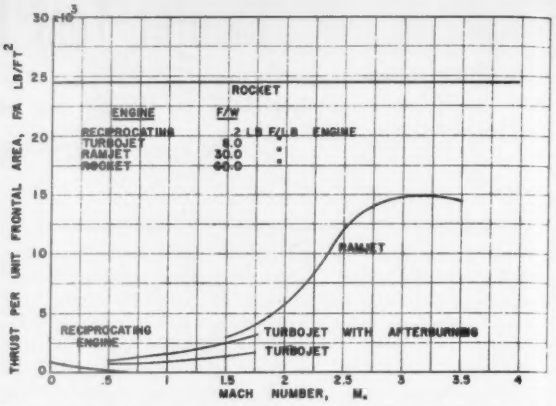

Fig. 3 Typical values of thrust/frontal area for various types of engines as a function of Mach number

be designed may increase due to advances in research on ramjet components and fuels or may decrease if strides are made in advancing rocket engine performance. The ramjet test facility planner must therefore carefully analyze research advances in ramjets and rockets as well as the relative complexity of development problems in the two types of engines in order to estimate the maximum Mach number for which ramjet test facilities should be designed.

A Mach number of 1.5 at altitudes between sea level and about 55,000 ft (*A-E*) comprises one limit of the operating envelope shown in Fig. 1. It is doubtful that ramjet engine free jet testing can be accomplished satisfactorily below Mach numbers of about 1.5 unless free jet testing philosophy is greatly changed. Below $M = 1.5$, the allowable over-all cross-section area at the engine inlet cowl is below 50 per cent of the Laval nozzle exit area. Choice of minimum Mach number was based on the practice in some ramjet engines of igniting the engine at low altitude, low Mach number conditions to assure ignition and to avoid the necessity of special geometry changes in the engine to make ignition possible at high flight Mach numbers.

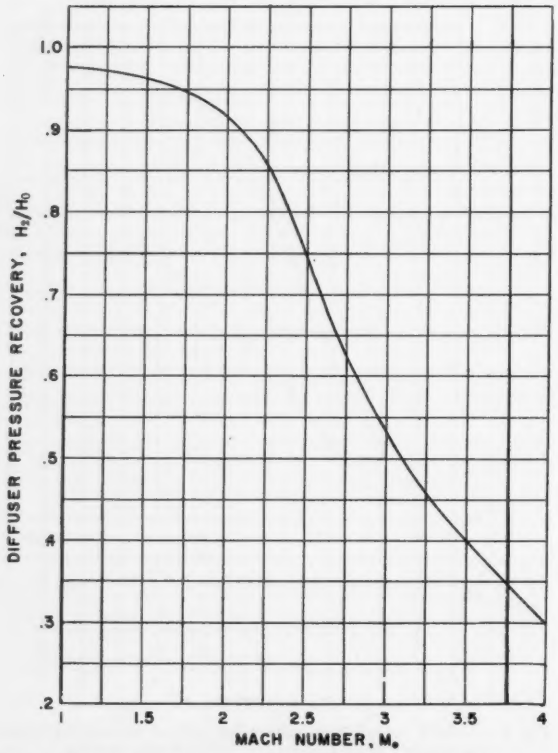

Fig. 4 Ramjet engine diffuser pressure recovery as a function of Mach number

Improvements in free jet test technique or the use of smaller engine inlet to free jet nozzle outlet area ratios to accommodate subcritical free jet testing would lower the minimum test Mach number. The engine test facility planner should, therefore, carefully follow the research results on such test techniques.

Maximum altitude to be simulated at each flight Mach number (*D-E*) was based on maintaining reasonable combustion chamber pressures. Experimental investigations of effects of combustor pressure on combustion efficiency indicate that minimum ramjet combustor pressures should not go below a critical value. One-third of an atmosphere was used as the minimum combustion pressure in this analysis. Total pressure recovery for a series of inlets, each designed for optimum recovery at the Mach number presented, is indicated in Fig. 4. These data were used along with the minimum allowable combustor pressure to calculate the maximum altitude operating limits in the following manner:

At a chosen Mach number, diffuser pressure recovery was read from Fig. 4. Minimum allowable combustor pressure was divided by the diffuser recovery to determine engine inlet total pressure.

$$\frac{H_2}{\eta_D} = H_0$$

where

H_0 = ambient total pressure, psfa
H_2 = combustor inlet total pressure, psfa
η_D = diffuser pressure recovery

Pressure ratio for the chosen Mach number was read from Mach number function tables (Reference 2) and ambient altitude pressure was calculated by use of the equation

$$H_0 \times \frac{p_0}{H_0} = p_0$$

where

p_0 = ambient static pressure, psfa

Altitude was determined by interpolation using a table of NACA standard properties of the atmosphere (2).

Maximum altitudes which should be simulated in the altitude facility at various Mach numbers were thus determined on this basis for the range of Mach numbers considered.

Ramjet research which results in increased diffuser pressure recovery or lower minimum combustor pressures would raise the maximum operating altitude of the ramjet.

Test Methods

Fig. 5 shows three methods in use for engine development testing. Direct-connect burner testing is used for preliminary phases of engine development and produces the least severe test facility requirements. Ducted-nozzle testing with choked inlet is a new and not yet universally accepted test method. Research is yet to be accomplished before it can produce completely acceptable test results for supercritical engine operating conditions. Free jet testing produces satisfactory inlet simulation and allows engine control system testing and diffuser-combustor matching studies. Each engine inlet simulation method may be used with sufficient pressure ratio across the engine exhaust nozzle to establish critical flow at the minimum area section of the nozzle, or ambient altitude pressure may be maintained at the engine outlet. Ambient-altitude exhaust pressure permits tests with variable geometry and fully expanded exhaust nozzles with ejectors. Ducted-nozzle and free jet test methods with choked engine exhaust nozzle and ambient altitude exhaust pressures were analyzed.

Facility Performance

Air flows presented in this paper are for the purpose of comparing facility requirements for different types of testing and are for an engine having a combustion chamber cross-sectional area of 1 sq ft. Prediction of changes in ramjet engine size, and therefore test facility capacity, requires study of ramjet component research results. At a fixed flight Mach number and L/D ratio for a missile, engine size would increase with increased altitude. As combustion and diffuser research produce the capability for high altitude operation of ramjets, engine size will increase.

Static pressure and temperature for operating conditions shown in the typical operating envelope in Fig. 1 were taken from NACA Standard Altitude Tables (2). Ambient total pressures and temperatures at each operating condition were calculated from the static values and the Mach number-pressure ratio-temperature ratio relations in (2). Engine air flow at each operating condition was determined in the following manner:

1 A burner inlet Mach number of 0.2 was assumed. This combustor inlet Mach number was assumed based on the fact that momentum pressure losses in a ramjet burner increase as burner inlet Mach number increases, and because it becomes very difficult to attain reasonable combustion efficiencies at high altitudes and high burner inlet Mach numbers.

2 Burner inlet total pressure was determined by multiplying ambient total pressure for each test condition by the diffuser pressure recovery shown in Fig. 4.

3 Burner inlet total temperature was assumed to be equal to ambient total temperature.

4 Burner inlet static pressure and temperatures were determined from the total pressure and temperature and Mach number-pressure ratio-temperature ratio relations presented in (2).

5 Air flow was calculated by use of the equation

$$W_a = p_2 A_2 M_2 \sqrt{\frac{\gamma g}{R t_2}}$$

where

p_2 = static pressure at combustor inlet, psfa
A_2 = combustor area, ft², assumed to be 1 in this study
M_2 = combustor inlet Mach number, 0.2
γ = ratio of specific heats, 1.4
g = gravitational constant, 32.2 fps²

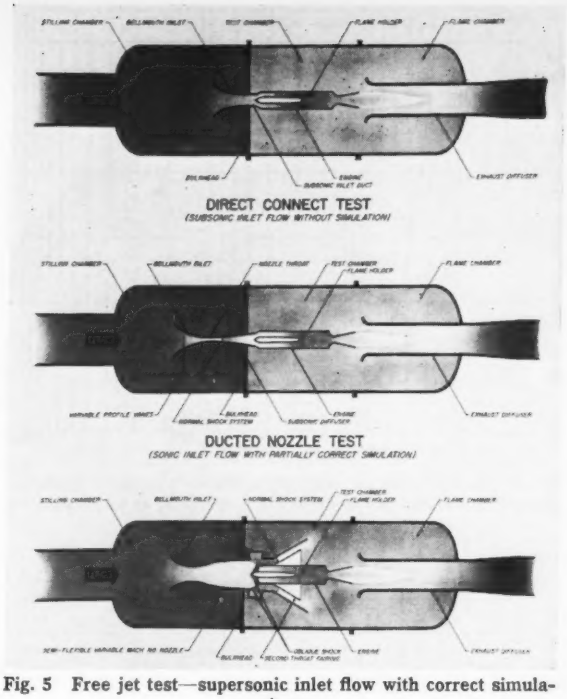
DIRECT CONNECT TEST
(SUBSONIC INLET FLOW WITHOUT SIMULATION)
DUCTED NOZZLE TEST
(SONIC INLET FLOW WITH PARTIALLY CORRECT SIMULATION)

Fig. 5 Free jet test—supersonic inlet flow with correct simulation

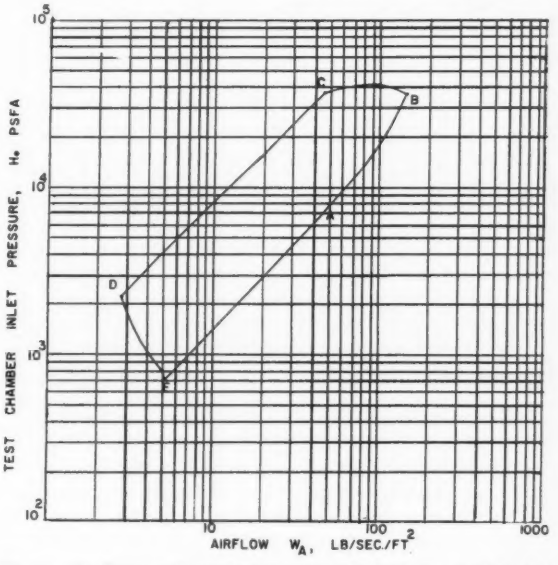

Fig. 6 Air flows and supply pressures required to simulate test conditions outlined by typical operating envelope ramjet, ducted nozzle test

R = gas constant for air, 53.3 ft lb/°R
t_2 = static temperature at combustor inlet, °R

Test chamber inlet total pressure as a function of air flow for ramjet ducted nozzle testing is shown in Fig. 6. Ambient total pressure was presented because testing with a ducted nozzle results in losses in the ducted nozzle which are equivalent to those which would occur in the ramjet diffuser. Letters shown on the curve in Fig. 6 correspond to those shown in Fig. 1 and permit correlation of the air flow and pressure requirements with Mach number and altitude. Maximum

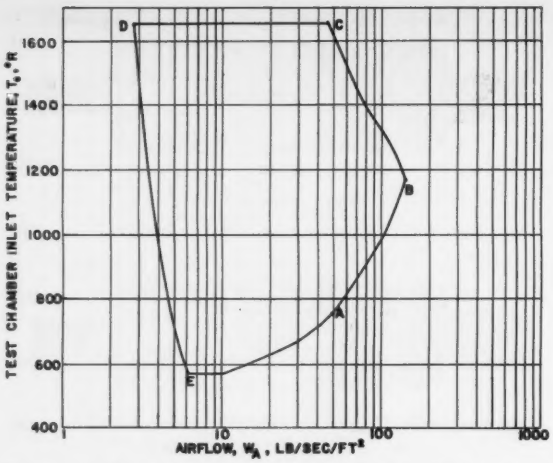

Fig. 7 Air flows and air supply temperatures required to simulate test conditions outlined by typical operating envelope ramjet, ducted nozzle test

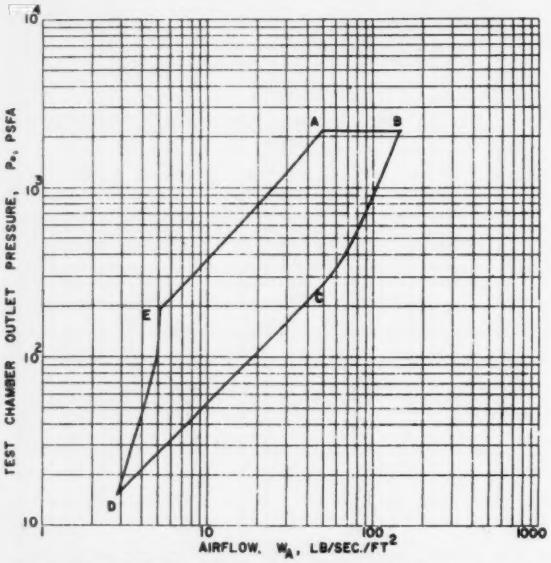

Fig. 8 Air flows and exhaust pressures required to simulate test conditions outlined by typical operating envelope—ramjet with ambient altitude exhaust pressure, ducted nozzle test

air flow required is about 142 lb/sec per sq ft of engine cross section area at a pressure of 36,200 psfa.

Test chamber inlet temperature is shown as a function of air flow for ducted-nozzle testing of the ramjet in Fig. 7. Maximum temperature required is about 1650 R at an air flow of 46 lb/sec. Temperature required at the maximum air flow condition of 142 lb/sec is 1165 R.

Test chamber exhaust pressure as a function of engine air flow for ducted-nozzle testing is presented in Fig. 8. This figure presents ambient altitude exhaust pressure. Ambient altitude pressure at the highest altitude considered is about 15 psfa, and engine air flow for operation at that altitude is 2.8 lb/sec per sq ft of engine cross-section area.

In order to determine exhaust pressure required to maintain critical pressure ratio across the ramjet engine exhaust nozzle, the total pressure losses through the ramjet downstream of the inlet diffuser were determined as follows:

1 A representative value of pressure drop for gutter flameholder of $2q$ was assumed.

2 A burner outlet temperature of 4000 R was assumed for all cases except those in which the engine outlet Mach number reached a value of 1 with no contraction in the exhaust nozzle. For these cases, temperature ratio required to produce choking at the burner outlet with no contraction was used.

3 A total pressure loss of 2 per cent due to losses in the engine exhaust nozzle was assumed.

4 Above values of temperature ratio were used with the assumed combustor inlet Mach number to calculate momentum pressure loss across the ramjet combustor.

Total pressure ratio H_5/H_2 across the ramjet burner including all of the losses discussed above are shown as a function of flight Mach number in Fig. 9. These burner pressure ratios were used with values of engine diffuser exit pressure to determine engine outlet total pressure at each flight condition on the envelope shown in Fig. 1. Test chamber outlet pressure required to maintain critical pressure ratio across the engine exhaust nozzle was determined by dividing engine outlet total pressure by two. Test chamber outlet pressure required to maintain critical pressure ratio across the engine outlet is shown as a function of air flow in Fig. 10. Maximum air flow at which exhausters are required is about 40 lb/sec per sq ft of engine cross section. Minimum exhaust pressure required is about 250 psfa at an air flow of about 5.2 lb/sec per sq ft of engine cross section.

Air supply requirements are the same for ducted-nozzle testing with ambient altitude exhaust and with choked engine outlet exhaust pressures. At an air flow of 2.8 lb/sec the exhaust pressure is 15 psfa for ambient altitude exhaust and 295 psfa for choked engine outlet testing. These two pressure levels indicate the difference in exhauster pressure ratio required for the two types of testing. Maximum volume flow through the exhausters for the choked engine outlet testing occurs at the minimum Mach number high altitude operating condition (E) rather than the maximum Mach number high altitude condition and is about $^1/_9$ as large as for ambient altitude exhaust.

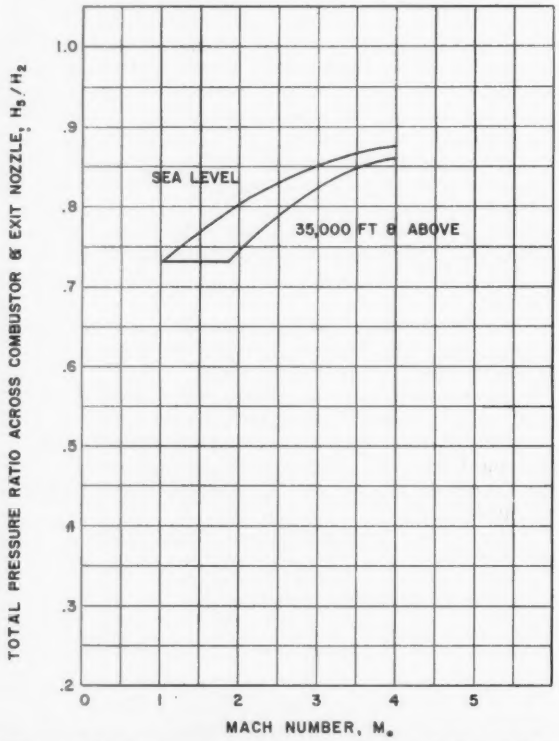

Fig. 9 Internal pressure losses in a ramjet exclusive of inlet diffuser losses

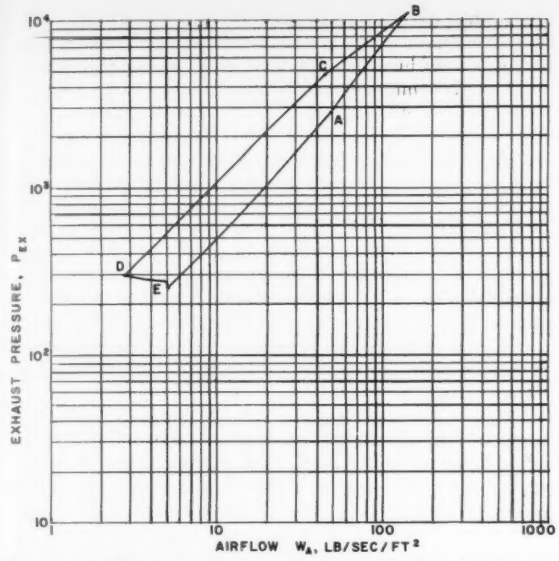

Fig. 10 Air flow and exhaust pressures required to simulate test conditions outlined by the typical operating envelope—ramjet with choked exhaust nozzle, ducted nozzle test

Free jet test facility requirements were based on the envelope shown in Fig. 1. Engine pressure losses and air flow requirements discussed for the ducted-nozzle test in this report were used in the free jet study.

Inlet total pressure and temperature required for free jet testing a ramjet engine throughout the operating envelope are the same as those required for ducted-nozzle tests. Air flow requirements for free jet testing the ramjet were determined in the following manner:

1 Engine air flow was taken from the ducted-nozzle calculations for each of the engine operating points. Free stream area through which this air flow would pass was obtained from

$$A_0 = \frac{W_a}{\rho_0 V_0}$$

where

A_0 = free stream or cowl lip area, ft²
W_a = engine air flow, lb/sec
ρ_0 = ambient density at the altitude at the operating condition chosen, lb/ft³
V_0 = velocity corresponding to the Mach number and altitude at the operating condition chosen, fps

2 Free stream or cowl inlet area as a function of Mach number is shown in Fig. 11. Cowl inlet area of the ramjet engine inlet is larger than the combustion chamber at Mach numbers above about 3.8 for the combustor Mach number and diffuser pressure recovery assumed in the calculations. An inlet area equal to the combustor area was used for determination of free jet testing requirements at Mach numbers above 3.8. A lower combustor inlet Mach number would, because of this assumption, exist in the ramjet at flight Mach numbers above 3.8.

3 Free jet nozzle exit dimension was then determined by using a value of about 50 per cent spill air flow for the high Mach number free jet test installation. Free jet tests have been run at high Mach numbers with spillage air flow as low as 35 per cent but these were tests in which the free jet nozzle exit was shaped to match the engine inlet, thereby precluding use of a variable Mach number free jet nozzle. Also, use of the figure of about 50 per cent spillage is justified by the need of tests at angle of attack. Justification of a much larger

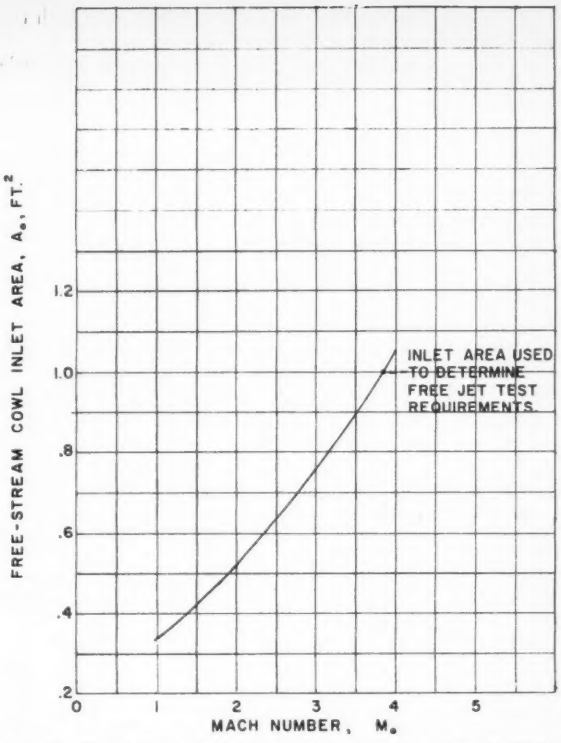

Fig. 11 Ramjet cowl inlet lip area as a function of flight Mach number

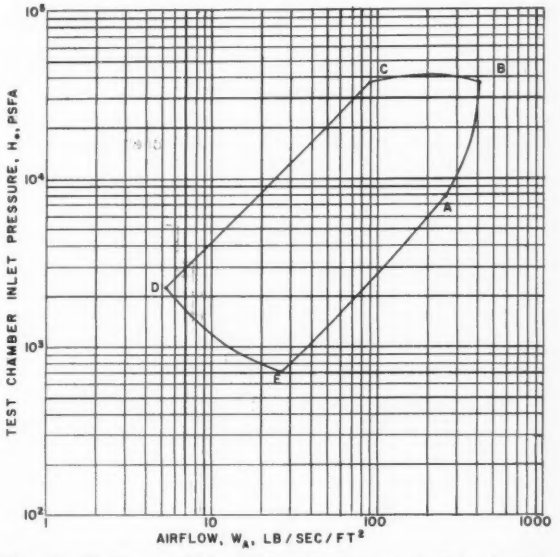

Fig. 12 Air flows and air supply pressures required to simulate test conditions outlined by typical operating envelope with free jet nozzle

spillage could have been made on the basis of the requirement for subcritical engine and control system testing. The maximum engine inlet area was doubled to arrive at a free jet nozzle exit area and further calculations are based on operating a constant outlet area-variable Mach number free jet nozzle over the range of conditions shown in Fig. 1. It was concluded that in the event it is necessary to test engines having asymmetric inlets in an altitude facility, a free jet

nozzle having the correct outlet area would be built with the proper exit dimensions for purposes of economy.

4 Air flow required for operation of the free jet nozzle was determined by use of the equation

$$W_a = A_N p_0 M_0 \sqrt{\frac{\gamma_0}{R t_0}}$$

where

A_N = nozzle exit area, ft²
p_0 = ambient static pressure, psfa
M_0 = flight Mach number
t_0 = ambient static temperature, °R

and other symbols are as previously presented.

Altitude facility air supply pressure is shown as a function of air flow for free jet testing in Fig. 12. A maximum air flow of about 412 lb/sec per sq ft of engine cross section at a pressure of 36,200 psfa is required. At an air flow of 26.5 lb/sec, inlet pressure as low as 710 psfa is required. These data show that use of a given size free jet nozzle which would permit tests of high Mach number engines over the complete range of Mach numbers results in a requirement for a broader range in air supply capacity. For instance, point *B* on the operating envelope represents Mach number 2.5 at sea level. The curve in Fig. 11 showed that at this lower Mach number the design engine inlet area would be about 65 per cent of the maximum value. Stated in other words, if the engine inlet, and the free jet nozzle, were to be tailored for operation at each Mach number, the maximum facility air flow would be 268 lb/sec for each square foot of engine cross section instead of 412 lb/sec. Comparison of maximum air flow for free jet testing on this figure with maximum air flows for ducted-nozzle testing previously presented shows that the free jet air flow is about three times the ducted-nozzle air flow for a given size engine.

Altitude facility air supply temperature is presented as a function of air flow for free jet testing in Fig. 13. Maximum temperature is required at an air flow of 89 lb/sec per sq ft of engine area. Temperature required at maximum air flow of 412 lb/sec is about 1165 R. The fact that maximum temperature is required only at air flows less than maximum shows the possibility of economizing on air heater capacity.

Test chamber exhaust pressures required for altitude facility free jet testing with ambient-altitude static pressure downstream of the free jet nozzle exit and the engine outlet are shown as a function of facility air flow in Fig. 14. Minimum test chamber exit pressure required for ambient altitude free jet testing is the same as the minimum pressure required for ambient altitude ducted-nozzle testing. Maximum air flow for free jet testing is about three times that required for ducted-nozzle testing.

Severity of the facility equipment requirements to maintain ambient static pressures in the test cell will probably

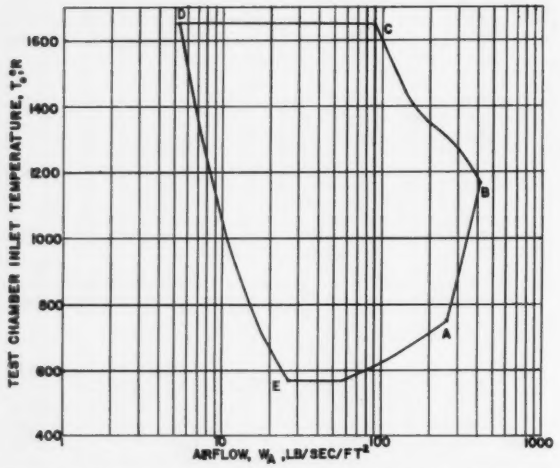

Fig. 13 Air flow and air supply temperatures required to simulate test conditions outlined by the typical operating envelope with free jet

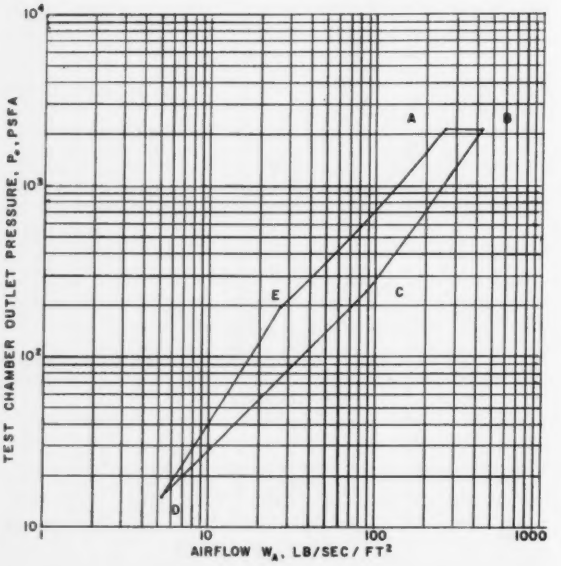

Fig. 14 Air flows and exhaust pressures required to simulate test conditions outlined by the typical operating envelope with free jet nozzle and ambient altitude exhaust pressure

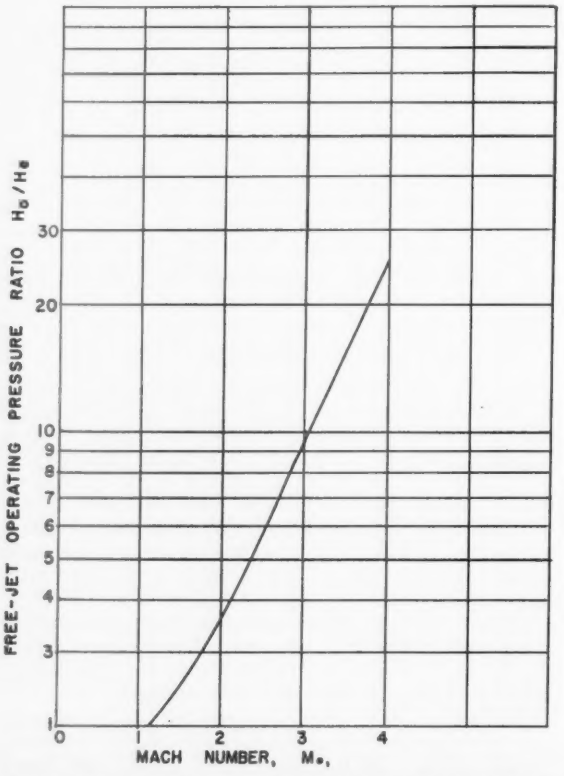

Fig. 15 Pressure ratio required to operate free jet test installations using two-dimensional variable Mach number nozzle

cause economic considerations to dictate use of test installation recovery devices.

Test chamber exit pressures for free jet test installations using second throat apparatus were calculated by use of the data presented in Fig. 15, and the free jet nozzle exit total pressures. Data presented in Fig. 15 were obtained experimentally with a variable Mach number free jet test installation. Exhaust pressure required for satisfactory free jet installation operation as a function of air flow is presented in Fig. 16. Minimum exhaust pressure required is 90 psfa compared with 15 psfa for ambient altitude free jet testing and 250 psfa with choked engine outlet ducted-nozzle testing. Air flow at the minimum exhaust pressure condition for free jet testing with both ambient exhaust pressure and second throat recoveries is 5.2 lb/sec compared to 3.04 lb/sec for ambient altitude ducted-nozzle testing, and 5.1 lb/sec for choked engine outlet ducted-nozzle testing. Taking choked engine outlet ducted-nozzle exhauster volume requirements as one, then volume requirements for ducted-nozzle ambient altitude testing would be about 9, for free jet testing with second throats about 4.5, and free jet ambient altitude testing about 17.

It is clear that the cost of facility equipment must be balanced against the relative advantages of ambient exhaust pressure testing. Factors such as greater facility utilization and decreased complexity and cost of test installations may compensate for the very large exhauster systems involved.

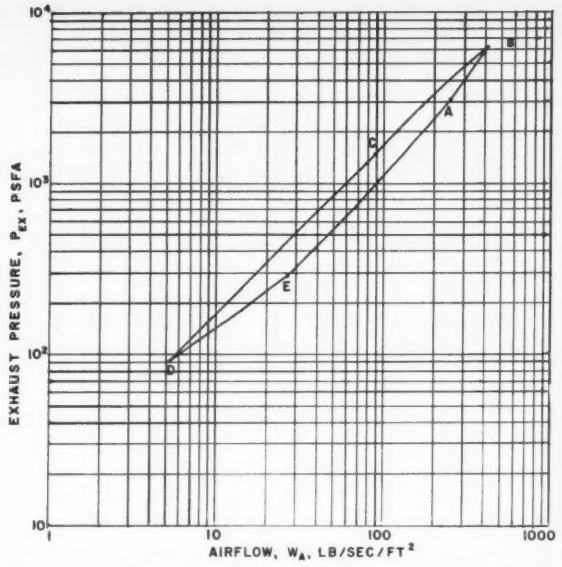

Fig. 16 Air flows and exhaust pressures required to simulate test conditions outlined by the typical operating envelope with free jet nozzle and second throat

Summary

From this analysis, it was concluded that the successful ramjet facility planner should continuously monitor ramjet research and development progress and try to anticipate the direction and magnitude of that progress so as to satisfactorily anticipate requirements for ramjet test facilities. Improvements in performance of ramjet inlets, combustors, fuels, tailpipes, as well as structural design, can produce major changes in the range of operation over which ramjets offer the best over-all performance potential. Research on ducted-nozzle testing and modified free jet testing may show that ramjet test facilities would require air supply and exhauster equipment greatly different from that currently considered necessary for such facilities.

References

1 Avery, William H., "Twenty-Five Years of Ramjet Development," JET PROPULSION, vol. 55, Nov. 1955, pp. 604–614.

2 Staff of the Ames 1- by 3-ft supersonic wind-tunnel section, "Notes and Tables for Use in the Analysis of Supersonic Flow," NACA TN 1428, Dec. 1947.

Spreading of Supersonic Jets From Axially Symmetric Nozzles

C. J. WANG[1] and J. B. PETERSON[2]

The Ramo-Wooldridge Corporation, Los Angeles, Calif.

This paper contains a formulation of the method of characteristics for computing the flow field in a supersonic jet. The method is programmed on an ERA-1103 computer. Nine of the cases calculated are reported in this paper. These cases represent jets issuing from two types of nozzles at various Mach numbers into a still or moving medium at a wide range of pressures. Different values of the ratio of specific heats of the gas have been assumed. Results include the effects of various parameters on the jet-spreading characteristics.

Presented at the ARS Semi-Annual Meeting, San Francisco, Calif., June 10–13, 1957.

[1] Head, Rocket Propulsion Systems, Space Technology Laboratories. Mem. ARS.

[2] Analyst, Space Technology Laboratories. Mem. ARS.

Nomenclature

b = defined by Equation [3c], boundary point
r = radial distance
A = defined by Equation [3a]
B = defined by Equation [3b]
C = defined by Equation [3d]
M = Mach number
P = pressure
R = radial distance
S = entropy divided by specific heat at constant pressure
U = defined by Equation [4a]
V = defined by Equation [4b]
W = velocity divided by maximum velocity; subscript 1 is before shock, subscript 2 is after shock
X = axial distance
α = initial condition points at nozzle exit

β = points on the singularity of the Prandtl-Meyer expansion
γ = ratio of specific heats
ϵ = nozzle area ratio
ζ = defined by Equation [7d]
η = defined by Equation [7c]
θ = flow angle measured from axis
θ_2 = defined by Equation [4d]
κ = defined by Equation [7b]
λ = defined by Equation [7a]
μ = Mach angle
ν = Prandtl-Meyer angle
ϕ = angle of shock with respect to upstream flow velocity

Subscripts

e = exit
b = boundary
c = chamber
t = stagnation
∞ = free stream
0 = refers to nozzle exit radius
RM = point where the boundary has a maximum value of radius
$\theta/2$ = point on boundary where θ is equal to one half its initial boundary point value

Introduction

KNOWLEDGE of the flow field of an axisymmetric supersonic gas jet has recently become important in the consideration of some jet propulsion problems. These problems include cooling the structures adjacent to or within the jet, and transmitting communication signals through the jet.

While it is difficult to obtain experimental data of jet spreading under high altitude pressures, the method of characteristics presents itself as a convenient tool for the theoretical calculation of the jet properties at any pressure. Furthermore, the effect of a supersonic external stream on the jet characteristics can be included in the calculation by properly determining the pressure variation on the jet boundary under interaction with the external stream.

For a gas jet the flow conditions at the nozzle exit are determined by the nozzle geometry and can be considered as initial conditions which are already known and from which the calculation of the jet can be started. The necessary boundary conditions are provided by the assumption of axisymmetry and the fact that the boundary is under pressure equilibrium with the surrounding medium. The only gas property needed in the calculation is the ratio of specific heats, gamma. In the usual temperature range of most supersonic jets, gamma can be assumed constant. With the initial conditions, the boundary conditions and gamma all given, the method of characteristics can be readily applied to calculate the jet flow field until a shock is encountered. The shock is to be handled by using a separate set of equations.

The finite-difference characteristic equations, as well as the machine programming and the equations for the shock wave, are given in this paper. The method of characteritics is programmed on an ERA-1103 computer. The computation can be carried out rapidly. The cases calculated include both the conical and the bell-shaped nozzle types; four exit Mach numbers, namely 2, 3, 4 and 5; three gamma values, namely 1.15, 1.25 and 1.35; a range of exit pressure to ambient pressure ratios from 2.8 to 6000; and three external stream Mach numbers, namely 4, 5 and 6. In all the cases the calculation was stopped before the shock caused difficulties in the isentropic computation. This was done because from consideration of a number of engineering problems it was concluded that the jet field would be of practical interest only in the vicinity of the nozzle exit. The calculation is carried out in most cases to at least 10 diam downstream.

It should be pointed out that the method of characteristics has its limitations. First, it does not consider the mixing between the jet and its surrounding medium. Second, the method of characteristics is based on a continuum theory.

[3] Numbers in parentheses indicate References at end of paper.

The book by Pai (1)[3] contains extensive references on supersonic jets.

Mathematical Formulation

Flow Variation Along Characteristic Lines

The supersonic flow equation, being of the hyperbolic type, has two families of real characteristics. Characteristics of the first family (left running) form an angle $(\theta + \mu)$ with the positive x-axis, where θ and μ are the local velocity angle and Mach angle, respectively. Characteristics of the second family (right running), on the other hand, form an angle $(\theta - \mu)$ with the positive x-axis. The characteristics have the property that the variations of flow properties along these lines are described by differential equations of the first order (2, Equations 512 and 513). These equations are given below in the difference form.

First Family

$$\Delta\theta = A\Delta M - B\Delta X + C\Delta S \quad [1]$$

Second Family

$$\Delta\theta = -A\Delta M + b\Delta X - C\Delta S \quad [2]$$

The various coefficients are defined as

$$A = \frac{\sqrt{M^2 - 1}}{M\left(1 + \frac{\gamma - 1}{2}M^2\right)} \quad [3a]$$

$$B = \frac{1}{(\sqrt{M^2 - 1}\cot\theta - 1)r} \quad [3b]$$

$$b = \frac{1}{(\sqrt{M^2 - 1}\cot\theta + 1)r} \quad [3c]$$

$$C = \frac{\sqrt{M^2 - 1}}{(\gamma - 1)M^2} \quad [3d]$$

The notation ΔS is dimensionless entropy change, and is defined by

$$\Delta S = \frac{\text{entropy change per lb m}}{C_p \text{ per lb m}}$$

When $r = 0$, it can be shown (3, p. 680) that Equation [1] takes the form

$$\Delta\theta = \tfrac{1}{2}(A\Delta M + C\Delta S) \quad [1a]$$

Flow Change Across Shock

Let subscript 1 denote the flow immediately upstream of the shock and subscript 2 denote the flow immediately downstream. If ϕ is the angle of shock with respect to the upstream flow velocity, the following equations can be used to calculate the downstream flow

$$U_2 = W_1 \cos\phi \quad [4a]$$

$$V_2 = W_1 \sin\phi \frac{\gamma - 1}{\gamma + 1}\left[\left(\frac{1}{W_2} - 1\right)\csc^2\phi + 1\right] \quad [4b]$$

$$W_2 = (U_2^2 + V_2^2)^{\frac{1}{2}} \quad [4c]$$

$$\theta_2 = \theta_1 + \phi - \arctan\frac{V_2}{U_2} \quad [4d]$$

The entropy increase across shock is given by

$$\Delta S = \left\{-\frac{\gamma + 1}{\gamma}\ln(\gamma + 1) - 2\ln(M_1\sin\phi) + \ln[2 + (\gamma - 1)(M_1\sin\phi)^2] + \frac{1}{\gamma}\ln[2\gamma(M_1\sin\phi)^2 - (\gamma - 1)]\right\} \quad [5]$$

Flow Around Nozzle Edge

The gas expands around the nozzle edge when leaving an underexpanded nozzle. For a sharp edge, the expansion at the edge follows Prandtl-Meyer solution exactly. Away from the edge, the flow is governed by the three-dimensional flow equations. For simplicity, a sharp nozzle edge is assumed for all the cases investigated.

Treatment of the External Stream

When a jet issues into atmosphere which is still with respect to the rocket, it may be assumed that the pressure on the jet boundary is constant and equals the atmospheric pressure. When the rocket is in motion, however, the jet boundary is no longer under a constant pressure and the interaction between the jet and the external stream must be determined in order to know the conditions at the jet boundary. In general, the determination of the interaction is not simple. However, if the Mach number range of the external stream is sufficiently high, the solution may be simplified by using some hypersonic approximation.

In practical considerations, it turns out that when the jet spreading becomes significant, which is normally at high altitude, the rocket speed is usually in or near the hypersonic range. Therefore, it appears justified to assume a hypersonic external stream in the present investigation. Under this assumption, the corpuscular theory of Newton, for example, will then be applicable and will greatly simplify the analysis of the interaction problem.

According to the Newtonian approximation, the local boundary slope of a body in a hypersonic stream is sufficient to determine the pressure on the boundary at the point and its neighborhood. This pressure, by isentropic relationship, is sufficient to further determine the local boundary Mach number of the jet flow. Knowing the Mach number, the characteristic equations will give a corresponding flow direction. This direction can be taken as the direction of the flow at the next boundary point. Thus the above procedure can be repeated.

The corpuscular theory (4) is represented by

$$\frac{P_b}{P_\infty} = \gamma_\infty M_\infty^2 \sin^2\theta + 1 \qquad (\theta > 0) \quad \ldots\ldots [6]$$

where P_b and P_∞ are the boundary pressure and the free stream pressure, respectively, M_∞ the free stream Mach number, γ_∞ the specific heats ratio of the external stream, and θ the local angle of the jet boundary with respect to the free stream. In the present investigation the free stream is assumed parallel to the jet axis.

Program of Numerical Computation

The numerical computation program employed in this investigation is briefly described here. Only essential features are given, since details of any program vary, depending on the taste of its programmer.

Input Data

The nozzle exit flow is represented by several discrete data points α in Fig. 1. Five pieces of information are given at each data point, namely X, r, M, θ and S. The α points may be on a spherical surface in the case of conical exit flow, may be on a plane in the case of a uniform parallel exit flow, and may be points after a shock.

The data also include the external flow properties M_∞, P_∞ and γ_∞. The jet gas properties to be included in the data are the ratio of specific heats γ, the boundary total pressure P_t, and the boundary Mach number M_{b0} to which the gas expands around the exit corner to reach a pressure equilibrium with the external stream.

In case the jet issues into still atmosphere, a constant Mach number M_b is stored in place of M_{b0} and it applies everywhere on the boundary.

Calculation of Corner Flow

The expansion of the flow at α_0 around the exit corner to the given boundary Mach number M_{b0} or M_b can be considered as consisting of many small steps. During each step the stream line turns through a small angle and gains an increase in Mach number according to the Prandtl-Meyer flow. Thus the points β_1, β_2 . . . are obtained as new data points. The point $\beta_0 = \alpha_0$ is given. From each β a characteristic can be started.

Simplifying Notations

In order to simplify the formulas to come up in the later sections, some new notations are introduced here.

$$\lambda = \tan(\theta - \mu) \quad \ldots\ldots [7a]$$

$$\kappa = \cot(\theta + \mu) \quad \ldots\ldots [7b]$$

$$\eta = (M^2 - 1)^{-1/2} \quad \ldots\ldots [7c]$$

$$\zeta = \tan\theta \quad \ldots\ldots [7d]$$

In addition to these, the notations defined in Equations [3a, b, c, d] are also to be frequently used.

In the following sections, difference equations are given which are essentially based on Equations [1, 2 and 1a].

Calculation of Interior Point from Two Noncentral Points

The unknown point 3 can be obtained from the two known points 2 and 1 by the following formulas (point 1 on left-running characteristic, 2 on right-running characteristic)

$$X_3 = \frac{X_1 + \kappa_1(r_2 - r_1 - \lambda_2 X_2)}{1 - \lambda_2\kappa_1} \quad \ldots\ldots [8]$$

$$r_3 = r_2 + \lambda_2(X_3 - X_2) \quad \ldots\ldots [9]$$

$$S_3 = S_1 + \frac{S_2 - S_1}{1 + \dfrac{X_3 - X_2}{X_3 - X_1}\kappa_1 \dfrac{M_1}{M_2}\sqrt{\dfrac{\lambda_2^2 + 1}{\kappa_1^2 + 1}}} \quad \ldots\ldots [10]$$

$$M_3 = \frac{-(\theta_1 - \theta_2) + A_1M_1 + A_2M_2 + B_1(X_3 - X_1) + b_2(X_3 - X_2) - C_1(S_3 - S_1) - C_2(S_3 - S_2)}{A_1 + A_2} \quad \ldots\ldots [11]$$

$$\theta_3 = \theta_1 + A_1(M_3 - M_1) - B_1(X_3 - X_1) + C_1(S_3 - S_1) \quad \ldots\ldots [12]$$

Calculation of Interior Point From One Central and One Noncentral Point

The unknown point 3 can be obtained from the two known

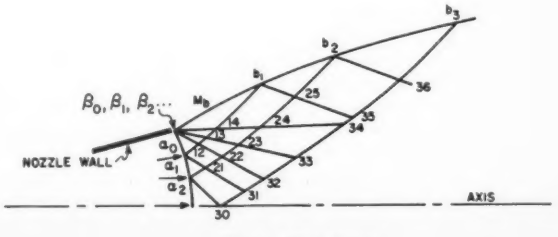

Fig. 1 Notations

points 1 and 2 by the following formulas, point 1 being on the axis

$$X_3 = \frac{-r_2 - \eta_1 X_1 + \lambda_2 X_2}{\lambda_2 - \eta_1} \quad [13]$$

$$r_3 = \eta_1 (X_3 - X_1) \quad [14]$$

S_3 by (10)

$$M_3 = \frac{-(\theta_1 - \theta_2) + A_1 M_1/2 + A_2 M_2 + b_2(X_3 - X_2) - C_1(S_3 - S_1) - C_2(S_3 - S_2)}{A_1/2 + A_2} \quad [15]$$

$$\theta_3 = \theta_1 + \tfrac{1}{2}[A_1(M_3 - M_1) + C_1(S_3 - S_1)] \quad [16]$$

Calculation of Boundary Point

The unknown point 3 can be obtained from the known points 1 and 2 by the following formulas, point 1 being on the boundary

$$X_3 = \frac{X_2 + \kappa_2(r_1 - r_2 - \zeta_1 X_1)}{1 - \zeta_1 \kappa_2} \quad [17]$$

$$r_3 = r_2 + \frac{1}{\kappa_2}(X_3 - X_2) \quad [18]$$

$$P_3 = P_\infty(\gamma_\infty M_\infty^2 \sin^2 \theta_1 + 1) \quad [19]$$

$$M_3 = \left\{ \frac{2}{\gamma - 1} \left[\left(\frac{P_{t3}}{P_3} \right)^{(\gamma - 1)/\gamma} - 1 \right] \right\}^{1/2} \quad [20]$$

$$\theta_3 = \theta_2 + A_2(M_3 - M_2) - B_2(X_3 - X_2) + C_2(S_3 - S_2) \quad [21]$$

The entropy S_3 is a constant along the boundary until a shock is encountered. The subscript t refers to the stagnation condition.

Calculation of Central Point

The unknown point 2 can be calculated from the known point 1 as follows

$$X_2 = X_1 - \frac{r_1}{\lambda_1} \quad [22]$$

$$r_2 = 0 \quad [23]$$

$$M_2 = M_1 + \frac{1}{A_1}\left[\theta_1 + b_1(X_2 - X_1) - C_1(S_2 - S_1) \right] \quad [24]$$

$$\theta_2 = 0 \quad [25]$$

Computing Procedure

The computing procedure is to a certain extent arbitrary. The procedure used in this investigation is briefly described below. Reference is made to Fig. 1.

1. Compute points β_1 and $\beta_2 \ldots \beta_n$ at the corner by the Prandtl-Meyer flow equation, the number of points depending on the mesh size desired.
2. Calculate interior points (12, 13, . . .) of the first left running characteristic $\alpha_1 b_1$.
3. Calculate the boundary point b_1.
4. Repeat steps 2 and 3 for all the left running characteristics which originate from the data points α until all the α are exhausted.
5. Calculate the central point 30.
6. Calculate the interior point 31.
7. Calculate all the remaining interior points (32, 33, . . .) on the characteristic 30-b_3.
8. Repeat steps 5, 6 and 7 for all the downstream characteristics until a shock is encountered, or until the computation is sufficiently far downstream.
9. In case the computation is stopped by a shock, locate the shock by tracing through the compression-wave crossings. Determine the flow downstream of the shock. Continue the calculation of flow by the method of characteristics essentially according to the foregoing procedure. Of course, the computation of corner expansion is to be omitted here.

Results

Cases Computed

In order to cover a reasonably wide range of operating conditions of the rocket jet, a total of nine computed cases is presented in this paper. The results of computation are plotted in equal number of figures showing equiproperty lines and streamlines. An index to these figures is provided in Table 1. Every equiproperty line is marked with a Mach number. The three streamlines shown in most of the figures are the boundary streamline, the axial streamline, and a typical streamline (dashed line) between these two.

Effect of External Stream

The effect of external stream is shown in Fig. 11 for various stream Mach numbers. It is seen that the jet boundary is squeezed in by the external stream. However, comparison of Figs. 5 and 10 and other cases (not given in this paper due to limited space) has led to the conclusion that the flow properties along the jet axis are practically unaffected by the external stream.

Effect of Ambient Pressure

The ambient pressure effect is illustrated in Fig. 12. It will be noted that, at a given station, $X/R_0 = 5$ in this case, the Mach number is a unique function of the distance R/R_0 irrespective of the pressure ratio P_e/P_b until the boundary is approached. Near the boundary, there is a sudden drop of the Mach number. The boundary itself, of course, flares out when the ambient pressure decreases.

Effect of Nozzle Type

Comparison of the curves in Fig. 13 quickly yields the conclusion that at a given distance from the exit, within the range of investigation, the jet from the conical exit always has larger radius than the jet from the parallel exit. This difference is amplified by increasing the pressure ratio P_e/P_∞ and the Mach number M_e. However, the Mach number distributions for the two nozzle types are not much different along the axis of the jet away from the exit.

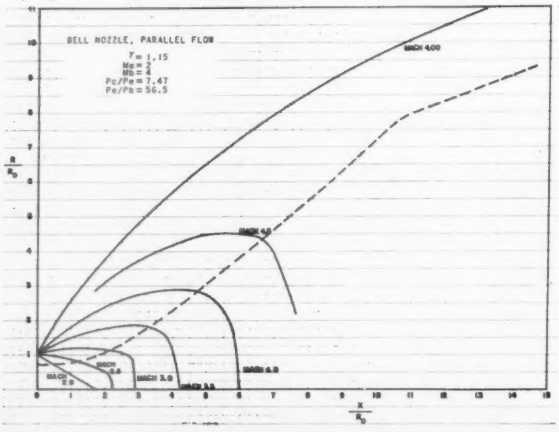

Fig. 2 Axial section of jet

Table 1 Summary of cases computed

Nozzle type: Parallel exit — Figure	Nozzle type: Conical exit No.	γ	ϵ	M_e	P_c/P_e	M_b	P_e/P_∞	M_∞
2	3	1.15	1.95	2	7.47	4.0	56.5	0
4	...	1.15	8.00	3	52.2	3.5	2.83	0
5	...	1.15	8.00	3	52.2	5.0	62.9	0
6	...	1.15	8.00	3	52.2	7.5	6080	0
7	8	1.15	230.6	5	3280	7.0	41.6	0
9	...	1.25	6.7	3.1	52.2	5.7	62.9	0
10	...	1.15	8.00	3	52.2	...	62.9	5

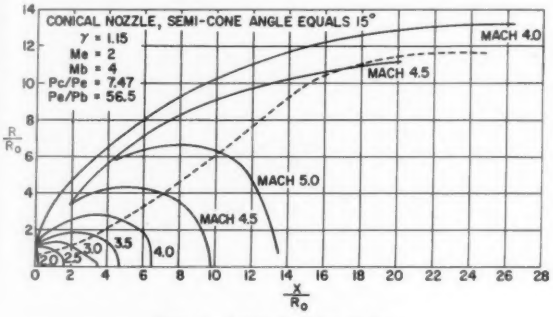

Fig. 3 Axial section of jet

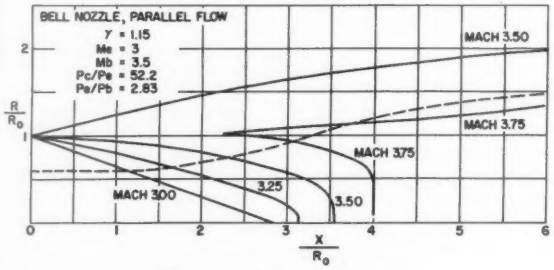

Fig. 4 Axial section of jet

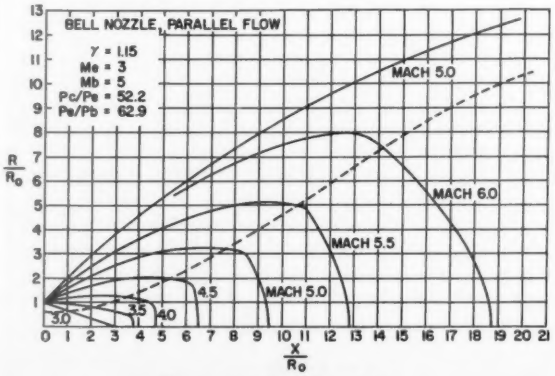

Fig. 5 Axial section of jet

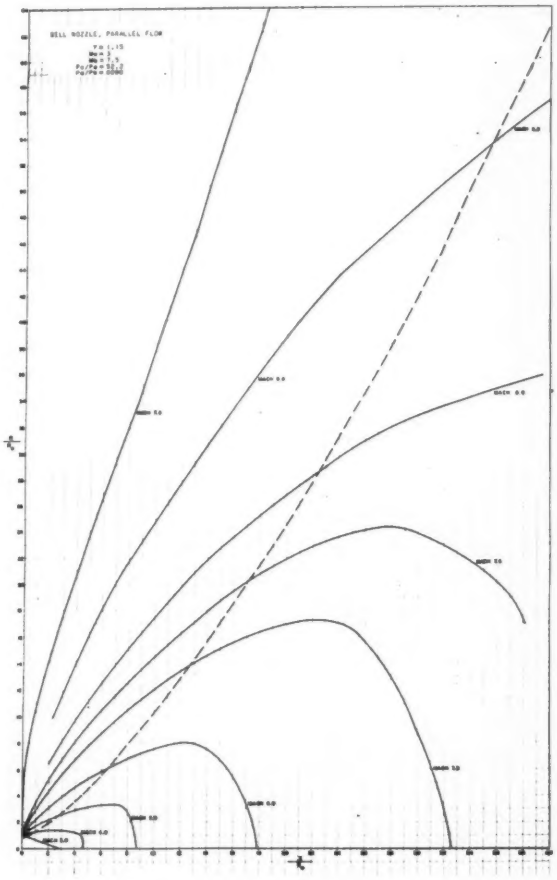

Fig. 6 Axial section of jet

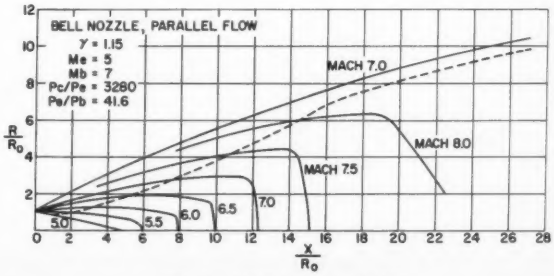

Fig. 7 Axial section of jet

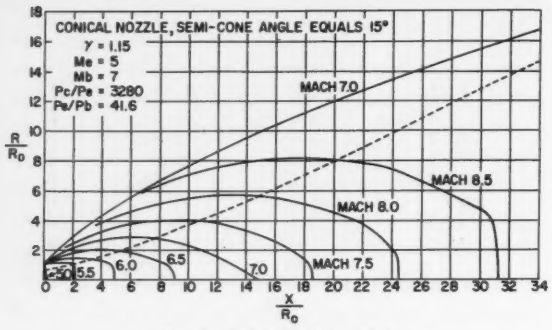

Fig. 8 Axial section of jet

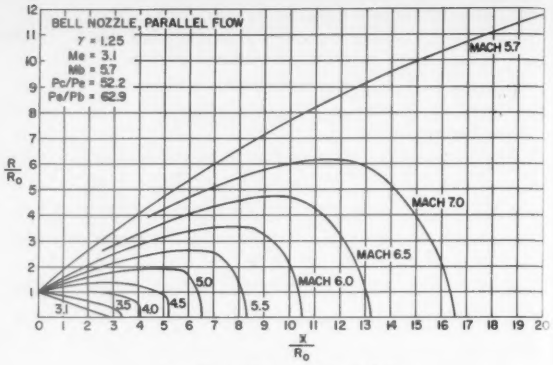

Fig. 9 Axial section of jet

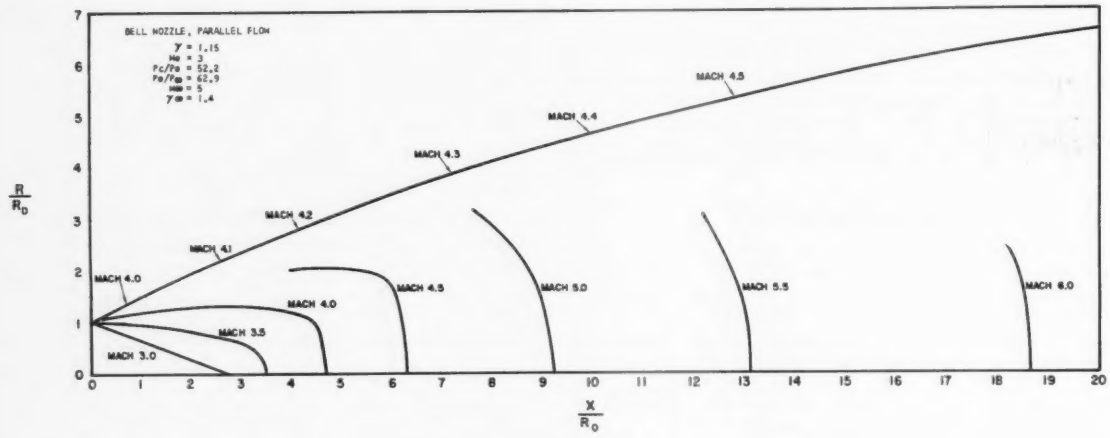

Fig. 10 Axial section of jet

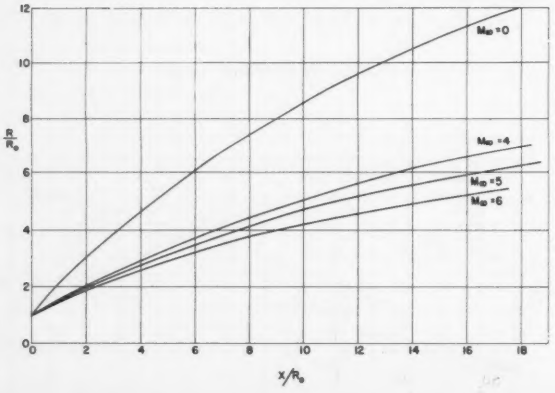

Fig. 11 Effect of external stream on jet boundary for constant P_∞/P_e

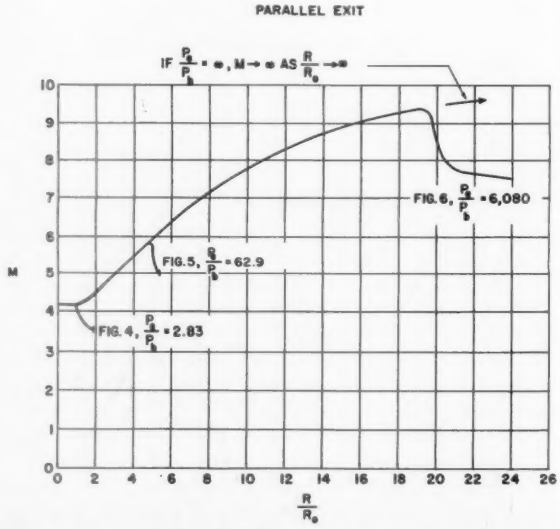

Fig. 12 M vs. R/R_0 for various P_e/P_b; $X/R_0 = 5$, $M_e = 3$, $\gamma = 1.15$

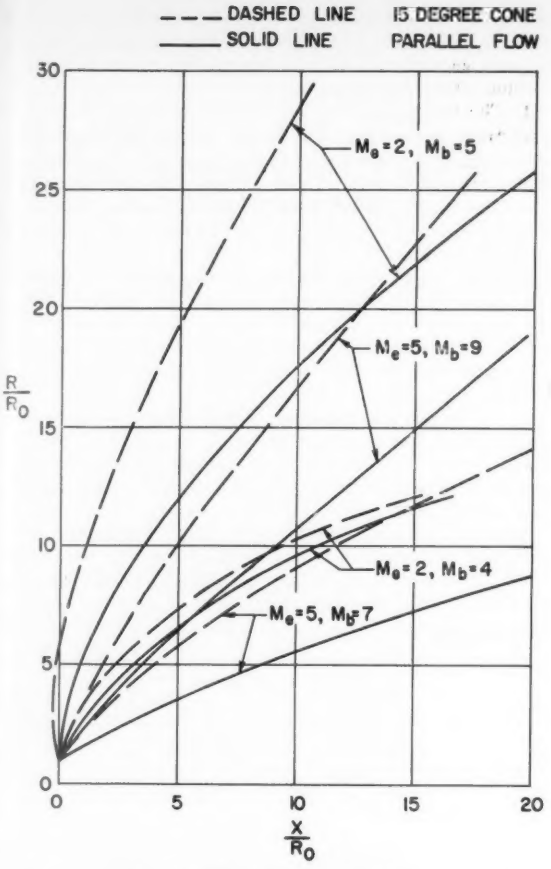

Fig. 13 Effect of nozzle types on boundary ($\gamma = 1.15$)

Effect of the Ratio of Specific Heats

The ratio of specific heats γ has a complex relationship with the nozzle area ratio ϵ, the Mach numbers M_e and M_b, and the pressure ratios P_c/P_e and P_e/P_∞. The first question involved in the study of γ effect is: What is to be kept constant in this study? Since the pressure ratios are known from the trajectory and are usually given as design conditions, it seems logical to investigate the γ effects on the basis of fixed pressure ratios. Results of this investigation are plotted in Figs. 14 and 15. It appears from Fig. 14 that at a given station the diameter of the jet is approximately proportional to the reciprocal of γ. Therefore the shape of the jet boundary given in this paper for $\gamma = 1.15$ can be used to estimate the jet boundary for other γ values. From Fig. 15, it can be noticed that for constant P_c/P_e and P_e/P_b the pressure distribution along the jet axis is not much affected by the value of gamma.

Investigation has also been carried out on the basis of fixed values of M_e and M_b. The conclusion is that for a given set of M_e and M_b, the jet spread rapidly becomes less diverged when the value of γ becomes larger. It should be pointed out, however, that under the condition of given Mach numbers, the area ratio ϵ and pressure ratios P_c/P_e and P_e/P_∞ vary rather rapidly with γ.

A Simplified Method for Predicting Jet Boundary

Curves are provided for getting an approximation to the jet boundary for $\gamma = 1.15$ and $M_\infty = 0$. Given the pressure ratios P_c/P_e and P_e/P_b, the two Mach numbers M_e and M_b and the two Prandtl-Meyer angles ν_e and ν_b can be determined. From Figs. 16 or 18, X_{RM/R_0} is determined from M_b which in turn determines R_{RM/R_0}. The two quantities

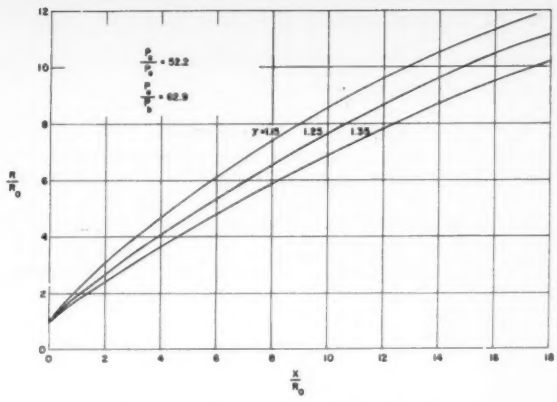

Fig. 14 Effect of γ on jet boundary

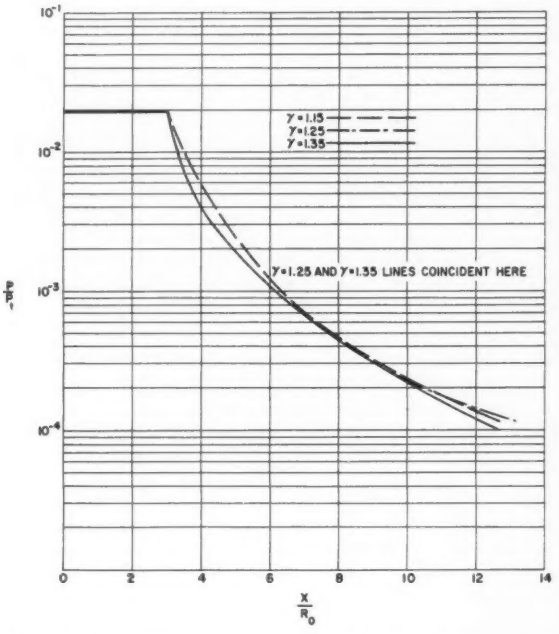

Fig. 15 Effect of γ on pressure on the jet axis; $P_c/P_e = 52.2$, $P_e/P_b = 62.9$

X_{RM/R_0} and R_{RM/R_0} are the coordinates of the boundary point where the jet radius is a maximum. Therefore a horizontal tangent to the curve is determined at this point. A tangent to the curve at the nozzle exit is obtained by adding the difference of the Prandtl-Meyer angles ($\nu_b - \nu_e$) to the wall angle of the nozzle exit. A third tangent to the curve is a line through point ($X_{\theta/2}/R_0$, $R_{\theta/2}/R_0$) with a slope equal to one half the initial angle. This point is obtaied from Figs. 17 or 18 by using the plot of M_b vs. $X_{\theta/2}/R_0$ and then the plot of $R_{\theta/2}/R_0$ vs. $X_{\theta/2}/R_0$. The curve is then drawn tangent to the three lines.

An example follows in which $M_e = 2$, $M_b = 3$, $\gamma = 1.15$ and the cone angle is 15 deg.

1) $\theta_{RM} = 0$

$$\frac{X_{RM}}{R_0} = 7.1 \qquad \text{from Fig. 16}$$

$$\frac{R_{RM}}{R_0} = 3.5 \qquad \text{from Fig. 16}$$

2) $\theta_{b0} = \nu_b - \nu_e + 15° = 69 - 33 + 15 = 51°$

$$X_{b0}/R_0 = 0, \quad R_{b0}/R_0 = 1$$

3) $\theta_{\theta/2} = \frac{1}{2}\theta_{b0} = 25.5°$

$$X_{\theta/2}/R_0 = 1.7; \quad R_{\theta/2}/R_0 = 2.3$$

Conclusions

1 The spread of a supersonic jet becomes significant at high altitudes. In general, the jet flow is rather complex and far from one-dimensional. However, with the computing program, it is a simple matter to calculate the flow if sufficient data are given as to the nozzle exit flow conditions, the gas property gamma, the pressure and the Mach number of the medium into which the jet issues.

2 The flow graphs reported in this paper cover a fairly wide range of operating conditions. A simplified method for predicting the jet boundary has also been derived on the basis of the calculated data. If for a particular application any doubt exists as to the applicability of these results, it is recommended that a special run be made on the computer for the particular case in question.

3 Other things being constant, an increase in divergence of the nozzle exit or in the pressure ratio P_e/P_∞ tends to increase the jet divergence; an increase in the exit Mach number or in the Mach number of the external stream tends to decrease the jet divergence; and an increase in the value of gamma tends to confine the jet.

4 When the jet boundary is under finite pressure, the highest Mach number region is usually somewhere in the core of the jet rather than at the boundary. Only when the boundary pressure is zero does the maximum Mach number exist at the boundary.

5 At a fixed point relative to the nozzle, the gas density is maximum when the jet boundary passes through the point.

6 In future work more emphasis should be put on gases with ratios of specific heats other than 1.15, and the computation should be carried beyond the shock.

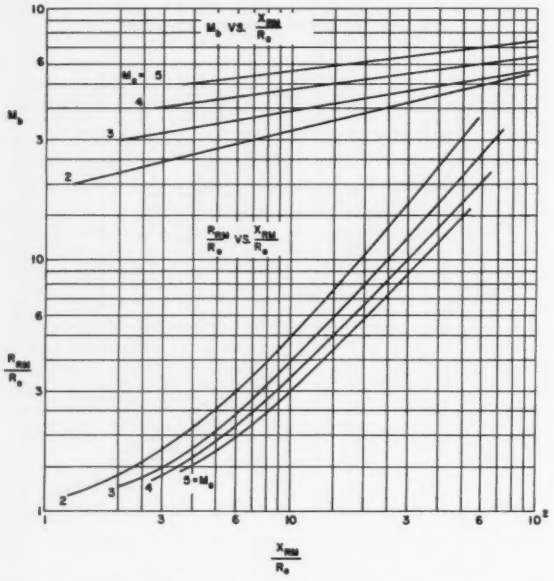

Fig. 16 Approximate jet boundary, 15-deg cone ($\gamma = 1.15$); M_b and R_{RM}/R_0 vs. X_{RM}/R_0

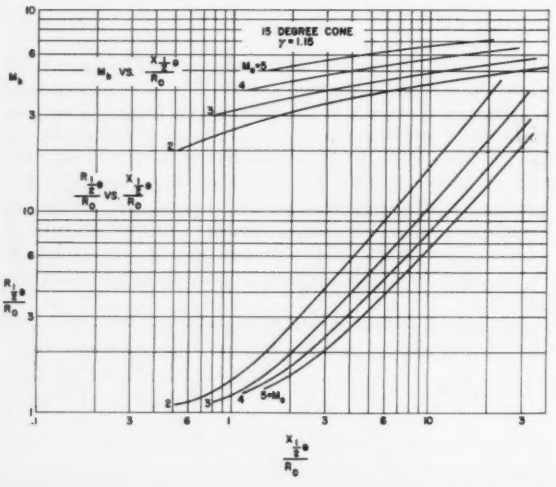

Fig. 17 Approximate jet boundary, 15-deg cone ($\gamma = 1.15$); M_b and $R_{\theta/2}/R_0$ vs. $X_{\theta/2}/R_4$

Acknowledgment

The work reported in this paper was initiated at the suggestion of H. R. Lawrence, associate director of aeronautical research and development at The Ramo-Wooldridge Corporation. The machine programming was carried out by Mrs. Janez Bordeaux.

References

1 Shih-I Pai, "Fluid Dynamics of Jets," Van Nostrand, 1954.

2 Ferri, Antonio, "Elements of Aerodynamics of Supersonic Flows," Macmillan, New York, 1949.

3 Shapiro, A. H., "Compressible Fluid Flow," Ronald Press, 1954.

4 Newton, Isaac, "Principia," University of California Press, 1950.

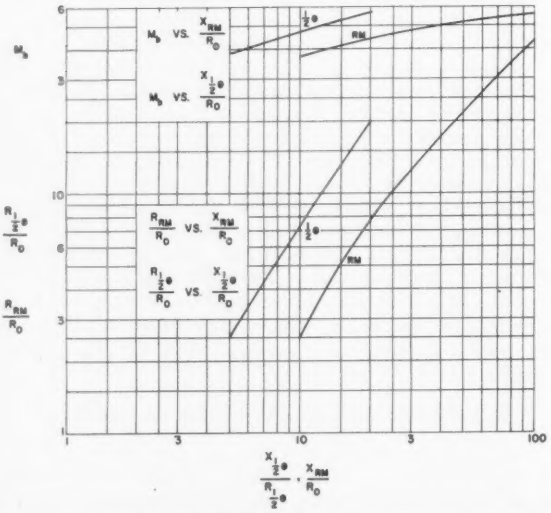

Fig. 18 Approximate jet boundary, uniform parallel flow ($\gamma = 1.15$, $M_e = 3$); M_b and R_{RM}/R_0 vs. X_{RM}/R_0, M_b and $R_{\theta/2}/R_0$ vs. $X_{\theta/2}/R_0$

Technical Notes

Vertical Re-entry into the Earth's Atmosphere for Both Light and Heavy Bodies

R. D. LINNELL[1]

Convair Division of General Dynamics Corp., San Diego, Calif.

Nomenclature

A = cross-sectional area of body, sq ft
C_D = drag coefficient, drag/$\frac{1}{2}\rho v^2 A$
E = function defined by Equation [5] and Table 1
g = acceleration of gravity, 32.174 fps^2
v = vertical re-entry velocity, positive downward, fps
W = weight of body, lb
y = altitude, ft
β = constant, ft^2/sec^2 (see Equation [2])
λ = $\beta/(W/C_DA)$, ft^4/lb sec^2
ρ = atmospheric mass density, slug/ft^3

Subscripts

B = conditions at base of an altitude interval of constant β
1 = conditions at top of an altitude interval of constant λ

A SOLUTION for the velocity of a body during vertical re-entry into the earth's atmosphere is presented. A piecewise-exponential density, a piecewise-constant drag coefficient and a constant acceleration of gravity are assumed. The solution involves use of a tabulated function of only a single variable.

Allen and Eggers (1)[2] give an equation for the velocity of a body re-entering an exponential-density atmosphere vertically under the influence of a constant drag coefficient and constant gravity acceleration. Their solution involves a series that converges slowly for some practical values of the parameters. A more tractable form is presented here for the more general case of a piecewise-exponential density and a piecewise constant drag coefficient.

The equation of motion is

$$v(dv/dy) = -g\{1 - (\rho v^2/2)/(W/C_DA)\} \quad [1]$$

where W/C_DA is assumed to be piecewise-constant. The piecewise-exponential density is given by

$$\rho = \rho_B \exp[-(y - y_B)g/\beta] \quad [2]$$

where the subscript B denotes the base of an altitude interval of constant β.

Using the density as the independent variable, Equation [1] becomes

$$dv^2/d\rho + \lambda v^2 = 2\beta/\rho \quad [3]$$

where $\lambda = \beta/(W/C_DA)$ is constant. The solution of Equation [3] is

$$v^2 = \{v_1^2 - 2\beta E(\lambda\rho_1)\} \exp[-\lambda(\rho - \rho_1)] + 2g(y_1 - y) \exp[-\lambda\rho] + 2\beta E(\lambda\rho) \quad [4]$$

where

$$E(\lambda\rho) = e^{-\lambda\rho} \int_0^{\lambda\rho} [(e^{+s} - 1)/s]\, ds \quad [5]$$

and the subscript 1 denotes conditions at the top of an interval of constant λ. The function E cannot be evaluated in closed form, but numerical values such as those given in Table 1 are easily obtained.

Table 1 Values of $E(\lambda\rho)$

$\lambda\rho$	$E(\lambda\rho)$	$\lambda\rho$	$E(\lambda\rho)$	$\lambda\rho$	$E(\lambda\rho)$
0.01	0.00995	0.2	0.1723	3.	0.4108
0.02	0.0197	0.3	0.2400	4.	0.3236
0.03	0.0294	0.4	0.2974	5.	0.2561
0.04	0.0388	0.5	0.3437	6.	0.2074
0.05	0.0482	0.6	0.3853	7.	0.1682
0.06	0.0574	0.7	0.4179	8.	0.1428
0.07	0.0664	0.8	0.4441	9.	0.1239
0.08	0.0753	0.9	0.4675	10.	0.1139
0.09	0.0841	1.0	0.4841	15.	0.0694
0.10	0.0927	2.0	0.4984	20.	0.0509

Equation [4] is valid for any altitude interval of constant λ. By applying the equation across each step of λ, several intervals of constant β can be used, in order to obtain a better representation of the atmospheric density. Similarly, several constant values of C_D, W or A can be used.

The accuracy of Equation [4] is quite good, as shown in Fig. 1 which presents the re-entry velocity for a body of $W/C_DA = 0.1$ falling from an altitude of 0.5×10^6 ft. The numerical solution was obtained by step-by-step integration of Equation [1], using the Model Atmosphere (2). The four-β atmosphere (3) shown in Table 2 was used with Equation [4].

Table 2 Approximate β atmosphere

y, ft	ρ_B, slug/ft^3	y_B, ft	β, ft^2/sec^2
0 to 0.05×10^6	2.377×10^{-3}	0	0.857×10^6
0.05×10^6 to 0.15×10^6	3.639×10^{-4}	0.05×10^6	0.695×10^6
0.15×10^6 to 0.25×10^6	3.564×10^{-6}	0.15×10^6	0.870×10^6
0.25×10^6 to 0.40×10^6	7.996×10^{-8}	0.25×10^6	0.633×10^6

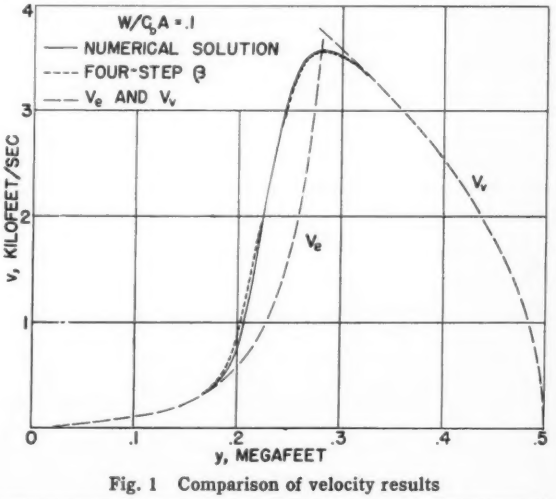

Fig. 1 Comparison of velocity results

Received Dec. 13, 1957.

[1] Staff Scientist, Scientific Research Laboratory. Mem. ARS.

[2] Numbers in parentheses indicate References at end of paper.

EDITOR'S NOTE: The Technical Notes and Technical Comments sections of JET PROPULSION are open to short manuscripts describing new developments or offering comments on papers previously published. Such manuscripts are published without editorial review, usually within two months of the date of receipt. Requirements as to style are the same as for regular contributions (see masthead page).

Some general features of the variation of the re-entry velocity can be obtained by consideration of Equation [4]. If the body starts from rest at a very great altitude ($\lambda\rho_1 \ll 1$), then during the first part of re-entry, where $\lambda\rho \ll 1$, Equation [4] reduces to the expression for the vacuum free-fall velocity

$$v^2 \simeq v_v^2 = 2g(y_0 - y) \quad [6]$$

where the subscript 0 denotes the conditions at great altitude. If, however, the velocity at a very great altitude is large, then Equation [4] reduces to

$$v^2 \simeq v_0^2 \exp(-\lambda\rho) \quad [7]$$

These approximations are valid for $\lambda\rho$ less than about unity, depending on the magnitudes of the release altitude and velocity. The lowest altitude for which they are valid depends on the magnitude of $\lambda = \beta/(W/C_DA)$; that is, on whether the body is light (small W/A) or heavy (large W/A). For high speed vertical re-entry of heavy bodies, it is known (1) that Equation [7] is valid almost to the earth's surface.

At sufficiently low altitudes ($\lambda\rho > 10$), the exponential factors are very small and Equation [4] reduces to the expression for the equilibrium free-fall velocity

$$v^2 \simeq v_e^2 = 2(W/C_DA)/\rho \quad [8]$$

For intermediate altitudes the complete Equation [4] gives the transition to Equation [8].

If the drag coefficient changes suddenly at low altitudes, then the new equilibrium velocity will be attained very rapidly, within a few hundred feet. This is due to the exponent $\lambda(\rho - \rho_1) = \lambda\rho_1[(\rho/\rho_1) - 1]$ becoming large for only a small increase of ρ/ρ_1 because the factor $\lambda\rho_1$ is large.

References

1 Allen, H. J., and Eggers, A. J., Jr., "A Study of the Motion and Aerodynamic Heating of Missiles Entering the Earth's Atmosphere at High Supersonic Speeds," NACA RM A53D28, Aug. 25, 1953.

2 Minzner, R. A., and Ripley, W. S., "The ARDC Model Atmosphere, 1956," Air Force Surveys in Geophysics no. 86, Air Force Cambridge Research Center TN-56-024, Dec. 1956.

3 Linnell, R. D., "Vertical Re-entry of Very Light-Weight Bodies into the Earth's Atmosphere," CSRL Research Note 9, Oct. 1957.

Air Density Determination by Observation of a Satellite

ROBERT E. ROBERSON[1]

Autonetics Division of North American Aviation, Inc., Downey, Calif.

Previous results on the relationship between orbital eccentricity and radius for a satellite affected by air drag are applied to the problem of inferring air density as a function of altitude.

AN APPLICATION envisioned for even the most rudimentary satellites is the determination of atmospheric density from observations of the descent. I am not aware of a published description of the analytical method by which the air density is to be inferred, but the fact that interest usually is expressed primarily in the decay of altitude with time or revolution number implies that one of these relations is intended to be used.

Such an approach is possible, but it does involve some difficulties. There are two major ones. First, there is the problem discussed by Petersen (1)[2] of the value of the drag coefficient to be used for flight under satellite conditions. Although its approximate value can be inferred rationally, the coefficient inevitably enters any relationship between altitude and time for revolution number and must be accepted as an additional unknown to be determined along with the density function. Second, there is the observation of DeNike (2), based on computer solutions of the equations of motion over an oblate earth in the presence of air drag: "We have an extremely complex motion . . . we have to be careful in using short portions of trajectory to extract such data as density." This implies that an extremely precise determination of the density-altitude function is likely to be a rather sophisticated operation involving a very complex and time-consuming program of numerical computation.

An alternative approach is outlined in this note. It provides a density function without reference to the drag coefficient by a very simple numerical process. These advantages are not without cost, of course, and the proposed method suffers in that it may provide a cruder approximation to the density function than can be obtained by more elaborate data reduction. Also, there is an implicit limitation to the case where the drag coefficient is essentially constant over the range of altitudes considered. However, tentative tests of the degree of approximation which may be expected indicate that the density can be estimated quite well this way, so that the results should be intrinsically adequate for most engineering applications. Furthermore, they should be useful as a first approximation in an iterative procedure for subsequent improvements in the density function.

The method is based on an approximate result obtained (3) by applying the method of variation of parameters to the same equations of motion as those given by Petersen. This is a relation between the orbital eccentricity ϵ and the radial distance R of the satellite from the center of the earth, involving the air density $\rho(R)$ but not the drag coefficient. (Strictly, R is a "characteristic" radius related to the perigee radius R_P by $R = R_P(1 + \epsilon)$.) For small eccentricities (of the order of $\epsilon = 0.001$ or less) and a spherical atmospheric shell it is

$$\sqrt{\frac{\rho(R)}{\rho(R_i)}} = \frac{\epsilon_i R}{\epsilon R_i} \quad [1]$$

where i designates initial values. Given observations of $\epsilon(R)$, one finds $\rho(R)/\rho(R_i)$ directly. The constant $\rho(R_i)$ can be evaluated when drag reduces R to the point where $\rho(R)$ can be identified with density accessible to direct measurement in the lower regions (say of the order of 100 km) of the atmosphere.

If the eccentricity is initially much larger than $\epsilon_i = 0.001$, a more accurate result

$$\sqrt{\frac{\rho(R)}{\rho(R_i)}} = \frac{\epsilon_i R}{\epsilon R_i} \exp\{\phi(\kappa_i\epsilon_i) - \phi(\kappa\epsilon)\} \quad [2]$$

can be used. Here

$$\phi(\xi) = \int_0^\xi \left[1 - \frac{2}{x}\frac{I_1(x)}{I_0(x)}\right]\frac{dx}{x} \quad [3]$$

(the functions I_1 and I_0 being Bessel functions of the first kind for imaginary argument) and

$$\kappa = -R\frac{d\ln\rho}{dR} \quad [4]$$

In the right-hand side of Equation [2], one uses the first approximation for κ and ϵ inferred from Equation [1], and by iteration could obtain a more precise $\rho(R)$. However, preliminary tests of the results against "exact" solutions of the complete equations of motion by IBM-701 computer indicate

Received Dec. 16, 1957.

[1] Specialist, Advanced Engineering Department. Mem. ARS.

[2] Numbers in parentheses indicate references at end of paper.

that the $\epsilon(R)$ results for $\epsilon_i = 0.01$ are, to within this order of approximation, in error by no more than about 1 per cent, corresponding to a density error of about 2 per cent. The error is not likely to become larger, except perhaps when R begins to change very rapidly as the satellite begins the precipitous portion of its descent. It should be noted that even a considerably larger density error might be acceptable, inasmuch as it is now uncertain as to order of magnitude.

It may be necessary to include the effect of the asphericity of the atmospheric shell arising from the oblateness of the earth. The analog of Equation [2] cannot be obtained unless the orbital eccentricity is much greater or much less than a factor $\tilde{\epsilon}$ related to the oblateness of the earth and defined

$$\tilde{\epsilon} = \frac{\kappa(a^2/b^2 - 1)}{4R} \sin^4\gamma \cos 2\beta_P \quad [5]$$

where a and b are respectively equatorial and polar radii of the earth, γ is the orbital inclination ($0 \leq \gamma \leq \pi$), and β_P is the angle from the ascending node to the perigee (measured positively in the direction of satellite motion). If $\kappa\epsilon \gg \tilde{\epsilon}$, the result is the same as Equation [2]. However, if $\kappa\epsilon \ll \tilde{\epsilon}$

$$\sqrt{\frac{\rho(R)}{\rho(R_i)}} = \frac{\epsilon_i R}{\epsilon R_i} \exp\left\{\frac{\tilde{\epsilon}}{4\kappa}\int_{R_i}^{R} \frac{d\ln\rho}{dR}\, dR\right\} \quad [6]$$

In Equation [6], the right-hand side is evaluated using the approximate density from Equation [1], as described following Equation [4]. In intermediate regions of $\tilde{\epsilon}$, one has recourse to an approximate first-order differential equation for $\epsilon(R)$, but its solution has not been explored with the present application in mind.

References

1 Petersen, Norman V., "Lifetimes of Satellites in Near-Circular and Elliptic Orbits," JET PROPULSION, vol. 26, 1956, pp. 341–351, 368.

2 DeNike, John, "The Effect of the Earth's Oblateness and Atmosphere on a Satellite Orbit," *Franklin Institute Monograph* 2, 1956, pp. 79–86.

3 Roberson, Robert E., "Effect of Air Drag on Elliptic Satellite Orbits," JET PROPULSION, vol. 28, 1958, pp. 90-96.

Lifetimes of Artificial Satellites[1]

ROBERT R. NEWTON[2]

Applied Physics Laboratory, The Johns Hopkins University, Silver Spring, Md.

Introduction

IN A recent paper (1),[3] Henry calculated the lifetimes of artificial satellites. If the orbit is not originally circular, he showed that the life of the satellite has two separate stages: In the first, the orbit changes from elliptical to circular; in the second, the satellite spirals in from a circular orbit. Unless the eccentricity is originally quite small, most of the lifetime is spent in the first stage.

Henry based the theories of these stages upon two particular assumptions. In the decay from a circular orbit, he assumed that the orbit parameters remain those appropriate to a circular orbit, with the radius changing slowly. In the decay from an elliptic orbit, he assumed that the altitude at perigee remains constant. While the errors in these assumptions are small, the lifetime is determined by only small changes in the orbit parameters. It is, therefore, necessary to examine these assumptions carefully to see if they are adequate for calculating lifetimes. We conclude that the first assumption is quite accurate, but that the second leads to an error which, for Sputnik I, amounts to about 40 per cent in the lifetime.

We retain the assumption that atmospheric density varies with altitude as

$$\rho = K \exp[-(r - R)/c] \quad [1]$$

where r is distance from the center of the earth, R is the earth's radius, and K and c are constants. Henry uses the value $c = 23.3$ km. Data on the orbital changes of Sputnik I are now available (2); from the rate of change of its period, we find that the average value of c applying up to the perigee altitude is about 12 km.

Lifetime in a Circular Orbit

The equations of motion of a particle in a gravitational field of force, subject to a drag force $\rho v^2 A$, are

$$\ddot{r} = (h^2/r^3) - (\gamma\mu/r^2) - (\rho A/M)\dot{r}[\dot{r}^2 + (h^2/r^2)]^{1/2} \quad [2]$$

$$\dot{h} = -(\rho A/M)h[\dot{r}^2 + (h^2/r^2)]^{1/2} \quad [3]$$

where $h = r^2\dot{\theta}$. If we neglect the vertical component of velocity $\dot{r}$, and let $h = 1/u$, these become

$$\ddot{r} = (1 - \gamma\mu r u^2)/r^3 u^2 \quad [4]$$

$$\dot{u} = \rho A/Mr \quad [5]$$

Using a subscript zero to denote initial values, the condition that the orbit be initially circular is that $\gamma\mu r_0 u_0^2 = 1$.

Unless the satellite is falling rapidly, ρ and r, and hence $\dot{u}$, change but slightly during one period. Hence, we have

$$u = u_0(1 + \beta t) \quad [6]$$

where β is small and slowly changing. Let

$$r = r_0 + y \quad [7]$$

Assuming that y is small and β is constant, Equation [4] becomes

$$\ddot{y} = -[(3 - 2\gamma\mu u_0^2 r_0)/u_0^2 r_0^4]y - (2\beta/u_0^2 r_0^3)t \quad [8]$$

From Equation [8], we see that y executes forced oscillations; using the initial conditions, we see that the period of these oscillations is the same as the period of revolution. The vertical component of velocity, $\dot{y}$ or $\dot{r}$, is found to be

$$\dot{r} = \dot{y} = -[2\beta r_0/(3 - 2\gamma\mu u_0^2 r_0)](1 - \cos\omega t)$$

We are interested only in the "center line" of the oscillations in $\dot{r}$; that is, we ignore $\cos\omega t$. If it is legitimate to assume that r and u are always connected by the relation appropriate to a circular orbit, we can apply this analysis at any time, and drop the subscript zero, obtaining

$$\dot{r} = -2\beta r/(3 - 2\gamma\mu u^2 r) \quad [9]$$

Since $\beta = \dot{u}/u$, this equation is found by substitution to have the solution

$$r = (\gamma\mu u^2)^{-1} \quad [10]$$

This is the relation satisfied by r and u on a circular orbit; therefore Henry's assumption is justified. Since $\dot{y} = 0$ at the beginning and end of each period, the satellite starts and ends each revolution tangent to a circle, with the speed and radius connected by Equation [10], which is Kepler's law for the period in a circular orbit. Each revolution, the orbit "steps" downward; Henry's results show that the steps increase exponentially, with most of the loss in altitude occurring during the last revolution.

Lifetime in an Elliptic Orbit

We begin by calculating the changes in the total energy E and in the angular momentum Mh during one period. We

Received Jan. 6, 1958.

[1] This work was supported by the Department of the Navy, Bureau of Ordnance, under Contract Nord 7386.

[2] Physicist, Research Center Division.

[3] Numbers in parentheses indicate References at end of paper.

shall continue to use $\rho v^2 A$ for the drag, and shall assume that the speed v is adequately given by $r\dot{\theta}$ or h/r. For the change in energy, we have, obviously

$$\Delta E = -\oint (\rho v^2 A) v dt = -Ah^2 \oint (\rho/r) d\theta \quad [11]$$

Neglecting $\dot{r}$ in Equation [3], we have

$$\dot{h} = -(\rho A/M)(h^2/r) = -(\rho A h/M) r\dot{\theta}$$

whence

$$\Delta h = -(Ah/M) \oint \rho r d\theta \quad [12]$$

From ΔE and Δh, we wish to calculate the changes in p, the height (from the center of the earth) at perigee, and q, the height at apogee. It is not accurate enough to obtain approximate values of ΔE and Δh from the integrals in Equations [11, 12], because Δp is a small difference in two large quantities. Instead, we must manipulate the integrals directly.

E and h are connected (3) with the semi-major axis a and the eccentricity ϵ by

$$E = -(\gamma\mu M/2a) \qquad h = [\gamma\mu a(1-\epsilon^2)]^{1/2} \quad [13]$$

From these, we find by routine manipulation

$$\left.\begin{aligned} \Delta a &= -2a^2(Ah^2/\gamma\mu M) \oint (\rho/r) d\theta \\ \Delta\epsilon &= -(Ah^2/\gamma\mu M\epsilon) \oint \rho\{(1-\epsilon^2)(a/r) - (r/a)\} d\theta \end{aligned}\right\} \quad [14]$$

p and q are related to a and ϵ by

$$p = a(1-\epsilon) \qquad q = a(1+\epsilon) \quad [15]$$

whence, after further manipulation, we find

$$\left.\begin{aligned} \Delta p &= -(Ah^2/\gamma\mu M) \oint \rho(r\epsilon)^{-1}\{r^2 - a^2(1-\epsilon)^2\} d\theta \\ \Delta q &= -(Ah^2/\gamma\mu M) \oint \rho(r\epsilon)^{-1}\{a^2(1+\epsilon)^2 - r^2\} d\theta \end{aligned}\right\} \quad [16]$$

It is now permissible to develop approximations for Δp and Δq.

Unless the eccentricity is quite small (of the order of 10^{-3}), most of the drag occurs near perigee. Choosing $\theta = 0$ at perigee, most of the values of the integrals come from small θ. Keeping only the first terms in θ which appear, but not assuming that ϵ is negligible compared with unity, Δp and Δq reduce to

$$\Delta p = -(Ah^2/\gamma\mu M) a[(1-\epsilon)/(1+\epsilon)] K \exp[-(p-R)/c] \times \int_{-\pi}^{\pi} \exp[-p\epsilon\theta^2/2c(1+\epsilon)]\theta^2 d\theta$$

$$\Delta q = -4(Ah^2/\gamma\mu M) a(1-\epsilon)^{-1} K \exp[-(p-R)/c] \times \int_{-\pi}^{\pi} \exp[-p\epsilon\theta^2/2c(1+\epsilon)] d\theta.$$

Replacing the limits of integration by $-\infty$ and ∞, the integrals are

$$(\sqrt{\pi}/2)[2(1+\epsilon)c/p\epsilon]^{5/2} \quad \text{and} \quad \sqrt{\pi}[2(1+\epsilon)c/p\epsilon]^{1/2}$$

respectively.

Finally, we eliminate a, ϵ and h in favor of p and q. Letting n be the number of revolutions, following Henry, $\Delta p = dp/dn$, $\Delta q = dq/dn$, and we obtain as differential equations satisfied by p and q

$$\left.\begin{aligned} dp/dn &= -4(AK\sqrt{\pi}/M)[cpq/(q-p)] \times [cq/p(q-p)]^{1/2} \exp[-(p-R)/c] \\ dq/dn &= -4(AK\sqrt{\pi}/M) q(q+p)[cq/p(q-p)]^{1/2} \times \exp[-(p-R)/c] \end{aligned}\right\} \quad [17]$$

These equations must be solved simultaneously for p and q.

While we cannot solve the equations accurately unless p is constant, we can readily estimate the total change in p which occurs during the lifetime in an elliptic orbit. Eliminating n

$$dq/dp = (q^2 - p^2)/pc \quad [18]$$

This can be solved exactly in terms of Bessel functions for pure imaginary argument; however, if the original eccentricity ϵ_0 is not too large, say a few per cent, there is a simpler procedure. Factoring $q^2 - p^2$ as $(q+p)(q-p)$, we can replace $q+p$ by its average value, which is very nearly $(2+\epsilon_0)p$. Equation [18] then integrates to

$$q = [2\epsilon_0 p_0 - c(2+\epsilon_0)^{-1}] \times \exp[(2+\epsilon_0)(p-p_0)/c] + p + c(2+\epsilon_0)^{-1} \quad [19]$$

where p_0 is the initial value of p, and we have approximated the initial value of q by $p_0(1+2\epsilon_0)$. The lifetime is nearly over when $q = p_0$; setting $q = p_0$, Equation [19] becomes, with $x = (2+\epsilon_0)(p_0 - p)/c$

$$[2\epsilon_0(p_0/c)(2+\epsilon_0) - 1]e^{-x} - x + 1 = 0 \quad [20]$$

Using $\epsilon_0 = 0.048$, $p_0 = 6600$ km, $c = 12$ km, which are approximate values for Sputnik I, this gives $x = 3.69$, and $p_0 - p = 21.6$ km. Over this change in altitude, the air density changes by a factor of 6, so that it is not legitimate to assume that the perigee altitude is constant.

We can now estimate the lifetime, using Henry's equation which follows his numbered Equation [16]:

$$\sqrt{a}(p+2a)^{-1}(p+a)^{-1} da = -2\sqrt{2\pi}(KA/M) \exp[-(p-R)/c]\sqrt{c}\, dn \quad [21]$$

The notation is the same as ours, except that a is not the semi-major axis; instead, $a = (q-p)/2$. The only place in this equation where changes in p are important is in the exponential; replacing $p+2a$ by its approximate average $p_0 + a_0 = p_0(1+\epsilon_0)$ and $p+a$ by $p_0(1+\epsilon_0/2)$

$$dn = -[\sqrt{a}M/2p_0^2(1+\epsilon_0)(1+\epsilon_0/2)\sqrt{2\pi}KA\sqrt{c}] \times \exp[(p-R)/c] da$$

From Equation [19], we get, neglecting c compared with $4a$, and ϵ_0 compared[3] with 2

$$\exp(p/c) = \sqrt{a/\epsilon_0 p_0} \exp(p_0/c)$$

Substituting this into dn and integrating from $a = a_0 = \epsilon_0 p_0$ to $a = 0$, we get as the lifetime in an elliptic orbit

$$n = [\epsilon_0^{3/2} M/4\sqrt{2\pi}KA(1+\epsilon_0)(1+\epsilon_0/2)\sqrt{cp_0}] \exp[(p_0 - R)/c] \quad [22]$$

This is less than Henry's result by a factor $(4/3)(1+\epsilon_0)\cdot(1+\epsilon_0/2)$. With $\epsilon_0 = 0.048$, this factor is 1.43. Some of this factor arises from differences in estimating terms of order ϵ_0, but most of it arises from the change in perigee.

Applications to Sputnik I

Analysis of Sputnik I is not the main purpose of this paper. However, we have made some slight use of deductions from observations of its orbit, which should be explained. The most easily measured change in the orbit is the change in the period P. If we calculate the derivation dP/dn, which is directly related to dE/dn, by the methods of the preceding section, we get

$$dP/dn = -3P\sqrt{\pi}(1-\epsilon)^{-1}(Ah^2/\gamma\mu M)[2c(1+\epsilon)/p\epsilon]^{1/2} K \times \exp[-(p-R)/c]$$

[3] The relative error produced by neglecting ϵ_0 here is only $\epsilon_0/8$; considerable algebra is needed to show this.

Using the values reported in (2), we can infer the factor $(AK/M)\exp[-(p-R)/c]$ unambiguously; this factor is 2.4×10^{-14} cm^{-1}. Using $M = 84$ kg and a diameter of 53 cm, we get $K \exp[-(p-R)/c]$, the density at the original perigee altitude, to be 9.0×10^{-13} gm/cm^3, about 7×10^{-10} times the standard sea level value. From this, we infer that c is about 12 km.

The estimate of density is uncertain by the error in the observed value of dP/dn, but this error should have a negligible effect upon c.

Having gone this far, it is necessary to go on and estimate the lifetime. From Equation [22], we find that the lifetime in an elliptic orbit is 1430 turns. From Henry's results, we find the lifetime after the orbit becomes circular to be 9 turns. This gives a total lifetime of 1439 turns, or 96 days.

References

1 Henry, Irvin G., "Lifetimes of Artificial Satellites of the Earth," JET PROPULSION, vol. 27, Jan. 1957, p. 21.

2 Staff of Royal Aircraft Establishment, Farnborough, "Observations of the Orbit of the First Russian Earth Satellite," *Nature*, no. 4593, Nov. 9, 1957, p. 937.

3 Page, Leigh, "Introduction to Theoretical Physics," 2nd Edit., sect. 30, Van Nostrand, New York, 1941.

Vertical Ballistic Trajectories Over an Oblate Earth

ROBERT E. ROBERSON[1]

Autonetics Division of North American Aviation, Inc., Downey, Calif.

Previous results on impact points of ballistic rockets on an oblate earth are modified to include the case of vertical trajectories.

IN A previous paper (1)[2] I developed expressions for the correction to ballistic missile impact points which result from the oblateness of the earth. One case was explicitly omitted, namely the case of vertical launch, and it was expected that this case would have to be developed separately ab initio. However, further consideration of the results has permitted this exceptional case to be included in the previous theory as described below.

Expressions for lateral deviation α_I, range deviation $\mu\Delta\phi^{(1)}$ and time deviation $\mu\tau^{(1)}$ are given by Equations [35, 36, 42], respectively, of that paper, in the general case. For short-range trajectories, the results specialize to Equations [45, 46, 47] which are in the form of the first terms of a power series development in the range angle $\Delta\phi$. (All notation is that of (1).)

For a near-vertical launch case it is evident that the short range form suffices. As $\theta \to \pi/2$, the range approaches zero. All of the higher order terms in the power series in $\Delta\phi$ can be neglected, for examination of the general equations shows that none of these can be multiplied by a coefficient that becomes infinite as $\theta \to \pi/2$. However, the coefficient of the series does have the latter property, and one is left with a dominant indeterminate term $(\tan\theta)\Delta\phi$ in each of the short range equations.

To evaluate the indeterminate term, we introduce h, the maximum altitude of the rocket above the reference sphere (of radius R_L) as it follows its elliptical reference path. It is easy to show that $\tan\theta \tan(\Delta\phi/4) = h/(R_L + h)$, so that

$$\lim_{\substack{\theta \to \pi/2 \\ \Delta\theta \to 0}} \left[(\tan\theta)\Delta\phi \right] = \frac{4h}{R_L + h} \quad \ldots\ldots\ldots\ldots [1]$$

Using this in Equations [45–47] of (1)

$$\alpha_I = -3\mu \frac{a^2}{R_L{}^2} \frac{4h}{R_L + h} \cos\gamma \sin 2\lambda_L \quad \ldots\ldots\ldots\ldots [2]$$

$$\mu\Delta\phi^{(1)} = -3\mu \frac{a^2}{R_L{}^2} \frac{4h}{R_L + h} \sin\gamma \sin 2\lambda_L \quad \ldots\ldots\ldots\ldots [3]$$

$$\mu\tau^{(1)} = -3\mu \frac{a^2}{R_L v_L} \frac{4h}{R_L + h} (1 - 3\sin^2\lambda_L)$$

$$= -12\mu a^2 \sqrt{\frac{h}{2KR_L(R_L + h)}} (1 - 3\sin^2\lambda_L) \quad \ldots\ldots [4]$$

The last equation is in view of the fact that the launching velocity and maximum altitude are related by

$$v_L{}^2 = 2Kh/R_L (R_L + h)$$

Next, turn to Equations [26, 32] of (1) which give latitude and longitude corrections to the impact point in terms of the variables of Equations [2–4]. Introduce $\Delta N = \lambda_I{}^{(1)}$ and $\Delta E = L^{(1)} \cos\lambda_I{}^{(0)}$ as northerly and easterly corrections. They are given by

$$\Delta N = -\frac{12\mu a^2}{R_L} \left(\frac{h}{R_L + h} \right) \sin 2\lambda_L \quad \ldots\ldots\ldots\ldots [5]$$

$$\Delta E = \frac{12\mu a^2}{R_L} \frac{\Omega}{\omega_{0L}} \sqrt{\frac{h}{R_L + h}} (1 - 3\sin^2\lambda_L) \cos\lambda_L \quad \ldots\ldots [6]$$

where $\omega_{0L} = \sqrt{K/R_L{}^3}$ is orbital angular velocity at the reference sphere.

For an illustrative calculation suppose $R_L = a$, whence $12\mu a^2/R_L = 41.8$ km and $\Omega/\omega_{0L} = 0.0588$. The behavior of ΔN and ΔE with nominal maximum height of trajectory and with launching latitude is shown in Fig. 1.

Reference

1 Roberson, R. E., "Oblateness Correction to Impact Points of Ballistic Rockets," ARS Preprint 548-57, presented at the ARS 12th Annual Meeting, New York, N. Y., Dec. 2–5, 1957.

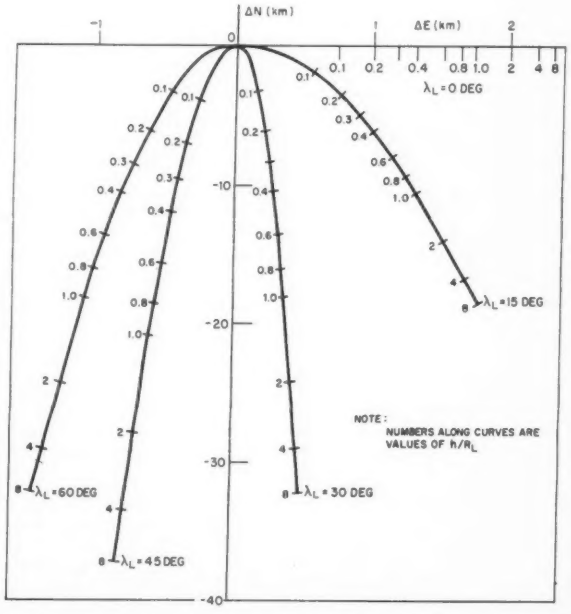

Fig. 1 Northerly and easterly deviation in vertical launch from several latitudes to various altitudes

Received Jan. 2, 1958.

[1] Specialist, Advanced Engineering Department. Mem. ARS.

[2] Numbers in parentheses indicate References at end of paper.

Evaluation of Flame Stability at High Reynolds Numbers[1]

LOREN E. BOLLINGER[2]

The Ohio State University, Columbus, Ohio

Nomenclature

- d = diameter of injector port
- g = velocity gradient evaluated at injector wall; superscript t = turbulent flow
- Re = Reynolds number $= (\bar{u}_g \cdot d)/\nu$
- $\bar{u}_g$ = average linear gas velocity
- ϵ = thickness of laminar sublayer; subscripts: 1 = using Equation [3] for λ and one-seventh power velocity distribution law; 2 = using Equation [3] for λ and one-tenth power velocity distribution law
- λ = friction factor
- ν = kinematic viscosity of gas mixture

LEWIS and von Elbe (1)[3] developed a theory by which the condition for flashback of laminar, premixed flames can be correlated to the velocity gradient of gas flow evaluated at the wall of a cylindrical burner tube. Edse (2, 3) extended this treatment to turbulent flames. Evaluation of the flame stability is straightforward for laminar flames; for turbulent flow, however, a solution is not readily obtainable because of the lack of an explicit analytical expression for the friction factor. The equation for the velocity gradient evaluated at the burner wall is obtained (4) by equating the pressure force that maintains the gas in a steady-state motion and the frictional force which opposes the gas flow. A general equation for the velocity gradient under steady-state flow conditions is:

$$g = \frac{\lambda \cdot \bar{u}_g^2}{8\nu} = \frac{\lambda \cdot Re \cdot \bar{u}_g}{8d} \quad \ldots\ldots [1]$$

This equation is applicable to either laminar or turbulent flow fields if appropriate values of the friction factor λ are employed. When the Reynolds number is less than 100,000, the Blasius expression for the friction factor fits the experimental data quite well for turbulent flow. Then the velocity gradient expression becomes

$$g^t = 0.03955(Re)^{3/4} \cdot \frac{\bar{u}_g}{d} \quad \ldots\ldots [2]$$

It has been found experimentally (2, 5) that the velocity gradients at flashback are dependent upon the burner diameter when the burners are not cooled. However, Edse (2) showed that if the burner tip is cooled adequately, the diameter of the tube has practically no effect on the flame stability for the range of burner diameters employed.

When the Reynolds number exceeds 100,000, the error in calculating friction factors from the Blasius expression becomes quite large. When the constants of the empirical formula of Prandtl and Lees (4, 6) are modified as follows

$$\lambda = 0.0067 + \frac{0.615}{(Re)^{0.35}} \quad \ldots\ldots [3]$$

the calculated values of the friction factor fit the experimental data for smooth tubes to within ± 3 per cent for the range $3 \times 10^3 < Re < 10^7$. The deviation of values of the various expressions from Moody's experimental data (7) is given in Fig. 1.

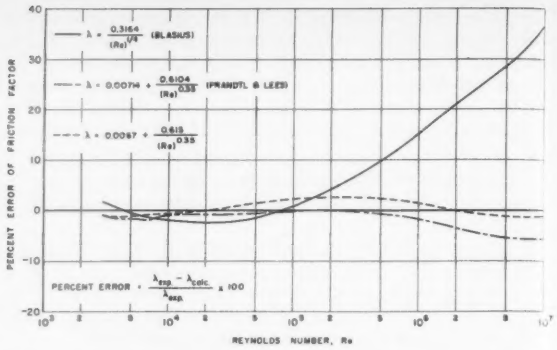

Fig. 1 Per cent error of various friction-factor equations as a function of Reynolds number for turbulent flow

Using Equation [3] to express λ, the velocity gradient equation becomes

$$g^t = 8.38 \times 10^{-4}[Re + 91.8(Re)^{0.65}] \cdot \frac{\bar{u}_g}{d} \quad \ldots\ldots [4]$$

Calculations of the depth of penetration of quenching for burners utilizing premixed gases under atmospheric and high pressure conditions (2, 3, 5) show that this distance is always less than the thickness of the laminar sublayer. From the theory of turbulent flow it can be seen that the distribution of linear gas velocity across a cylindrical tube varies according to the one-seventh power of the distance and that a laminar sublayer exists in a region very close to the wall itself. The sublayer thickness, obtained by considering the balance of pressure and frictional forces, the pressure drop along the tube, and Newton's law of viscosity, is

$$\epsilon = \frac{16.25d}{(\lambda \cdot Re)^{7/8}} \quad \ldots\ldots [5]$$

Values for the fricton factor can be calculated from the Blasius expression or from Equation [3] for very high Reynolds numbers. In the latter case the resulting expression is

$$\epsilon_1 = \frac{5586d}{(Re)^{0.76}[195 + (Re)^{0.41}]} \quad \ldots\ldots [6]$$

At a Reynolds number of 10^6, the calculated sublayer thickness is 10 per cent larger when the Blasius expression for λ is used instead of Equation [3]; at $Re = 10^7$, the difference increases to 63 per cent.

According to Prandtl (4) the one-seventh power law of velocity distribution changes gradually to a one-tenth power law variation at a Reynolds number of 4×10^6. Under these conditions the laminar sublayer thickness is

$$\epsilon_2 = \frac{2505d}{(Re)^{0.72}[152 + (Re)^{0.39}]} \quad \ldots\ldots [7]$$

Laminar sublayer thicknesses as calculated by Equations [6, 7] show that at a Reynolds number 10^7 the thickness calculated by the one-tenth power law distribution is only 16 per cent larger. Thus it appears reasonable to conclude that the thickness of the sublayer is relatively insensitive to the law governing the velocity distribution for the range of exponents considered.

Received Dec. 24, 1957.

[1] This research was supported in part by the U. S. Air Force under Contract AF 33(616)-2078, monitored by the Aeronautical Research Laboratory, WCRRD, Wright Air Development Center, with The Ohio State University Research Foundation. Material in this paper was used in partial fulfillment of the requirements for the degree M.Sc.

[2] Research Associate, Rocket Laboratory and Department of Aeronautical Engineering. Mem. ARS.

[3] Numbers in parentheses indicate References at end of paper.

Acknowledgment

The author gratefully acknowledges the assistance given during this study by R. Edse of the Department of Aeronautical Engineering, The Ohio State University.

References

1 Lewis, B., and von Elbe, G., "Stability and Structure of

Burner Flames," *Journal of Chemical Physics*, vol. 11, 1943, pp. 75–97. "Further Studies of the Structure and Stability of Burner Flames," ibid., vol. 13, 1945, pp. 89–100.

2 Edse, R., "Studies on Burner Flames of Hydrogen-Oxygen Mixtures at High Pressures," Wright Air Development Center Technical Report 52–59, April 1952.

3 Edse, R., "Studies on Bunsen Burner Flames at High Pressures with Hydrogen-Oxygen Mixtures," Second Midwestern Conference on Fluid Mechanics, March 17–19, 1952.

4 Prandtl, L., and Tietjens, O., "Applied Hydro- and Aeromechanics," McGraw-Hill, New York, first ed., 1934.

5 Bollinger, L. E., and Edse, R., "Effect of Burner-Tip Temperature on Flash Back of Turbulent Hydrogen-Oxygen Flames," *Industrial and Engineering Chemistry*, vol. 48, April 1956, pp. 802–807.

6 Lees, C. H., "On the Flow of Viscous Fluids through Smooth Circular Pipes," *Proceedings of The Royal Society of London*, Series A, vol. 91, 1914, p. 46.

7. Moody, L. F., "Friction Factors for Pipe Flow," *Trans. ASME*, Nov. 1944, pp. 671–684.

Effect of High Altitude Conditions on Atomization Phenomena

C. C. MIESSE[1]

Armour Research Foundation, Chicago, Ill.

THE demands of modern defense tactics require that aircraft and/or rockets maintain combustion at extreme altitudes. Since the combustion of liquid propellants is predicated upon adequate atomization, evaporation and penetration, the effect of high altitude conditions on these contributory phenomena is of paramount importance.

The behavior of sprays under high altitude conditions was investigated experimentally by Garner and Henny (1)[2] who used an air blast atomizer to determine that the SMD increased slightly as the pressure decreased. The data which they obtained with five different hydrocarbons are presented in Fig. 1, which reveals that the sprays of toluene and benzene deteriorate markedly as pressure is reduced, with lesser effects for the other liquids. Replotting of these data on logarithmic coordinates in Fig. 2 suggests that the pressure dependence can be represented by

$$\text{SMD} = D_0 = kP^{-n} \quad [1]$$

where the appropriate evaluation of n is noted on each curve.

This effect of lower ambient pressures, which is accompanied by lower densities, was predicted theoretically by Weber (2), whose analysis of stream disintegration was used by Miesse (3) to correlate his experimental data obtained under sea-level conditions. In the same report, the finer atomization effected by higher pressures was demonstrated by comparing Miesse's data with those of Kuehn (4), Lee (5) and Wöltjen (6). The data of these investigators are presented in Fig. 3, which gives further indication of the decrease of drop size with ambient pressure. More closely akin to the air blast atomization is the phenomenon of secondary atomization, a simple criterion for which was given by Littaye (7)

$$\rho' U^2 D/\sigma = \text{const} \quad [2]$$

where ρ' is the ambient density, U is the droplet velocity, D is diameter and σ is the surface tension of the liquid. Equation [2] thus predicts a value of unity for exponent n of Equation [1], under the assumption that the density of the gas varies as its pressure.

Received Jan. 20, 1958.

[1] Supervisor, Combustion Research Section. Mem. ARS.

[2] Numbers in parentheses indicate References at end of paper.

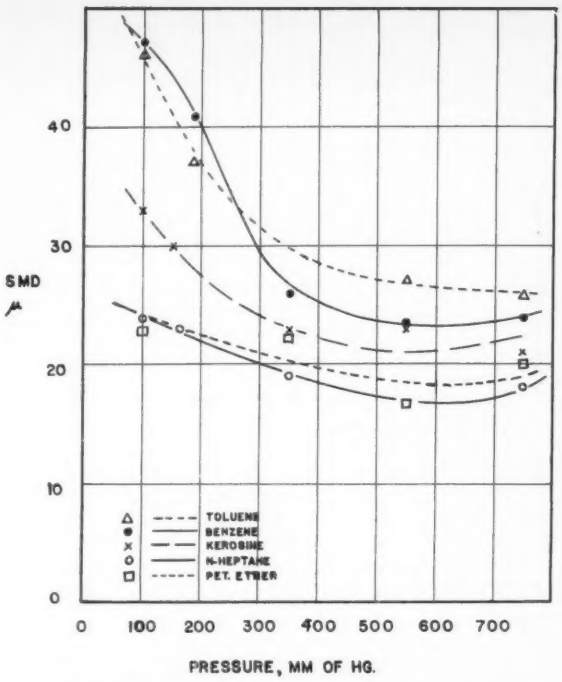

Fig. 1 Variation of Sauter mean diameter of spray with ambient pressure (Garner and Henny)

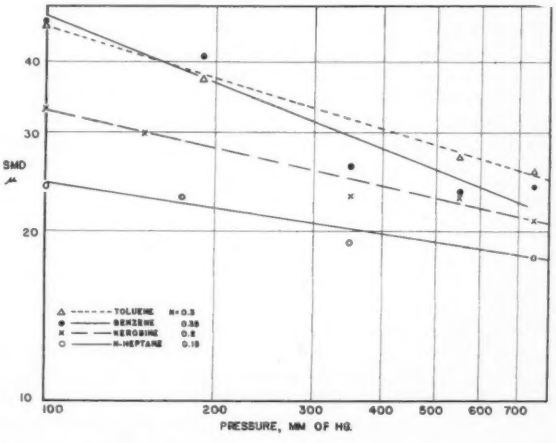

Fig. 2 Logarithmic variation of Sauter mean diameter with ambient pressure: n = negative slope

The effect of ambient pressure on the vaporization rate for a single droplet is given by Langmuir (8)

$$\frac{dm}{dt} = \frac{-2\pi DYc_0m_2}{P} \quad [3]$$

which indicates an inverse variation with ambient pressure, other factors being the same. Since the SMD of a spray is defined as the single diameter which represents the vaporization characteristics of the distributed spray, the vaporization rate of the collective spray of N droplets can be expressed by assuming a monodisperse spray

$$\frac{dM}{dt} = N\frac{dm}{dt} \quad [4]$$

where N can be defined in terms of the total volume V of

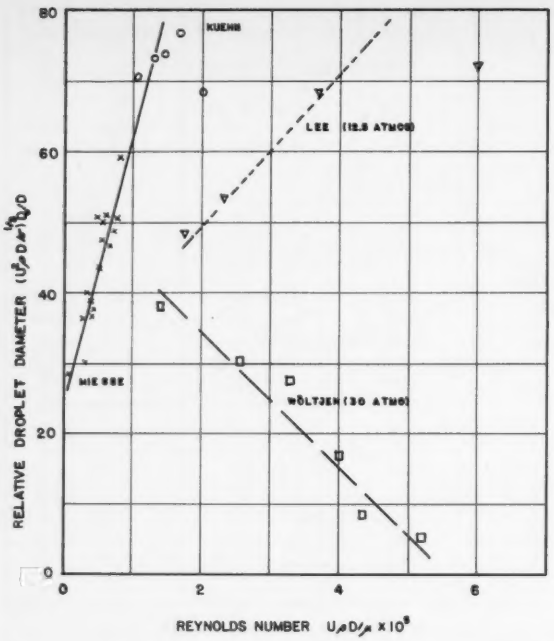

Fig. 3 Variation of relative droplet diameter with Reynolds number for various ambient pressures (Miesse)

liquid in the spray

$$N = \frac{6V}{\pi D_0^3} \quad \ldots\ldots [5]$$

The over-all effect of pressure on the initial vaporization of a spray, which provides the gaseous fuel for ignition, can be determined by simultaneous consideration of Equations [1, 3, 4, 5]. For kerosene which approximates current jet fuels, $n = 0.2$, and

$$\frac{dM}{dt} = -\frac{6V}{\pi D^3} \cdot \frac{2\pi D_0 Y c_0 m_2}{P}$$

$$= -12VYc_0m_2(P^{0.6})\left(\frac{(P^{-0.2}}{P}\right) = KP^{-0.6} \quad \ldots\ldots [6]$$

Hence it is apparent that a decrease in ambient pressure by a factor of ten will result in an increase in initial vaporization of a kerosene-type fuel by a factor of four.

The lifetime of an evaporating droplet can be determined from consideration of Equation [3] which can be written in the form

$$D^2 = D_0^2 - \lambda t \quad \ldots\ldots [7]$$

where λ varies inversely as P, as indicated by Equation [3]. From Equation [6], the droplet lifetime T can be expressed as

$$T = D_0^2/\lambda \quad \ldots\ldots [8]$$

Simultaneous consideration of Equations [1, 3, 8] then reveals that the lifetime of a kerosene droplet produced by a given injection system varies as $P^{0.6}$.

The penetration distance of a spray can be determined from an equation developed by Miesse (9) for the distance traveled by an evaporating droplet with an injection velocity U_0

$$L = \frac{D_0^2 U_0}{\lambda\left(\frac{k\mu}{\rho'\lambda} + 1\right)} \quad \ldots\ldots [9]$$

Since Equation [3] and the previous assumptions regarding the proportionality of ρ' and P indicate that the product $\rho'\lambda$ is independent of pressure, Equation [9] predicts that the penetration distance L varies as the droplet lifetime. Hence, from Equations [1, 3, 8]

$$L = K'P^{1-2n} \quad \ldots\ldots [10]$$

again indicating that the penetration distance is decreased under high altitude conditions for $n < 0.5$.

Actually, the evaporation rate of a decelerating droplet is dependent upon both the Schmidt and Reynolds numbers, as described by Frössling's equation (10)

$$\frac{d(D^2)}{dt} = -\lambda_0(1 + 0.3\sqrt[3]{Sc}\sqrt{R})$$

$$= -\lambda_0(1 + 0.3\sqrt[3]{\mu/\rho\mathfrak{D}}\sqrt{Up'D/\mu}) \quad \ldots\ldots [11]$$

Since the diffusion coefficient $\mathfrak{D}$ varies inversely as the pressure, it is apparent that the Schmidt number Sc is unaffected by pressure variations. The Reynolds number however varies as P^{1-n} by virtue of Equation [1] and the assumed pressure dependence of the density ρ'. Simultaneous consideration of Equation [11] and Stokes' drag equation by Miesse (11) led to the following equations (with suitable approximation) for the droplet lifetime and penetration distance, respectively

$$T = \frac{D_0^2\rho'}{36b\mu(1 + 4bA)}\left[1 + \frac{16b^2A(1 - bA)}{(1 + b)(1 + 5b)}\right] \quad \ldots\ldots [12]$$

and

$$L = U_0\left\{T - \frac{D_0^2\rho'}{9\mu(1 + 4bA)}\left[\frac{1}{2 + 4b} + \frac{4bA(1 - bA)}{(1 + b)(3 + 5b)}\right]\right\} \quad \ldots\ldots [13]$$

where

$$A = 0.3\sqrt[3]{Sc}\sqrt{U_0\rho' D_0/\mu} \quad \ldots\ldots [14]$$

and $b \ll 1$ is independent of pressure. Because of the small relative magnitude of b, it is apparent from inspection of Equations [1, 12, 13] that both T and L vary essentially as P^{1-2n}; hence they can be expected to decrease at high altitudes, provided $n < 0.5$, as noted previously regarding Equations [8, 9]. Since the effect of the Reynolds number is determined primarily by the $(1 + 4bA)$ term in the denominator of Equations [12, 13], it is apparent that a decrease in pressure leads to a decrease in the value of A, and hence to a slight increase in both droplet lifetime and penetration distance. This increasing effect, however, is of secondary importance, as shown by the following equations, derived from Equations [1, 12]

$$\frac{\partial T}{\partial P} = \frac{\partial}{\partial P}\left[\frac{KP^{1-2n}}{1 + kbP^{1-n}}\right]$$

$$= K\left[\frac{(1 - 2n)P^{-2n}}{1 + kbP^{1-n}} - \frac{kb(1 - n)P^{1-2n}}{(1 + kbP^{1-n})^2}\right]$$

$$= \frac{K}{P^{2n}(1 + kbP^{1-n})^2}[(1 - 2n) - (1 - n)kbP] \quad \ldots\ldots [15]$$

Inspection of Equation [15] reveals immediately that the droplet lifetime, and hence the penetration distance, decreases as the pressure decreases, since the second term in the brackets is of second order because of the smallness of both b and P at high altitudes.

As a result of the foregoing analysis, it is apparent that the effect of high altitude, which is evidenced by lower ambient pressures, is threefold: (a) The initial Sauter mean diameter (SMD) of the spray formed by primary disintegration or secondary atomization is slightly larger than the corresponding SMD at sea level pressures, (b) the vaporization rate is greater and (c) the penetration distance is decreased as a consequence of the shorter droplet lifetime.

References

1 Garner, F. H., and Henny, V. E., "Behavior of Sprays under High Altitude Conditions," *Fuel*, vol. 32, 1953, p. 151.

2 Weber, C., "Zum Zerfall eines Flüssigkeitsstrahles," *ZAMM*, vol. II, 1931, p. 136.

3 Miesse, C. C., "Correlation of Experimental Data on the Disintegration of Liquid Jets," *Industrial and Engineering Chemistry*, vol. 47, 1955, p. 1690.

4 Kuehn, R., "Über die Zerstäubung flüssiger Brennstoffe," *Motorwagen*, vols. 27 and 28, 1924 and 1925. Also NACA TM 329, 330, 331, 1925.

5 Lee, D. W., "The Effect of Nozzle Design and Operating Conditions on the Atomization and Distribution of Fuel Sprays," NACA TR 245, 1932.

6 Wöltjen, A., "Über die Feinheit der Brennstoff-zerstäubung in Ölmaschinen," Technische Hochschule, Darmstadt, 1925.

7 Littaye, G., "Sur une Theorie de la Pulverisation des Jets Liquides," *Comptes Rendus (Paris)*, vol. 217, 1943, p. 99.

8 Langmuir, I., "The Evaporation of Small Spheres," *Physical Review*, II, vol. 12, 1918, p. 368.

9 Miesse, C. C., "Ballistics of an Evaporating Droplet," JET PROPULSION, vol. 24, 1954, p. 237.

10 Frössling, N., "Über die Verdungstung fallender Tropfen," *Gerlands Beitrage zur Geophysik*, vol. 52, 1938, p. 170.

11 Miesse, C. C., "The Effect of a Variable Evaporation Rate on the Ballistics of Droplets," *Journal of the Franklin Institute*, vol. 264, 1957, p. 391.

Celestial Iconospherics, the Ultimate Astronomy[1]

WILLIAM J. BERGER[2]

***Celestial Iconospherics* is defined as the study and utility of images formed by the refractional, diffractional and gravitational bending of electromagnetic radiation around large celestial bodies. The thesis is that, according to known laws of physical optics, a large spherical celestial body must function as a telescopic positive lens forming real images of almost everything in the universe; the focal surface of such a lens is a sphere, called an *iconosphere*, which is concentric with the celestial body. A spherical celestial body has iconospheres of many different sizes depending upon the wave length and the mode of bending of the electromagnetic waves.**

Physical investigation of the iconospheres requires controllable space-traveling vehicles carrying radio, image-transformer and television equipment. Because of the high optical resolving power available on the iconospheres, the method may suffice to detect the most remote of celestial objects and to detect other important objects of small angular diameter, such as the planets of other stars. Techniques of celestial iconospherics may make radio communication possible over interstellar distances.

Iconospheres

BY WELL-KNOWN laws of physical optics, there are three natural modes of wave-bending whereby a spherical body acts as a positive lens on incident electromagnetic radiation which are refraction, diffraction and gravitation. Since a celestial spherical body presents the same aspect to all directions of space, the result of its positive lens action on incident radiation is that the body is concentrically surrounded by a series of spherical optically real focal surfaces, herein called *iconospheres*. The radius of any particular iconosphere depends upon the mode of bending of the radiation and upon the ratio of body-diameter to radiation wave length.

Received Dec. 23, 1957.

[1] This article was developed independently by the author without affiliation to any corporation or institution.

[2] Research engineer, Convair-Astronautics, San Diego, Calif.

A celestial body with an atmosphere generally has iconospheres of all three principal types, which, in the increasing order of magnitude of their radii, are *refractional, diffractional* and *gravitational*. A body without an atmosphere has no refractional iconospheres.

A spherical celestial body is in fact a lens which looks simultaneously in all directions, and its iconospheres contain images of almost everything in the universe. Since the resolving power of a lens, as measured by the smallest angular diameter detectable, depends upon the ratio of radiation wave length to lens diameter, it follows that the optical resolving power on the iconospheres is extremely high, at least for the refractional type, and hence that the iconospheres contain information of the greatest importance in astronomy.

Compound Telescopes

The fact that most moons are inside the iconospheres of their respective planets causes the existence of other kinds of optical foci. The moon may be entirely inside a conical bundle of rays which have been deflected by the planet and which have a focus on an iconosphere of the planet. Some of these rays, in passing the moon, are further deflected by diffraction and gravitation and thus arrive at other foci, so that the planet-moon system acts as a compound lens. Such a compound iconospherical system, however, because of its narrow view of the universe, is generally less useful than the ordinary complete iconospheres.

Physical Investigation

Since the minimum radius of an iconosphere is thousands of times greater than that of the celestial body which generates it, and since the iconospherical images can be oberved only by a detector placed on or outside the iconosphere, physical investigation of the iconospheres evidently requires use of a controllable space-traveling vehicle of some sort. The vehicle may be manned or not. It might be a robot ship cruising for a long time in a gravitational orbit just outside an iconosphere, recording its observations by image-transformer and television methods and occasionally correcting its orbit by small bursts of power until eventually covering all areas of interest. The first attempt at physical investigation may well be much simpler: A ship sent out from the earth to make a loop around some particular image (for instance, that of Mars) on a refractional iconosphere of the earth and thence somehow to return its observational data to earth.

Image detection on visual iconospheres, i.e., those caused by light in the visual spectrum (including also ultraviolet and infrared), is complicated by the fact that the detector may often be illuminated not only by the desired image but also either by direct sunlight or by sunlight reflected from the celestial body generating the iconosphere. Such difficulty can be practically eliminated by methods of shielding, filtering, and image-transformation or television. Since the ratio of visual iconospherical brightness to albedo of the generating body is a maximum for moons in eclipse by their respective planets, the visual iconospheres of the Galilean moons of Jupiter are very useful. Gravitational iconospheres have radii so great in comparison to diameter of their generating body that useful visual images probably occur on gravitational iconospheres generated even by the sun itself since at such distances the sun appears only as a moderately bright star.[3]

Because of fewer shielding difficulties, image detection on iconospheres in the radio spectrum is usually simpler than in the case of the visual spectrum.

Utility

Celestial iconospherics has important uses in astronomy of the solar system, in cosmology, and in the possibility of interstellar radio communication.

[3] Zwicky's 20-year-old theory of gravitational lenses is most recently described in: Zwicky, F., "Morphological Astronomy," Springer-Verlag, 1957, pp. 215–218.

Before visiting other planets, we could learn much about them by studying their images on iconospheres of the earth. To illustrate in the simplest way the order of the magnitudes involved, let us consider the visual iconosphere of earth for the red light commonly seen when the sun is on the horizon. Since this light is refracted by nearly half a degree of arc in passing through our atmosphere, its focus is an iconosphere, having a radius of some 458,000 miles. On this iconosphere, the image-diameters of the sun, Jupiter, Mars and the nearer stars are about 4000 miles, 89 miles, 33 miles and 500 ft, respectively. With such resolving power, the planetary systems of other stars are definitely observable, and it may even be possible to determine whether or not the number of galaxies is finite.

Iconospheres in the radio spectrum are useful not only in "seeing" across great distances through the intergalactic dust and gas but also in communicating over interstellar distances. Certain kinds of interstellar radio signals may be too weak to be detected on earth itself but they have strong foci on the radio iconospheres of the earth; thus by detecting alien radio signals of characteristic information-carrying type, we may prove that intelligent beings exist in other solar systems.

By placing a radio transmitter on a suitable radio iconosphere of the earth and sending a signal toward the earth, we cause the signal to pass as a plane wave beyond the earth. Thus, by the search-light principle, we may expect the signal to travel with virtually undiminished intensity over a vastly greater distance than it could achieve in its normal form of a diverging wave. Moreover, the cross-sectional area of the search-light beam produced by the earth-lens is obviously much greater than any which can be realized by man-made antennas alone, and hence by this method we may achieve communication over interstellar distances. Radio iconospheres of the sun are even more effective for this purpose. By the same principle, experiments in interstellar radar are possible. Of course, a peculiarity of two-way interstellar experiments is the long time interval (perhaps nine years) between transmission and reception of signals.

Conversely, since all of these things are possible to us, they are possible also to intelligent beings in other planetary systems, and so we may eventually communicate with such beings. Celestial iconospherics is the master key to exploration of the universe. Since it uses the most powerful of all lenses, namely the large celestial bodies themselves, it may indeed be called the "ultimate astronomy."

Closure

This brief essay leaves many questions not explicitly answered, but the purpose has been to introduce and define celestial iconospherics, to forecast the proper conduct of the exploration of the universe, and to open the way to further discussion.

Computation of Rocket Step Weights to Minimize Initial Gross Weight

RICHARD P. TEN DYKE[1]

The Ramo-Wooldridge Corp., Los Angeles, Calif.

The technique of dynamic programming is applied to the problem of finding optimum step weights of multistage rockets. If the design velocity requirement of the rocket system is determined, the velocity may be allocated to the various stages in such a manner that the initial gross weight is minimized. This approach permits the study of rockets with three and more stages, where the specific impulses for the stages are unequal, and where the jettison weight relations are nonanalytic. It is also possible to determine the relative flatness of optima with respect to any particular staging ratio with slight additional calculation. The approach outlined in this paper supplements but does not replace the use of calculus in solving the same problem where certain simplifying assumptions may be necessary.

Received Jan. 17, 1958.

[1] Member of the Technical Staff. Mem. ARS.

Definitions[2]

Step Rocket: A rocket system employing the technique of jettisoning structure weight during flight to increase performance. Also multistage rocket.

Stage: The period of time starting just after the jettison of one structural package and lasting until just after the jettison of the next, or the time from take-off to just after the first jettison (first stage) or, if no weight is jettisoned at last-stage burnout, from just after the last jettison to burnout.

Rocket weight: The initial gross weight at the start of a stage.

Step Weight: The sum of the propellant ejected during a stage and the weight jettisoned at the end of the stage. Also, the change of weight from the start of one stage to the start of the next.[2]

Stage Payload: All weight which remains after the jettison at the end of the stage. Rocket weight of next stage.

Rocket Payload: Payload of last stage.

Nomenclature

$f_k[V]$	=	minimum weight of rocket k achieving velocity V
g	=	gravitational constant 32.2 fps^2
I_i	=	specific impulse of stage i (thrust ÷ flow rate of fuel)
N_i	=	ratio of initial thrust to weight of rocket i
n	=	number of steps (the rocket payload may be considered the $(n + 1)$-step)
r_i	=	burnout mass ratio $W_i/(W_{i+1} + \sigma_i w_i)$
V_i	=	velocity ideally added by rocket i; rocket i design velocity
V_{bo}	=	actual burnout velocity of rocket system
V_t	=	design velocity of rocket system; also V_1
v_i	=	velocity ideally added during stage i
δV	=	velocity lost by rocket to effects of atmosphere and gravitation
W_i	=	initial gross weight of rocket i
W_L	=	rocket system payload weight
w_i	=	initial gross weight of step i
w_{zi}	=	that portion of stage i jettison weight which is constant (independent of step size or thrust)
$\alpha_i w_i$	=	portion of stage i jettison weight dependent on step weight
$\beta_i N_i W_i$	=	portion of stage i jettison weight dependent on thrust
$\sigma_i w_i$	=	total jettison weight of stage i

Subscripts

i = denotes ith step, stage or rocket
k = denotes kth rocket

Introduction

MANY authors (1–4)[3] have considered the problem of determining the optimum stage sizes as a straightforward minimization using calculus, and their results are very useful. To make hand computation possible certain simplifying assumptions are necessary, such as: (a) Two stages or less, (b) same specific impulse in all stages, or (c) structure proportional to size of step. For many problems the assumptions are quite reasonable, and the results are found to compare favorably with actual practice; however, problems arise where the simplifying assumptions must be verified or the problem solved by use of an alternate approach.

Such an alternate approach is outlined here. The use of

[2] Fig. 1 shows graphically the definitions of *rocket* and *step*.

[3] Numbers in parentheses indicate References at end of paper.

dynamic programming (5), a technique found useful in allocation problems, permits the operator to use structure factors which are nonanalytic with discontinuities. It also helps the operator to determine flatness of optima, which is valuable if the rocket must be designed away from the "ideal optimum" for any reason. It is particularly helpful in the study of rockets with three or more stages.

Hand computation with this approach is lengthy, but suitable for rockets of three or fewer stages. The technique is ready-made for machine computation if a large number of cases are to be investigated.

Suitable Optimization Parameters

The well-known rocket equation

$$v_i = I_{ig} \ln r_i \quad [1]$$

yields a relationship, independent of time, between the velocity ideally added to a rocket during a stage and the stage burnout mass ratio. This independence does not hold for actual surface-to-surface rockets because two time-dependent effects, atmosphere and gravitation, erode some of this velocity. The effects of atmosphere are: (a) Drag which increases with increasing velocity (and therefore acceleration) at low altitudes and (b) reduction of engine thrust due to atmospheric pressure. The effect of gravitation is to penalize the use of low acceleration in nonhorizontal trajectories.

However, studies of rockets flying realistic trajectories have yielded gratifying results. If we consider a given rocket with engines of constant flow rate, the velocity lost to gravitation and atmosphere, δV, is principally dependent on the ratio of initial thrust to initial weight for each stage, N_i, and is independent of range above 500 nautical miles. Fig. 2 presents this result. Thus, the simplified rocket equation, [1], may be used for design purposes if it is corrected by the additive constant δV. The sum of the stage design velocities is termed the rocket design velocity V_t.

$$V_t = \Sigma v_i = \Sigma I_{ig} \ln r_i = V_{bo} + \delta V \quad [2]$$

Of course range, not burnout velocity, is usually the desired result. The same studies show that for the maximum range trajectory, the burnout velocity essentially defines the range irrespective of other parameters. Although the actual burnout velocity required for a given range will depend on the burnout conditions, namely altitude, angle and down-range distance, deviations from nominal values will be comparatively small. Since burnout conditions are also greatly dependent upon the thrust-time program, corrections can be considered a part of the quantity δV. A curve of burnout velocity as a function of maximum range appears in Fig. 3.

It appears from the foregoing that the treatment of this optimization as an allocation (of velocity) problem is a practical approach where Equation [2] is the constraint and V_t is determined by the range requirement.

The General Optimization

The general optimzation assumes that the designer has the following "inputs" to the problem: (a) The specific impulse of fuel for each stage and (b) the jettison weight for each stage as a function of step weight or step propellant weight, of stage thrust and/or of velocity added or burnout mass ratio of each stage. For (a) the specific impulse is assumed constant for the duration of a stage but may vary in value from stage to stage. For (b) the function may be in analytic or tabular form except that if it is of certain forms computation is simplified.

Equation [1] yields a relationship between the design velocity of a stage and the stage burnout mass ratio. The inverse relation also holds.

$$r_i = \exp\left[\frac{v_i}{I_{ig}}\right] \quad [3]$$

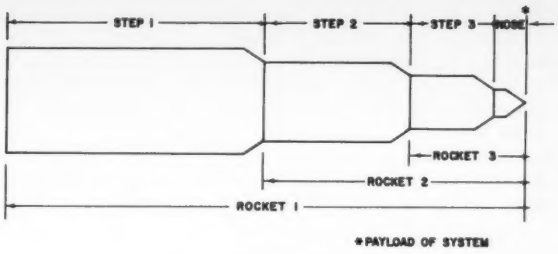

Fig. 1 Three-stage rocket

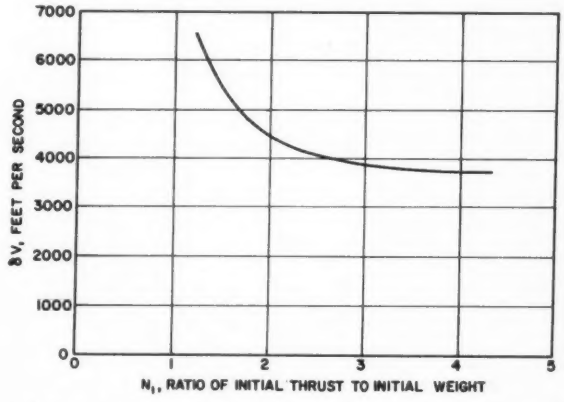

Fig. 2 Velocity lost to gravitation and atmosphere, δV, for a typical single-stage rocket

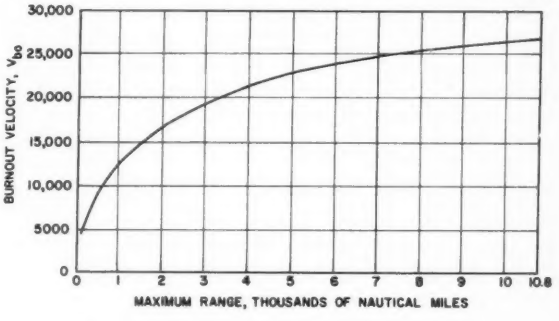

Fig. 3 Burnout velocity vs. maximum range

From the definitions

$$W_i = W_{i+1} + w_i \quad [4]$$

Solving for the weight of propellant

$$(1 - \sigma_i)w_i = \left(\frac{r_i - 1}{r_i}\right)(W_{i+1} + w_i) \quad [5]$$

From item (b) of the assumptions we say the jettison weight is a function h of the items listed

$$\sigma_i w_i = h[w_i, N_i, v_i] \quad [6]$$

Combining [5] and [6]

$$w_i = \left(\frac{r_i - 1}{r_i}\right)(W_{i+1} + w_i) + h[w_i, N_i, v_i] \quad [7]$$

For the nth stage of an n-stage rocket, the value W_{n+1} is simply the payload for the last stage, W_L, and is known. Solving for w_i we find it dependent upon three quantities.

$$w_i = w[W_{i+1}, v_i, N_i] \quad [8]$$

$$w_n = w[W_L, v_n, N_n] \quad [9]$$

These equations yield a dynamic programming problem in two variables, v and N. This can be reduced to a problem in one variable if N is held fixed. For considerations of performance only, the ratio of initial thrust to initial weight of the first stage should fall between one and four. For succeeding stages values above one are preferred, but lower values are acceptable for nearly horizontal thrust vectors. Conditions other than optimality may dictate a choice of N, but no attempt will be made here to consider these constraints.

Assume values for N_i are selected, then

$$w_i = w[W_{i+1}, v_i] \quad [8a]$$

$$w_n = w[W_L, v_n] \quad [9a]$$

Now define

$$f_k[V] = \underset{0 \le v_k \le V}{\text{minimum}} \left\{ w[f_{k+1}[V - v_k], v_k] + f_{k+1}[V - v_k] \right\} \quad [10]$$

where $f_{k+1}[V - v_k]$ is the minimum initial gross weight of the $k + 1$ rocket which achieves a velocity of $V - v_k$ and $w[f_{k+1}[V - v_k], v_k]$ is the weight of step k which achieves the velocity v_k. The sum $(V - v_k) + v_k$ is the velocity V, and v_k is selected to minimize the sum of the weights. This cannot be accomplished unless the weight of the payload, rocket $k + 1$, is known as function of the velocity added by the payload. This is known for the nth stage where the payload is known and the velocity added by the payload is zero.

$$f_n[V] = w[W_L, V] + W_L \quad [11]$$

When $f_n[V]$ is found and plotted against V, then f_{n-1} can be found using [10] and so on to f_1. Equations [10, 11] are the typical recurrence relationships found in allocation problems of one variable and are solved quickly by digital machines.

Sample Case

If n is small, say three or less, and the function $w[W_{i+1}, v_i]$ is simple to compute, a hand solution is practical. Consider the case where the stage jettison weight is

$$\sigma_i w_i = \alpha_i w_i + \beta_i N_i W_i + w_{xi} = h[w_i, N_i, W_{i+1}] \quad [12]$$

where α_i, β_i, and w_{xi} are constants. From [7]

$$w_i = \left(\frac{r_i - 1}{r_i} \right) (W_{i+1} + w_i) + \alpha_i w + N_i \beta_i (W_{i+1} + w_i) + w_{xi}$$

Substituting [3]

$$W_i = \frac{(1 - \alpha_i) W_{i+1} + w_{xi}}{\exp\left[\dfrac{-v_i}{I_{ig}} \right] - \beta_i N_i - \alpha_i} \quad [13]$$

If N_i are selected, the weight W_i is dependent only on the velocity gained, v_i, and the recurrence relations are

$$f_k[V] = \underset{0 \le v_k \le V}{\text{minimum}} \left\{ \frac{w_{xk} + (1 - \alpha_k) f_{k+1}[V - v_k]}{\exp\left[\dfrac{-v_k}{I_{kg}} \right] - \beta_k N_k - \alpha_k} \right\} \quad [14]$$

$$f_n[V] = \frac{w_{xn} + (1 - \alpha_n) W_L}{\exp\left[\dfrac{-V}{I_{ng}} \right] - \alpha_n - \beta_n N_n} \quad [15]$$

Flatness of Optima

For two-stage rockets, a single plot of f_1 vs. v_1 is sufficient to solve for a minimum and to get a picture of its flatness. For three or more stages additional plots will be required as functions of particular staging ratios. Fortunately, the information is available from the calculations.

References

1 Goldsmith, M., "On the Optimization of Two Stage Rockets," JET PROPULSION, vol. 27, April 1957, p. 415.

2 Malina, F. J., and Summerfield M., "The Problem of Escape from the Earth by Rocket," *Journal of the Aeronautical Sciences*, vol. 14, Aug. 1947, pp. 471–480.

3 Schurmann, Ernest E. H., "Optimum Staging Technique for Multi-staged Rocket Vehicles," JET PROPULSION, vol. 27, Aug. 1957, pp. 863–865.

4 Vertregt, M., "A Method for Calculating the Mass Ratios of Step Rockets," *Journal of the British Interplanetary Society*, vol. 15, March–April 1956, p. 95.

5 Bellman, R., "Dynamic Programming," Princeton University Press, Princeton, N. J., 1957.

Surface Combustion in Dissociated Air

SINCLAIRE M. SCALA[1]

General Electric Co., Philadelphia, Pa.

Nomenclature

A	=	atom
B_n	=	$X_n/\overline{\mathfrak{M}}$
f	=	similarity stream function
f_η	=	u/u_e
l	=	$\rho\mu/\rho_w\mu_w$
$\dot{m}_w$	=	combustion rate
$\mathfrak{M}_n$	=	molecular weight of the nth species
$\overline{\mathfrak{M}}$	=	$\sum_n x_n \mathfrak{M}_n$ mean molecular weight
M_1	=	first molecular species
M_2	=	second molecular species
M_n	=	$\mathfrak{M}_n/\overline{\mathfrak{M}}$
M_{ni}	=	$M_n - M_i$
Le	=	Lewis number
Pr	=	Prandtl number
T	=	temperature
u, v	=	tangential and normal components of velocity
x, y, r_0	=	body oriented coordinate system
X_n	=	mole fraction of nth species
$\left(\dfrac{du_e}{dx}\right)_s$	=	stagnation point velocity gradient
θ	=	T/T_e dimensionless temperature
μ	=	viscosity
ρ	=	density
η	=	similarity variable

Subscripts

e	=	outer edge of boundary layer
i	=	atomic species
j	=	first molecular species
k	=	second molecular species
n	=	nth species
s	=	stagnation point
w	=	wall
$\dot{\eta}$	=	denotes differentiation with respect to η

THE need for structural materials which are suitable for use as aerodynamic members at high temperature initiates the requirement for analytical techniques for studying the interaction between different classes of materials and chemically reacting flow fields. In order to explore the features involved in the theoretical determination of the combustion rate of a material immersed in a stream of dissociated air, two different models are considered for the combustion of graphite.

Some typical boundary layer profiles, near a surface at which combustion occurs, are shown in Fig. 1. It is noted that the physical extent of the boundary layer is not known a priori. Rather, in the absence of external forces, the various boundary layer profiles are governed by the presence of transport processes whose influence appears in the form of dimensionless groups such as the Reynolds, Prandtl and Lewis num-

Received Jan. 24, 1958.

[1] Research Engineer, Aerophysics Laboratory, Missile and Ordnance Systems Department. Mem. ARS.

bers. It is also noted that in the general treatment of compressible boundary layers with surface reactions, the equations of change can be uncoupled and solved individually only for special circumstances, such as isothermal flows over flat plates.

In addition, unlike surface catalysis (1, 2),[2] in which the macroscopic gas velocity vanishes at the surface, during surface combustion the normal component of velocity is not zero at the surface but is related to the rate at which the surface is consumed.

Reactions at surfaces generally occur in five steps, the slowest of which will determine the over-all rate of the process. It is usually considered that these successive steps include the transport of reactants to the surface, adsorption of the gases, combustion, desorption of the products or reactants, and transport of the liberated products back to the main stream by convection and diffusion.

If the surface reactions are extremely rapid, the rate-controlling step will be the diffusion process. That is, the combustion rate will depend on the quantity of reactant that can diffuse to the surface, in the presence of a counter-diffusion of combustion products.

For simplicity, it will be assumed here that gas phase reactions can be neglected; i.e., the boundary layer is frozen. Then, upon utilizing a similarity transformation, the stagnation point boundary layer equations for a three-component compressible chemically reacting gas, in which homogeneous reactions are frozen, become (3)

$$[lLe\overline{\mathfrak{M}}^{-1}(M_kX_{i\eta} + M_{kj}X_{j\eta})]_\eta + fPrB_{i\eta} = 0 \quad [1]$$

$$[lLe\overline{\mathfrak{M}}^{-1}(M_kX_{j\eta} + M_{ki}X_{i\eta})]_\eta + fPrB_{j\eta} = 0 \quad [2]$$

which are the equations for the conservation of the ith and jth diffusing species

$$(lf_{\eta\eta})_\eta + ff_{\eta\eta} + \frac{1}{2}\left[\frac{\overline{\mathfrak{M}}_e}{\overline{\mathfrak{M}}}\theta - f_\eta^2\right] = 0 \quad [3]$$

which is the momentum equation, and

$$(l\theta_\eta)_\eta + fPr\theta_\eta + lLe[M_{ki}M_jX_{i\eta} + M_{kj}M_iX_{j\eta}]\theta_\eta = 0 \quad [4]$$

which is the energy equation. In deriving Equations [1–4] which constitute a coupled ninth order system of nonlinear differential equations, it was assumed that the Prandtl and Lewis numbers were constant, and that the specific heats were constant and equal for all species.

In the theoretical models considered here, it was assumed that by appropriate "lumping" of those species whose thermal and chemical behavior is sufficiently similar, dissociated air and the gaseous combustion products may be represented by a three-component system, denoted by subscripts i, j and k (see Fig. 2).

The two models considered were: (a) Nitrogen is an inert diluent (model I). (b) Oxygen and nitrogen react completely to form CO and CN, i.e.

$$X_{iw} = X_{jw} = 0 \text{ (model II)}$$

The relevant surface boundary conditions were derived and solutions were obtained (3) by means of a Reeves analog computer (REAC).

The combustion rate is given by

$$\dot{m}_w = -\sqrt{2\rho_w\mu_w\left(\frac{du_e}{dx}\right)_s}\, f_w \quad [5]$$

and a universal solution for all combinations of free stream conditions and wall temperatures is shown in Fig. 3 for model II, a Prandtl number of 0.75 and a Lewis number of 1.2. Note that since X_{k_e} is always zero (see Fig. 1), and since $\Sigma X_n = 1$, the specification of X_{i_e} determines the free stream dissociation level. That is, when $X_{i_e} = 0$, the free-stream air is undissociated and when $X_{i_e} = 1.0$, it is entirely dissociated.

The solutions obtained for model I yielded values for $\dot{m}_w$ which were of the order of 25 per cent of those obtained for model II.

[2] Numbers in parentheses indicate References at end of paper.

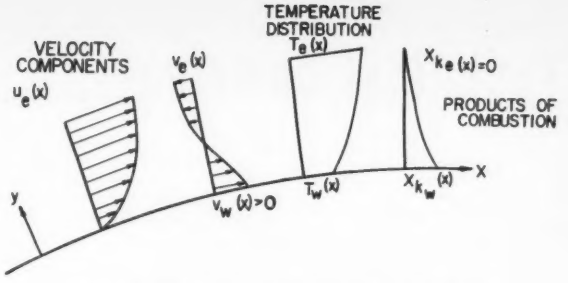

Fig. 1 Typical combustion boundary layer profiles

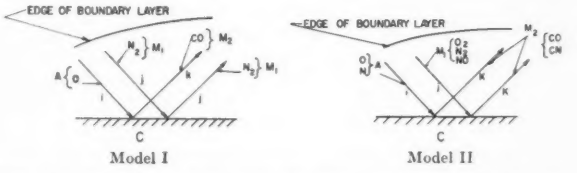

Fig. 2 Models for the combustion of graphite. Model I: no nitrogen reactions; model II: nitrogen reactions allowed

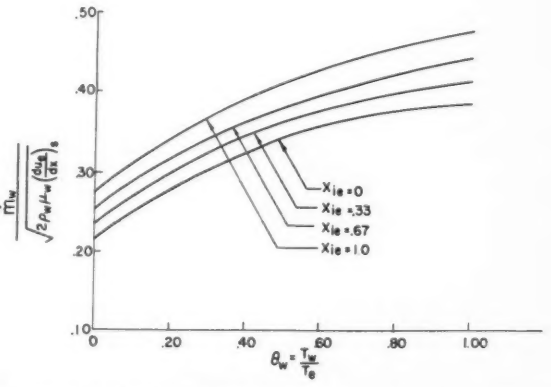

Fig. 3 Variation of combustion rate with surface temperature, model II

Acknowledgments

The author would like to acknowledge the assistance of Miss M. C. FitzGibbon in obtaining the analog results, and Miss K. J. Burke in reducing the data.

References

1 Chambre, Paul L., "On Chemical Surface Reactions in Hydrodynamic Flows," *Applied Scientific Research*, Section A, vol. 6, pp. 97–113.

2 Scala, Sinclaire M., "Hypersonic Heat Transfer to Surfaces Having Finite Catalytic Efficiency," General Electric Co., Aerophysics Laboratory Memo. 4.

3 Scala, Sinclaire M., "The Laminar Diffusion Boundary Layer with Surface Combustion," General Electric Co., Aerophysics Laboratory Memo. 6.

Technical Comments

Comment on 'Stresses in Rocket Grains'[1]

W. T. COX[2]

Aerojet-General Corp., Azusa, Calif.

IN ATTEMPTING to apply Equation [9] of "Preliminary Photoelastic Design Data for Stresses in Rocket Grains,"[1] we have arrived at unreasonably high calculated circumferential stress on the internal surface of a case-bonded propellant charge. Moreover, the sign of the estimated stress was opposite from what one would expect. Subsequently this matter was called to the attention of one of the authors, M. L. Williams, who has explained the discrepancy as being the result of omitting certain terms in expanding the denominator of Equation [8]. This omission limits the applicability of Equation [9] to cases in which the ratio Ec/E is of the order one.

Since this ratio may be several hundred, even for low temperature conditions and high rates of strain under which the mechanical properties of the propellant approach those of an elastic material, caution should be used in employing the simplified Equations [8a and 9].

Received Feb. 7, 1958.

[1] Ordahl, D. D., and Williams, M. L., "Preliminary Photoelastic Design Data for Stresses in Rocket Grains," JET PROPULSION, vol. 27, June 1957, pp. 657–662.

[2] Senior Technical Specialist. Mem. ARS.

Corrections to 'Comments on the Powered Flight Trajectory of a Satellite'[1]

BURTON D. FRIED[2]

The Ramo-Wooldridge Corp., Los Angeles, Calif.

THE optimum steering program for the powered flight trajectory of a satellite launcher is given by[3]

$$\tan \psi = a - bt \qquad [1]$$

where ψ is the angle between the thrust vector and the horizontal at time t and a and b are constants whose values depend on the thrust and mass programs. The conditions for the validity of [1] are: (a) The missile is treated as a point particle. (b) The distance covered during *powered* flight is small compared to the earth's radius R_e, so that the gravitational force field may be taken as uniform during powered flight. (c) Aerodynamic forces are neglected. (d) The quantity W to be optimized (i.e., made stationary) is a function only of burnout velocity and altitude, for instance, the orbit altitude at perigee (if W depends also on the range at burnout, $\tan \psi$ simply becomes instead a quotient of two linear functions of t).[4] (e) The time of powered flight is short compared to[5]

$$t^* \equiv \sqrt{R_e/2g} = 9.5 \text{ min}$$

where g is the gravitational acceleration.

In a recent note,[1] Edelbaum remarks that the analysis leading to [1] does not include "the effect of centrifugal force, which is significant for satellite launching vehicles," thereby inferring that "centrifugal force" effects may invalidate [1]. This is incorrect. So long as conditions (a) through (e) are satisfied, the program [1] will give a stationary solution for a W of the form specified in (d) *independent* of whether the velocity during powered flight becomes equal to or even greatly exceeds the standard satellite velocity $v_s = \sqrt{gR_e}$.

Edelbaum's error is an understandable one, stemming from a common misinterpretation of "centrifugal force." The point is simply that *if (b) is satisfied*, then we may analyze the powered flight trajectory in Cartesian coordinates. The total force acting on the missile consists only of the thrust force and the gravitational force; there is *no* "centrifugal force" (the earth's rotation being neglected, of course), *regardless* of the magnitude of the missile's velocity. Of course, one may choose to use polar coordinates (r, θ) in place of (x, y) to describe the motion, as Edelbaum does, and one then finds in the equations of motion a "centrifugal" pseudo-force, $mv^2\mathbf{r}/r^2$. However, so long as (b) is satisfied the choice of coordinates clearly cannot affect the answer and a correct calculation in any coordinate system must again lead to [1].

To demonstrate this analytically, we use the general result[5] that if condition (b) is absent and the equation of motion for the point mass missile is assumed to be

$$\ddot{\mathbf{r}} = n\mathbf{N} + \boldsymbol{\alpha} \qquad (t_0 \leq t \leq t_1) \qquad [2]$$

where n is the acceleration due to thrust, $\mathbf{N}$ is a unit vector along the thrust, and $\boldsymbol{\alpha}$ is the gravitational acceleration

$$\boldsymbol{\alpha} = -gR_e^2\mathbf{r}/r^3 \qquad [3]$$

then the optimum direction of thrust is along the vector $\boldsymbol{\lambda}(t)$ defined by the differential equation

$$\ddot{\boldsymbol{\lambda}} - \nabla\boldsymbol{\alpha}\cdot\boldsymbol{\lambda} = 0 \qquad [4]$$

and boundary conditions which depend on the particular optimization problem at hand. For instance, if we wish to make stationary a function $W(\mathbf{r}_1, \mathbf{v}_1)$ of the burnout position and velocity for given initial conditions $\mathbf{r}_0$, $\mathbf{v}_0$ and given $n(t)$, then we have

$$\boldsymbol{\lambda}(t_1) = -\nabla_{\mathbf{v}_1} W \qquad \dot{\boldsymbol{\lambda}}(t_1) = \nabla_{\mathbf{r}_1} W \qquad [5]$$

As a result of the vector methods, it is clear that when condi-

Received Feb. 28, 1958.

[1] Edelbaum, T. N., "Comments on the Powered Flight Trajectory of a Satellite," JET PROPULSION, vol. 27, Dec. 1957, pp. 1260–1261.

[2] Physical Research Laboratory.

[3] Fried, B. D., "On the Powered Flight Trajectory of an Earth Satellite," JET PROPULSION, vol. 27, June 1957, pp. 641–643.

[4] Lawden, D. F., "Optimal Flight Trajectories," JET PROPULSION, vol. 27, Dec. 1957, p. 1263.

[5] Fried, B. D., "Space Technology," Wiley and Sons, Chap. 2b (to be published).

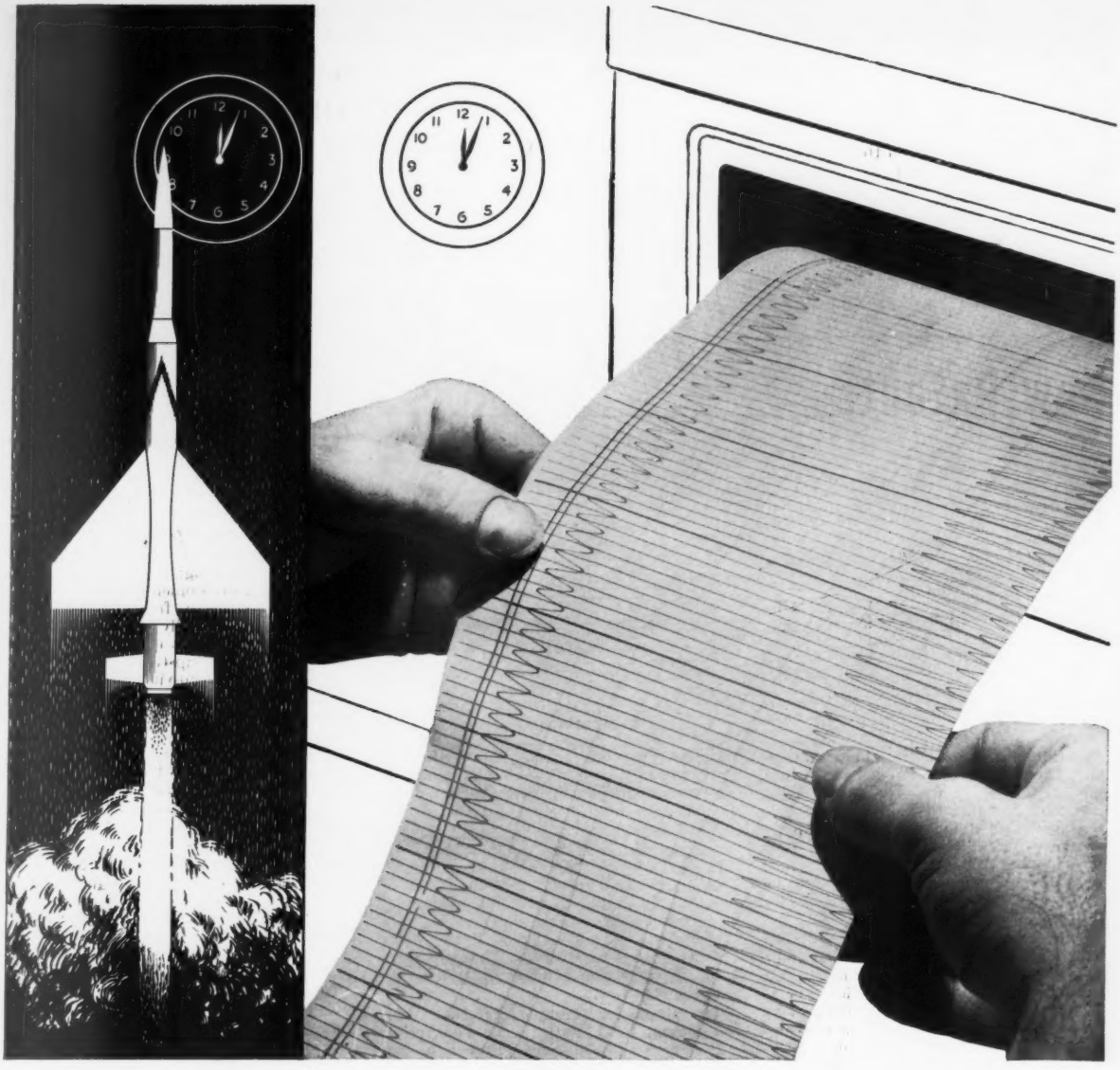

For records you can read at once . . . new Kodak Linagraph Direct Print Paper

This paper is designed for use when you must know what's happening while it's happening . . . in such applications as rocketry, control, computing, product design, component testing and nuclear research. It requires no processing, comes out of the recording instrument ready to read.

To get such instant monitoring of high-speed variables you eliminate the powerful energy amplification factor of photographic development. Traces must be put down by a high-intensity u-v light source.

Kodak Linagraph Direct Print Paper gives you a wide range of recording speeds—from 0 to 3,000 cps. Records have adequate permanence for extended storage. If used under sunlight or fluorescent lamps they should be stabilized. The surface of the paper takes notations in pencil or ink. Records are suitable for use in recording system readers.

Several major manufacturers now offer recording instruments based on the characteristics of Kodak Linagraph Direct Print Paper. We'll gladly send you their names on request. If you want more detailed information on the paper, we'll send that too.

EASTMAN KODAK COMPANY
Graphic Reproduction Division
Rochester 4, N. Y.

Kodak

tion (b) is satisfied so that we can set $\nabla\alpha = 0$, then $\ddot{\lambda} = 0$, and for the boundary conditions [5]

$$\lambda = \nabla_{v_1} W + (t_1 - t)\nabla_{r_1} W \quad \ldots\ldots\ldots\ldots [6]$$

When $\partial W/\partial x_1 = 0$, this is just equivalent to [1]. One may, as stated above, resolve [2, 4] into polar coordinates and then solve for λ_r and λ_θ, but in the resultant algebraic complexity it is possible to lose sight of the simple result [6].

Of course, when $\nabla\alpha \neq 0$, [1, 6] are no longer valid and we must solve the coupled system of Equations [2, 4]; but this is simply a consequence of the failure of condition (b) and *not* of any "centrifugal force" effects. It is interesting to note that the first correction to the $\nabla\alpha = 0$ result, obtained by neglecting the distance from launch to burnout *after* computing $\nabla\alpha$ rather than before, gives

$$\nabla\alpha = \omega^2 \begin{pmatrix} -1 & 0 \\ 0 & 2 \end{pmatrix} \qquad (\omega^2 \equiv g/R_e) \quad \ldots\ldots\ldots [7]$$

and hence, from [4 and 5] in Cartesian coordinates

$$\left.\begin{aligned} \lambda_x &= -(\partial W/\partial v_{1x}) \cos \omega(t - t_1) + \\ &\qquad [(\partial W/\partial x_1) \cdot \sin \omega(t - t_1)]/\omega \\ \lambda_y &= -(W/\partial v_{1y}) \cos h\sqrt{2}\,\omega(t - t_1) + \\ &\qquad [(\partial W/\partial y_1) \cdot \sin h\sqrt{2}\,\omega(t - t_1)]/\sqrt{2}\,\omega \end{aligned}\right\} \quad \ldots [8]$$

If $(t_1 - t_0) \ll 1/\sqrt{2}\,\omega$, as required by condition (e), then [8] reduces to [6].

New Patents

George F. McLaughlin, *Contributor*

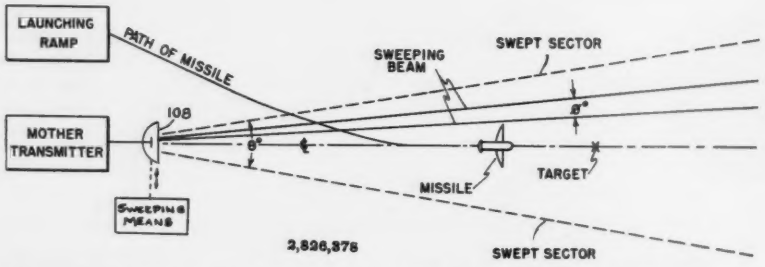

Apparatus for radio control of guided missiles (2,826,378). J. N. Childs Jr., Wyndmoor, Pa.

Mother equipment is a directional transmitter for providing a very narrow rapidly sweeping radio beam. When the time intervals between successive signals at the missile are equal, the missile is traveling down the center line of the swept sector directly toward the target.

Control system for guided missiles (2,824,710). A. C. Hale, Bloomfield Township, Mich., assignor to U. S. Air Force.

Homing missile of the glider type in which aerodynamic control is effected by elevons. Homing information is provided in the form of right-left and up-down error signals and means for measuring differences between roll and pitch angles.

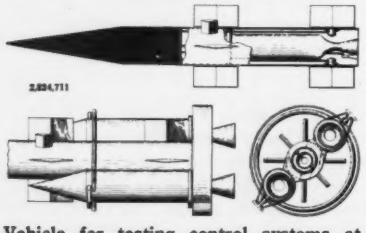

Vehicle for testing control systems at supersonic speeds (2,824,711). H. H. Porter, Washington, D. C., assignor to U. S. Navy.

Rocket engine powered guided missile having a forward compartment for containing guidance equipment to be tested.

Device for indicating the relative movement of the earth and a heavenly body (2,825,151). R. H. Farguhar, Philadelphia, Pa.

Time ring within a transparent globe and fixed to a shaft passing through its axis of rotation. A second shaft carries a head representing a satellite rotatable in a great circle path adjacent to the outer surface of the globe.

Aerodynamic valves (2,825,203). J. H. Bertin and A. R. Mihail, Asnieres, France, assignors to SNECMA Co.

Pulsejet unit with resonant firing combustion chamber. Valveless unilaterally conductive air inlet device offers greater resistance to backflow of hot gases from the chamber than the flow of fresh air into the chamber.

Jet propulsion units (2,825,204). M. Kadosch, F. G. Paris, J. Le Foll and J. Bertin, Neuilly-sur-Seine, France, assignors to SNECMA Co.

Combustion apparatus for generating a continuous flow of motive gas. Two divergent jet pipes have means for urging the gas to flow successively and intermittently toward one inlet and then the other.

Combustion devices especially suitable for gas turbine engines and propulsion units for aircraft (2,825,205). G. Racine, Paris, France, assignor to SNECMA Co.

Jet propulsion engine with a flame-holding device comprising an auxiliary compressor which discharges fluid into the combustion chamber at an inclination from the axial flow, forming transverse fluid jets creating a wake zone in which a flame can be held.

Polycyclic aldehydes as hypergolic fuels (2,826,037). C. R. Scott and J. V. Smith, Bartlesville, Okla., assignors to Phillips Petroleum Co.

Separate and simultaneous injection of an oxidant and fuel into contact with each other in the combustion chamber of a reaction motor. Fuel is composed of an aldehyde of hydrogen atom, a methyl radical, a hydrogen atom and an alkyl radical having carbon atoms.

Gas inlet structure for combustion chambers (2,826,039). P. F. Ashwood, Farnham, England, assignor to Power Jets (Research and Development) Ltd.

Channel extending from the combustion chamber wall inwardly across the combustion reaction flow path. The open side of the channel faces upstream and a part of the gas is directed into it from the chamber.

Vortex tube free air thermometer (2,826,070). H. C. Box and L. S. Packer, Eggertsville, N. Y.

Cylindrical inlet conduit with a portion terminating in a right angle defining an elliptical-shaped opening for exhausting the air. A fairing maintains a static pressure region in the air stream adjacent to the exhaust opening.

High speed sampler (2,826,075). R. J. Vernier, Baltimore, Md., assignor to U. S. Army.

Atmospheric sampler comprising a filter disk locked in a hollow holder ring to which a suction tube is attached. Suction applied to the ring causes ejection of the disk.

Torpedo suspension band (2,826,119). A. H. Barrowman, Attleboro, Mass., assignor to U. S. Navy.

Apparatus for suspending a missile from an aircraft having a bombrack and movable supporting hook.

Mechanism for ejecting rockets from an aircraft (2,826,120). J. M. Land and R. P. Graham, Stratford, Conn., assignors to Chance Vought Aircraft, Inc.

Pair of drums mounted within the body of an airplane. Plungers eject rockets from opposite sides of the aircraft through openings in the drums.

Signal device (2,826,144). Yukichi Inata, Tokyo, Japan.

Tubular waterproof container having a storage chamber with inflammable powder. Release of a spring-tensioned trigger causes a rod composed of ignitable material to rub against an abrasive surface on the container wall.

Alloy steel for use at high temperatures (2,826,380). W. R. Kegerise, Reading, Pa., assignor to Carpenter Steel Co.

Alloy capable of being hardened to show a martensitic structure, good corrosion resistance, ductility and life at temperatures up to 1200 F, high impact strength, and machineable at room temperature.

EDITORS NOTE: Patents listed above were selected from the Official Gazette of the U.S. Patent Office. Printed copies of patents may be obtained from the Commissioner of Patents, Washington 25, D. C., at a cost of 25 cents each; design patents, 10 cents.

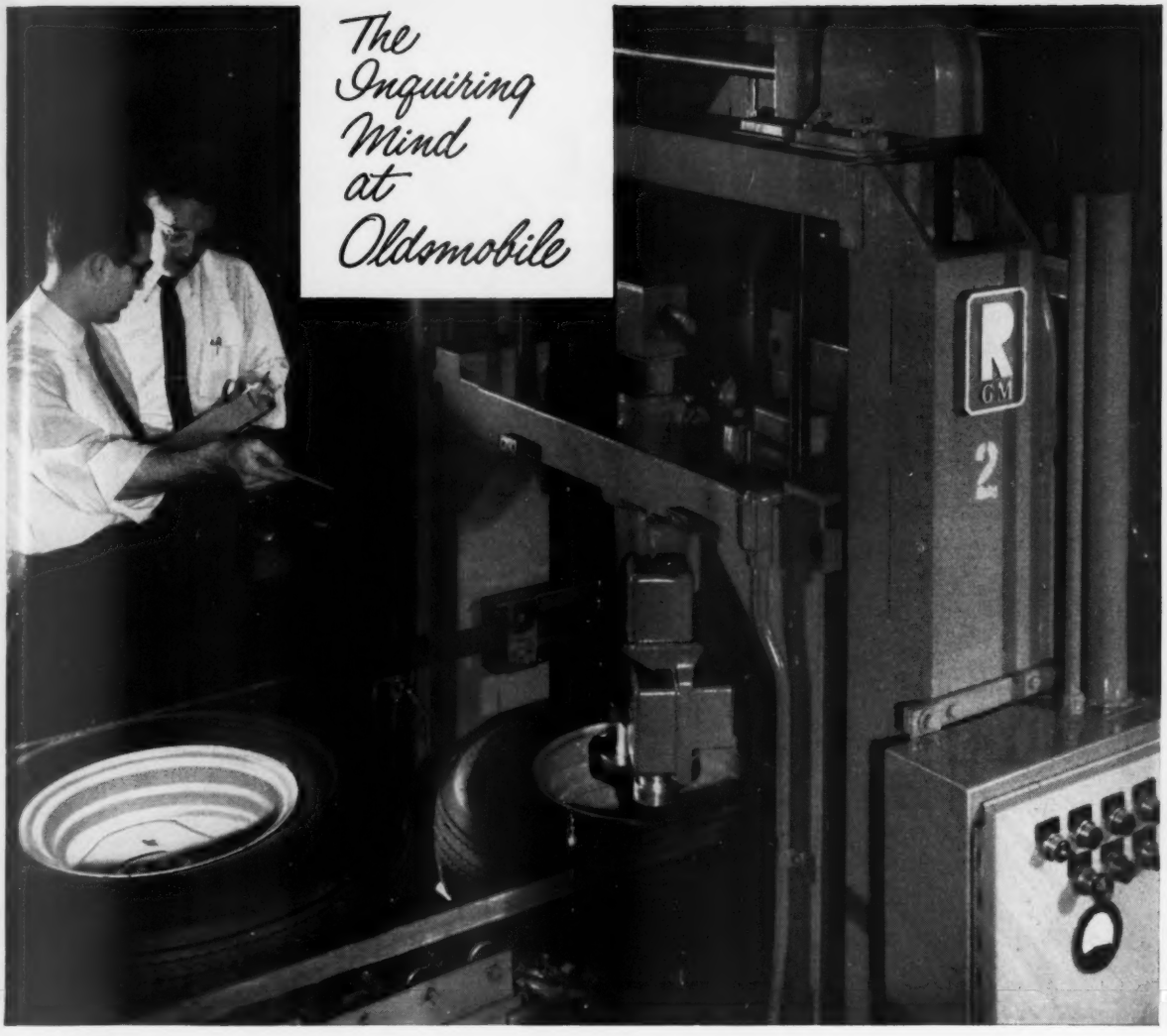

no. 3 OF A SERIES

TIPPING THE BALANCE IN YOUR FAVOR

New Olds-developed machine makes wheel balancing three times more accurate!

Out-of-balance wheels and tires are not only a source of annoyance and tire wear, but also in extreme cases, a detriment to safety by causing excessive shimmy at higher speeds.

To virtually eliminate this problem, Oldsmobile engineers, in conjunction with the General Motors Research Section, have developed a machine that automatically balances every wheel and tire with a degree of precision not previously possible on a production basis. With this equipment, balancing is now accurate to 2 inch-ounces, or approximately three times more precise than before.

The heart of such accuracy is an automatic electronic computing device. After the tire and wheel are located on a delicate sensing table, supported on an air bearing, four differential transformers signal the out-of-balance to an electronic computor. This computor then resolves the vector forces and a signal of the proper magnitude and direction is transmitted to the stamping head which automatically revolves to the correct location on the wheel. The stamping head then prints the correct weight, accurate to .25 ounce. The entire assembly is then moved to a station where the weights are attached.

It has often been said that "Olds really knows how to put a car together." This reputation grew from a sincere concern for just such little-noticed details. A warm welcome awaits you at your Olds dealer's. He invites you to try a '58 Olds on the road.

OLDSMOBILE DIVISION
GENERAL MOTORS CORP.

OLDSMOBILE

Pioneer in Progressive Engineering ...Famous for Quality Manufacturing

MISSILE HARDWARE

By

NEWBROOK

• • • we have the "Know-How!"

We have developed new techniques, new methods, new processes that effect production economy so necessary to a successful missile program.

Here at Newbrook you will find men with experience gained from doing . . . a modern plant with up-to-date equipment . . . precision inspection to meet your most exacting quality control requirements.

And most important, Newbrook specialization results in strict reliability ! Let us help you with your Missile Hardware problems.

Specializing in

- **Motor Cases** *Solid and Liquid propellants*
- **Jato Cases**
- **Nozzles**
- **Plenum Chambers**
- **Blast Tubes**
- **Fuel Injectors**

Phone or Write

NEWBROOK MACHINE CORPORATION

20 Mechanic Street ***Phone 45***

SILVER CREEK, NEW YORK

Contains carbon, silicon, manganese chromium, molybdenum, copper, nitrogen and iron.

Bearing cooling system (2,826,895). W. P. English, Northport, N. Y., assignor to Fairchild Engine and Airplane Corp.

Gas turbine engine housing with a discharge opening and an exhaust nozzle forming an air chamber in which the exhaust gases create an aspirating effect for cooling the tail cone interior.

Rocket dispensers (2,826,961). J. J. White, Washington, D. C., assignor to ACF Industries, Inc.

For installation on high speed aircraft, an outer shell with a conical nose spaced from a tubular body. A dispensing tube in the shell has a conical sheath with its rear end attached to a bulkhead. The sheath expands radially to permit passage of a rocket between the nose and body.

Container for high pressure fluids (2,827,195). T. F. Kearns, Arlington, Va.

Spherical liner over which a wire mesh is wound in layers. Tension in the wires is increased in each layer, moving outwardly from the liner.

Gas turbine aircraft powerplant (2,827,759). B. W. Bruckmann, Dayton, Ohio, assignor to the USAF

Engine with contraflow air-fuel combustion system. An air-fuel escape nozzle is directed forwardly in the combustion chamber to deliver the mixture directly against the oncoming compressed air. A gas exhaust jet leads from the outlet side of the turbine to free air.

Combined anti-icing and generator cooling arrangement for a gas turbine engine (2,827,760). F. C. I. Marchant and J. E. Bell, Mangotsfield, England, assignor to Bristol Aero Engines, Ltd.

Air outlets from hollow spider arms discharge compressed air to a double-walled entry nose bullet housing the electrical generator.

Constant speed reaction motor (2,827,762). M. C. Towns Jr., Morristown, N. J., assignor to Reaction Motors, Inc.

Means for admitting a propellant to the reaction chamber in regulated amounts to automatically maintain a given speed, the supply being unaffected by centrifugal forces.

Ion tracer airspeed indicator (2,827,786). B. Boyd, R. G. Dorsch and G. H. Brodie, Bedford, Ohio, assignors to U. S. Navy.

Apparatus for indicating the speed of an airstream flowing along a surface by means of an ion bundle created in the airstream by corona discharge.

Gyroscope (2,827,788). A. M. Campbell, Weston, Mass., assignor to Minneapolis-Honeywell Regulator Co

Internally threaded hollow stator mounted within a hollow rotor. Static balance is achieved by an externally threaded mass in the stator moved along the rotor axis upon rotation of the mass.

Control arrangements for craft operable in space (2,827,789). K. A. Oplinger and I. M. Holliday, Venice, Calif., assignors to Westinghouse Electric Corp.

Gyroscope with an inertia member mounted for rotation about a pivot axis. The pointed end of an electromagnet core remains within the boundary of an opening in an armature over the range of relative movement of the frame members.

Planetarium projector (2,827,827). A. N. Spitz, Lansdowne, Pa.

Spherical mirror centered in a hemispherical perforated globe. High intensity light source in the zenith position in the globe directs rays to the mirror, passing through perforations and reflected to the globe.

AUXILIARY POWER for the U.S. Army's deadly NIKE HERCULES

AiResearch units power the controls of America's most potent defense weapons

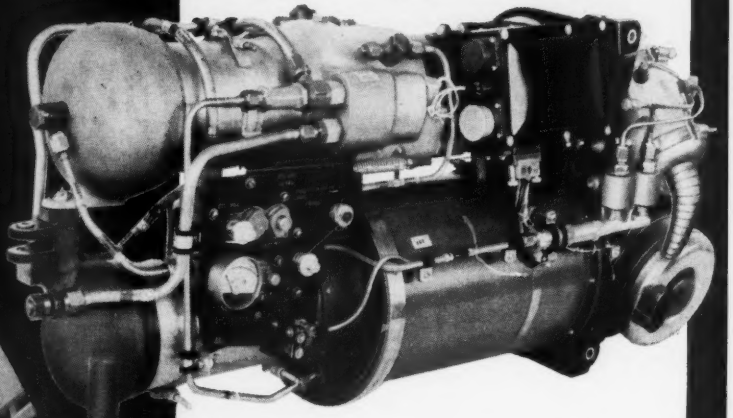

Key defense and population centers are now being ringed with batteries of Army Nike Hercules missiles to deter or destroy aggressors. *Supplying power for flight controls* is the AiResearch auxiliary power unit pictured above, now in production.

As a member of the Army-industry team producing the Nike Hercules (Army Ordnance, Western Electric-Bell Telephone Laboratories and Douglas Aircraft), AiResearch was chosen to design, develop and manufacture this vital accessory power source for the missile because of nearly two decades of experience in lightweight turbomachinery.

This experience includes applications utilizing solid propellants, liquid mono-propellants, bi-propellants, atomic power, cryogenic gases as well as gasoline and air. AiResearch's ability for high capacity production as well as in research and development, made it the logical choice.

Garrett's AiResearch divisions have also designed systems and components for 18 other missiles and rockets in the U.S. defense arsenal.

We invite your inquiries.

ENGINEERING REPRESENTATIVES: AIRSUPPLY AND AERO ENGINEERING, OFFICES IN MAJOR CITIES

THE GARRETT CORPORATION

AiResearch Manufacturing Divisions

Los Angeles 45, California • Phoenix, Arizona

Systems, Packages and Components for: AIRCRAFT, MISSILE, ELECTRONIC, NUCLEAR AND INDUSTRIAL APPLICATIONS

Technical Literature Digest

M. H. Smith, *Associate Editor*, and M. H. Fisher, *Contributor*
The James Forrestal Research Center, Princeton University

Jet and Rocket Propulsion Engines

Propellant Vaporization as a Criterion for Rocket-Engine Design; Calculations Using Various Log-Probability Distributions of Heptane Drops, by Richard J. Priem, *NACA TN* 4098, Oct. 1957, 29 pp.

Design and Evaluation of a Turbojet Exhaust Simulator, Utilizing a Solid-Propellant Rocket Motor, for Use in Free-Flight Aerodynamic Research Models, by Carlos A. deMoraes, William K. Hagginbothom Jr. and Ralph A. Falanga, *NACA RM* L54I15, Dec. 1954, 25 pp. (Declassified from Confidential by authority of *NACA Res. Abstracts* 120, p. 11, 10/3/57.)

Investigation of Blade Failures in a J34, Eleven-Stage Axial-Flow Compressor, by Howard F. Calvert, Andre J. Meyer Jr. and C. Robert Morse, *NACA RM* E52I16, May 1953, 24 pp. (Declassified from Confidential by authority of *NACA Res. Abstracts* 120, p. 8, 10/3/57.)

Jet Engine Thrust Reversers, by Robert C. Kohl and Joseph S. Algranti, *SAE J.*, vol. 65, no. 11, Oct. 1957, pp. 38–40.

Experiment Investigation of a Rocket Source for a High Temperature Wind Tunnel, by F. K. Hill and H. A. Wallskog, *Johns Hopkins Univ., Applied Phys. Lab.*, CM-907, July 1957, 46 pp.

Dynamic Response Characteristics of Gas Turbines, by S. L. Soo and William W. S. Charters, *ASME Prep.* 57-F-22, Sept. 1957, 17 pp.

General Design Considerations for Smaller Gas Turbines, by W. T. von der Nuell, *ASME Paper* 57-F-13, Sept. 1957, 17 pp.

British Aero Engines, *Aeronautics*, vol. 37, Sept. 1957, pp. 102–127.

Designing the World's Most Powerful Turbojet, by Randolph Hawthorne, *Aviation Age*, vol. 28, Oct. 1957, pp. 26–31.

Scale Effect in a Gas Turbine Combustion Chamber Fitted with a Swirl Atomizer, Part 1, by M. V. Herbert and J. A. Bamford, *Combustion and Flame*, vol. 1, no. 3, Sept. 1957, pp. 360–378.

Mach 4 Turbojets, by J. S. Butz Jr., *Aviation Week*, vol. 67, no. 17, Oct. 28, 1957, pp. 86–89.

Aerodynamics of Jet Propelled Vehicles

Theoretical Aerodynamic Force and Moments for a Slender Body Moving Through the Flow Field of a Slender Body, by Henry W. Woolard, *Cornell Aeron. Lab. Inc., Rep.* QC-910-C-15, Oct. 1956, 25 pp

Laminar Boundary Layer on a Spinning Circular Cone in Supersonic Flow at a Small Angle of Attack, Part II, by Martin Fiebig, *Cornell University, Grad. School of Aeron. Engng.* (*AFOSR-TN*-57-68; *ASTIA AD* 120410), Feb. 1957, 14 pp.

Inviscid Hypersonic Flow over Blunt Nosed Slender Bodies, by Toshi Kubota, *Stanford Univ., Stanford, Calif., Preprints of papers, Heat Transfer and Fluid Mechanics Inst.*, 1957, 439 pp., pp. 193–210.

Measurement of the Moment of Inertia of Missile-Type Bodies, by A. B. Schwartz, S. Malick and J. R. Friesen, *Aircraft Engng.*, vol. 29, Sept. 1957, pp. 271–274.

Formulas for the Velocity Potential of Linear Subsonic and Supersonic Flow for Not-so-slender Bodies at Zero Lift, by Friedrich Keune, *Z. Flugwiss.*, vol. 5, Aug. 1957, pp. 243–247 (in German).

Heat Transfer and Fluid Flow

Condensation Interfaces in Two Phase Flows, by P. Chiarulli and R. F. Dressler, *Nat. Bur. Standards Rep.* 5341, April 1957, 14 pp.

On Menard Inserts in Supersonic Nozzles, by J. L. Amick, S. A. Harrington and H. P. Leipman, *Univ. Michigan, Engng. Res. Inst., Tech. Rep.* CF 2656, May 1957, 8 pp.

Mass Transfer Cooling of a Laminar Boundary Layer by Injection of a Light Weight Foreign Gas, by E. R. G. Eckert, P. J. Schneider, A. A. Hayday and R. M. Larson, *Univ. Minnesota, Inst. Tech., Mech. Engng. Dept., TN* 14 (*AFOSR-TN*-57-323; *ASTIA AD* 1382395), June 1957, 45 pp.

Growth of Drops by Condensation, by Ignace I. Kolodner, *N. Y. Univ., Inst. Math. Sci., Rep.* IMM-NYU 215 (*ASTIA AD* 121943), March 1955, 28 pp.

Evaporation of Fuel Sprays, II: Experimental Work, by G. W. Bensor and R. J. Brisebois, *Canada, Nat. Aeron. Estab., Lab. Rep.*, LR-182 (*ASTIA AD* 121802), Nov. 1956, 15 pp.

The Thermal Properties of Carbon Dioxide, Nitrogen, Air, Hydrogen and Helium, by A. W. Nicklin, *Gt. Brit., Atomic Energy Authority, Industrial Group, TN* 36, Nov. 1956, 9 pp.

The Sound Generated by Interaction of a Single Vortex with a Shock Wave, by G. I. Ram and H. S. Ribner, *Preprints of papers, Heat Transfer and Fluid Mechanics Inst.*, 1957, pp. 1–22.

The Chemical Kinetics of Air at High Temperatures; a Problem in Hypersonic Aerodynamics, by Saul Feldman, *Preprints of papers, Heat Transfer and Fluid Mechanics Inst.*, 1957, pp. 173–192.

An Investigation of Stagnation Point Heat Transfer in Dissociated Air, by Peter H. Rose and F. R. Riddell, *Preprints of papers, Heat Transfer and Fluid Mechanics Inst.*, 1957, pp. 231–248.

An Experimental Investigation of the Secondary Flow Occurring in a Compressor Cascade, by W. D. Armstrong, *Aeron. Quart.*, vol. 8, Aug. 1957, pp. 240–256.

The Smoothing of Temperature Fluctuations by Radiative Transfer, by Edward A. Spiegel, *Astrophysical J.*, vol. 126, July 1957, pp. 202–207.

Heat Transfer to Boiling Methanol, by A. J. Lowery Jr. and J. W. Westwater, *Indust. Engng. Chem.*, vol. 49, Sept. 1957, Pt. 1, pp. 1445–1448.

Combustion, Fuels and Propellants

What's All This Talk about Exotic Propellants? by John F. Tormey, *Missiles and Rockets*, vol. 2, Sept. 1957, pp. 93–94.

Fluorine: Tamed for Rockets, by H. R. Neumark and F. L. Holloway, *Missiles and Rockets*, vol. 2, Sept. 1957, pp. 97, 99–100.

Liquid Propellants for Manned Rocket Aircraft, by William Mitchell, *Missiles and Rockets*, vol. 2, Sept. 1957, pp. 109–110, 112, 114.

Dimazine Comes of Age as Rocket Fuel, by William G. Strunk, *Missiles and Rockets*, vol. 2, Sept. 1957, pp. 116–118, 120.

LOX—Mainstay Oxidizer for the Missile Age, by William H. Thomas, *Missiles and Rockets*, vol. 2, Sept. 1957, pp. 131–132.

An Investigation of the Behavior and Reaction Mechanisms of Nitric Acid-Hydrocarbon Flames, by M. H. Boyer and P. E. Friebertshauser, *Combustion and Flame*, vol. 1, no. 3, Sept. 1957, pp. 264–280.

Extraction of Ions from a Flame, by J. Deckers and A. van Tiggelen, *Combustion and Flame*, vol. 1, no. 3, Sept. 1957, pp. 281–286.

Predicting the Laminar Flame Speed in Gases with Temperature-Explicit Reaction Rates, by D. B. Spalding, *Combustion and Flame*, vol. 1, no. 3, Sept. 1957, pp. 287–295.

One-Dimensional Laminar Flame Theory for Temperature-Explicit Reaction Rates, by D. B. Spalding, *Combustion and Flame*, vol. 1, no. 3, Sept. 1957, pp. 296–307.

Flame Decomposition of the Propyl Nitrates, by J. Powling and W. A. W. Smith, *Combustion and Flame*, vol. 1, no. 3, Sept. 1957, pp. 308–320.

Notes on Problems in Combustion Instability of Rocket Motors, by T. Paul Torda, *Aeron. Engng. Rev.*, vol. 16, no. 11, Nov. 1957, pp. 34–37, 47.

Shift to Solid Propellants, *Aviation Week*, vol. 67, no. 17, Oct. 28, 1957, p. 34.

The Premixed Ozone-Cyanogen Flame, by A. G. Streng and A. V. Grosse, *J. Amer. Chem. Soc.*, vol. 79, no. 20, Oct. 20, 1957, p. 5583.

Studies in Bomb Calorimetry, VII: Principles for the Design of Calorimeter Systems, by R. A. Mott, *Fuel*, vol. 36, Oct. 1957, pp. 447–468.

Rocket Thrust and the Energy Power of Ergols, by P. Glansdorff, A. Jaumotte and J. Passelecq, *Fusées Recherche Aeron.*, vol. 2, no. 3, July 1957, pp. 205–212 (in French).

Stabilization of Concentrated Solutions of Hydrogen Peroxide, by W. C. Schumb, *Indust. Engng. Chem.*, vol. 49, no. 10, Oct. 1957, pp. 1759–1762.

Borane High Energy Fuels, *Interavia*, vol. 12, no. 10, Oct. 1957, p. 1023.

Density of Liquid Ozone, by Robert I. Brabets and John M. McDonough, *J. Chem. Phys.*, vol. 27, Oct. 1957, pp. 880–882.

EDITOR'S NOTE: Contributions from E. R. G. Eckert, J. P. Hartnett, T. F. Irvine Jr. and P. J. Schneider of the Heat Transfer Laboratory, University of Minnesota, are gratefully acknowledged.

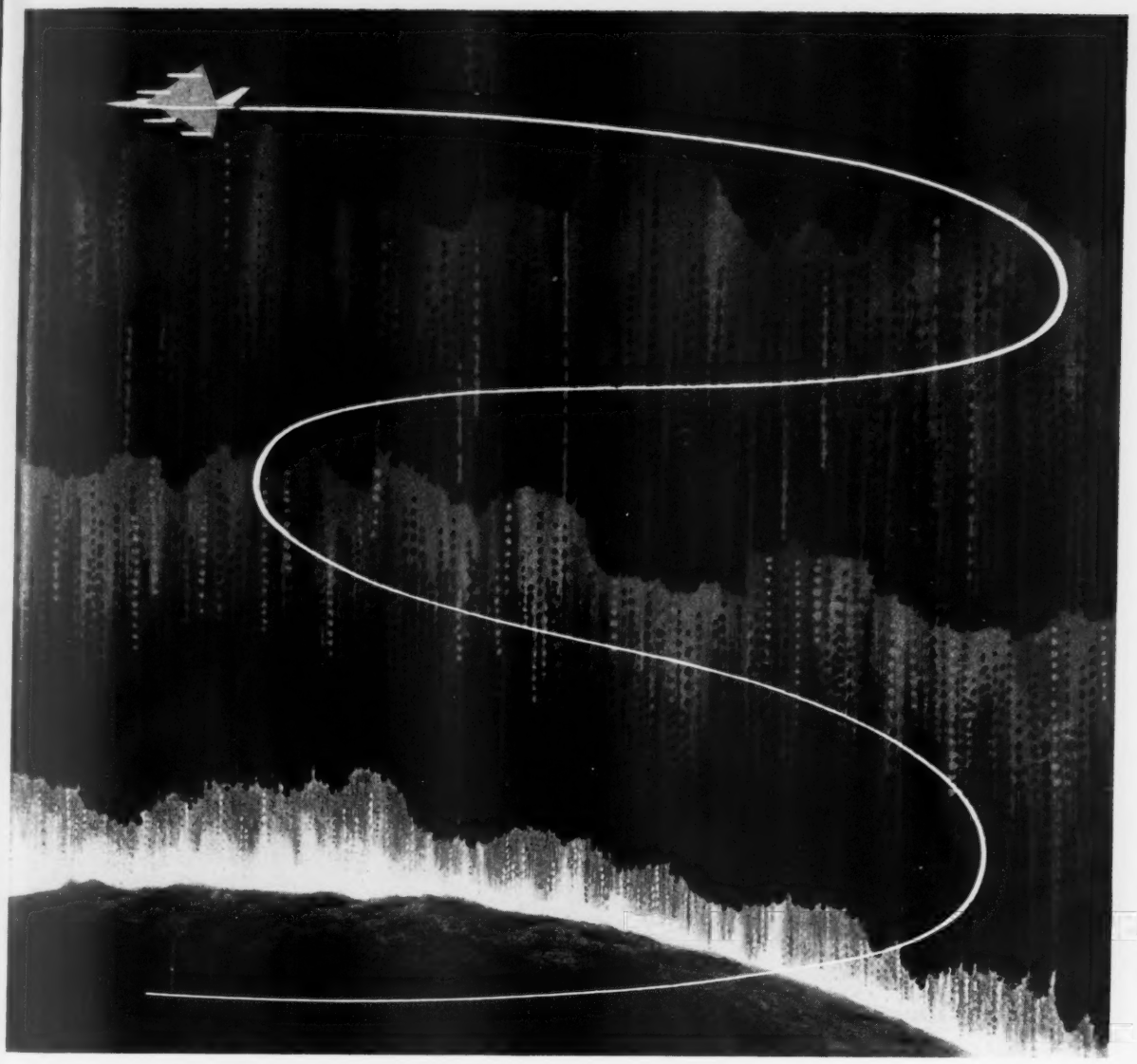

New extreme-high-temperature lubricants for missiles and supersonic aircraft **SHELL ETR GREASES**

One of the serious lubricating problems faced by designers of missiles and supersonic aircraft has been solved by scientists at Shell Research Laboratories.

The problem: to find a grease which would permit components to operate with certainty under extreme high temperatures. Co-operation with representatives of bearing manufacturers and military personnel resulted in a completely new class of greases—SHELL ETR GREASES.

These greases can easily withstand temperatures up to 600°F. They give superior lubricating performance because of a special thickener—an organic vat dye—which has exceptional heat stability and jelling efficiency.

If you are presently in the market for an ultra-high-temperature-range grease, we will be glad to provide more information on Shell ETR Greases.

SHELL OIL COMPANY

50 West 50th Street, New York 20, N.Y.
100 Bush Street, San Francisco 6, Calif.

SHELL

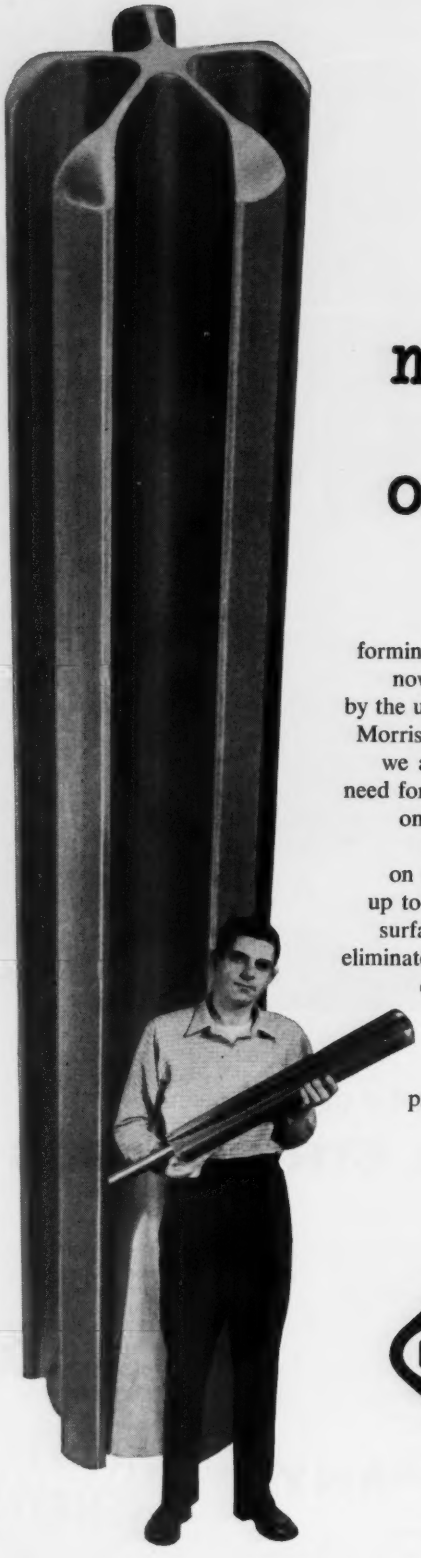

cast mandrels or cores?

Aluminum mandrels for forming solid fuel propellant are now being cast in production by the unusual foundry methods of Morris Bean & Company. While we assume there is no present need for a mandrel as large as the one on the left, it *can* be cast. Currently we are working on solid and hollow mandrels up to 8 feet long. Their smooth surfaces and accurate contours eliminate much difficult machining; cost is drastically reduced. In addition to large size, we would be happy to explore with you ways to produce intricate star-lobes. *Telephone or write.*

Morris Bean & Company,
Yellow Springs 6, Ohio.

BEAN

Materials of Construction

Effect of Overheating on Creep-rupture Properties of S-816 Alloy at 1,500°F, by John P. Rowe and J. W. Freeman, University of Mich., *NACA TN* 4081, Dec. 1957, 75 pp., diagrs., photos., tabs.

Effect of Overheating on Creep-rupture Properties of HS-31 Alloy at 1,500°F, by John P. Rowe and J. W. Freeman, University of Mich., *NACA TN* 4083, Dec. 1957, 78 pp., diagrs., photos., tabs.

The Useful Heat Capacity of Several Materials for Ballistic Nosecone Construction, by Jackson R. Stalder, *NACA TN* 4141, Nov. 1957, 19 pp., diagrs.

Preliminary Investigation of the Strength and Endurance of Plansic-impregnated Fiberglas Compressor Blades, by Donald F. Johnson and Andre J. Meyer Jr., *NACA RM* E54I27a, Jan. 1955, 21 pp., diagrs., photos. (Declassified from Confidential by authority of *NACA Res. Abs.* 122, p. 9, 12/3/57.)

Buckling at High Temperature, by N. J. Hoff, *J. Roy. Aeron. Soc.*, vol. 61, Nov. 1957, pp. 756–774.

Study of Chemical Factors Affecting Corrosion of Carbon Steel A1S1 1020 by Liquid Phase Fuming Nitric Acid, by John B. Rittenhouse and David M. Mason, *Calif. Inst. Techn., Jet Propulsion Lab. Mem.* 20–147, Oct. 1957, 31 pp.

Strength of Cylinders, by W. R. D. Manning, *Ind. & Engng. Chem.*, vol. 49, Dec. 1957, pp. 1969–1978.

Stress Concentration in Heavy-walled Cylindrical Pressure Vessels, by J. G. Faupel and D. B. Harris, *Ind. & Engng. Chem.*, vol. 49, Dec. 1957, pp. 1979–1986.

Instrumentation, Data Recording, Telemetering

French Telemetering Equipment, by J. Idrac, *North Atlantic Treaty Organization, Advisory Group for Aeron. Res. and Dev., Rep* 33, Feb. 1956, 18 pp. (in French).

Weapon System Requirements for Air Data Computers, by A. K. Hammell, *Aeron. Engng. Rev.*, vol. 17, Jan. 1958, pp. 32–35.

Transistor Inverters Supply 400-Cycle Power to Aircraft and Missiles, *Aviation Age*, vol. 28, Dec. 1957, pp. 112–118.

Investigation of the Conditions in the Plasma in Mercury-vapor Arc Discharges and Oscillating Electron Ion Sources, by Max Hoyaux and Paul Gans, *Ateliers Construc. Elec., Charleroi, Rep.* EOARDC TR 54 (AFOSR TR 56–23), (AD 88353), 1956, 51 pp.

Guidance Systems and Components

Bomarc Guidance Spawns New Testing Techniques, by Henry P. Steier, *American Aviation*, vol. 21, Dec. 30, 1957, pp. 32–33.

Theoretical Investigation of the Performance of Proportional Navigation Guidance Systems—Effect of Missile Configuration on the Speed of Response, by Marvin Abramovitz, *NACA RM*, A52-J22, Jan. 1953, 20 pp. (Declassified from Confidential by authority of *NACA Res. Abs.* 121, p. 14, 11/4/57.)

Application of Statistical Theory to Beam-rider Guidance in the Presence of Noise, I: Wiener Filter Theory, by Elwood C. Stewart, *NACA RM* A55E11, Aug. 1955, 40 pp. (Declassified from Confidential by authority of *NACA Res. Abs.* 121, p. 15, 11/4/57.)

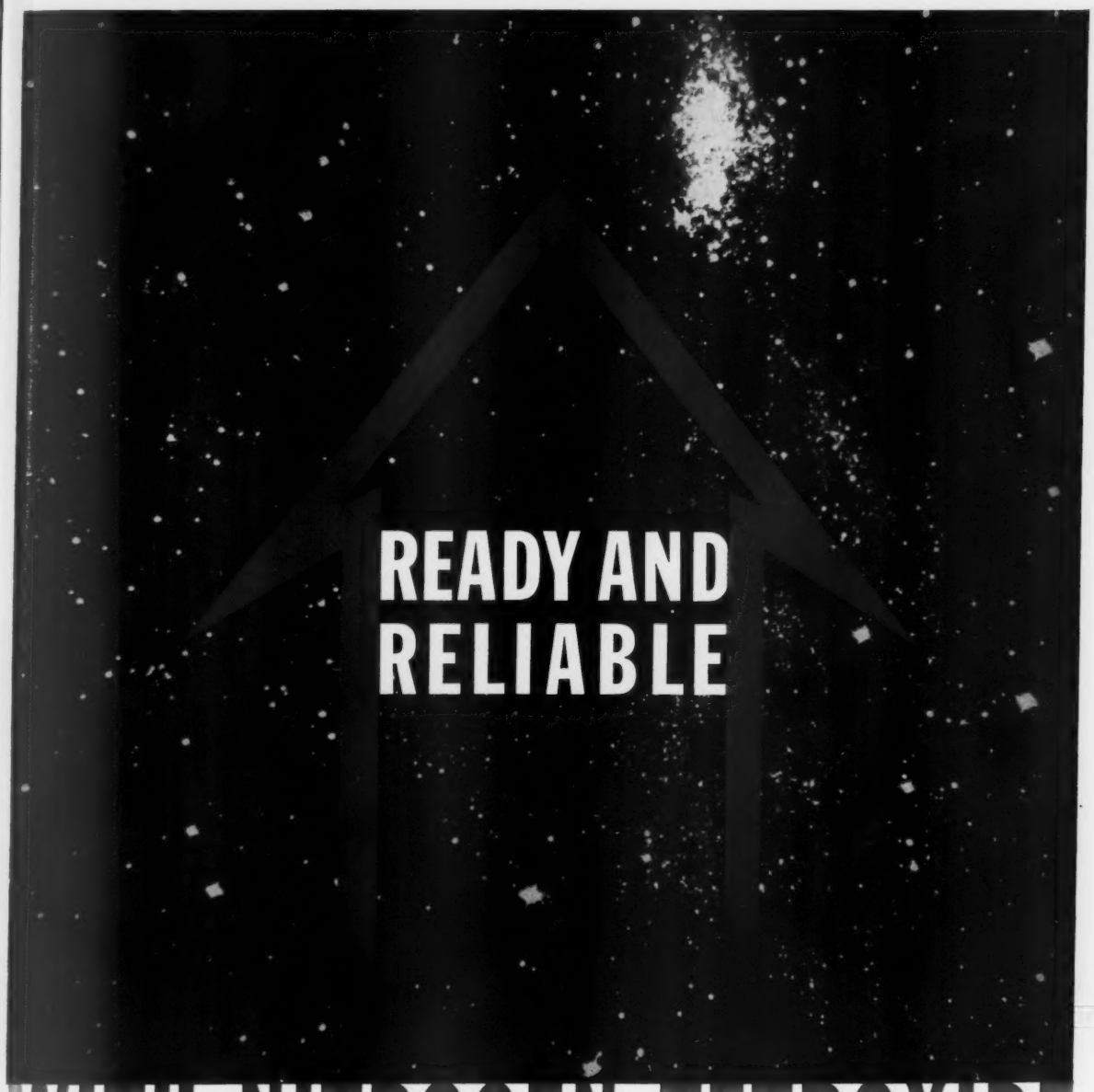

WITH NITROGEN TETROXIDE

. . . Requires no refrigeration . . . Easier to store than liquid oxygen

Performance of Nitrogen Tetroxide as an oxidizer for many fuels is comparable to that of liquid oxygen. In convenience it is far superior to liquid oxygen.

N_2O_4 can be shipped easily and stored indefinitely without refrigeration in ordinary carbon steel containers. It is a dense, mobile liquid that is noncorrosive if kept dry. The quantity of oxygen contained per unit volume of N_2O_4 is 1.01 Kg/liter at 20°C.

N_2O_4 is available in tonnage quantities from Allied's Hopewell, Virginia plant. For experimental purposes, N_2O_4 is available in 125 lb. cylinders and 2000 lb. containers. Write for technical data, and information on prices and delivery.

N_2O_4 Oxidant for liquid rocket propellants

Molecular weight	92.02
Boiling Point	21°C
Freezing Point	−11.3°C
Latent Heat of Vaporization	99 cal/gm @ 21°C
Critical Temp.	158°C
Critical Pressure	99 atm
Specific Heat of Liquid	0.36 cal/gm −10 to 20°C
Density of Liquid	1.45 gm/ml at 20°C
Density of Gas	3.3 gm/liter 21°C, at 1 atm
Vapor Pressure	2 atm at 35°C

Allied Chemical

Ethanolamines • Ethylene Oxide • Ethylene Glycols • Urea • Formaldehyde • U. F. Concentrate—85 • Anhydrous Ammonia • Ammonia Liquor • Ammonium Sulfate • Ammonium Nitrate • Sodium Nitrate • Methanol • Nitrogen Solutions • Nitrogen Tetroxide • Fertilizers & Feed Supplements

Nitrogen Division • Department NT4-12-1 • 40 Rector Street, New York 6, New York

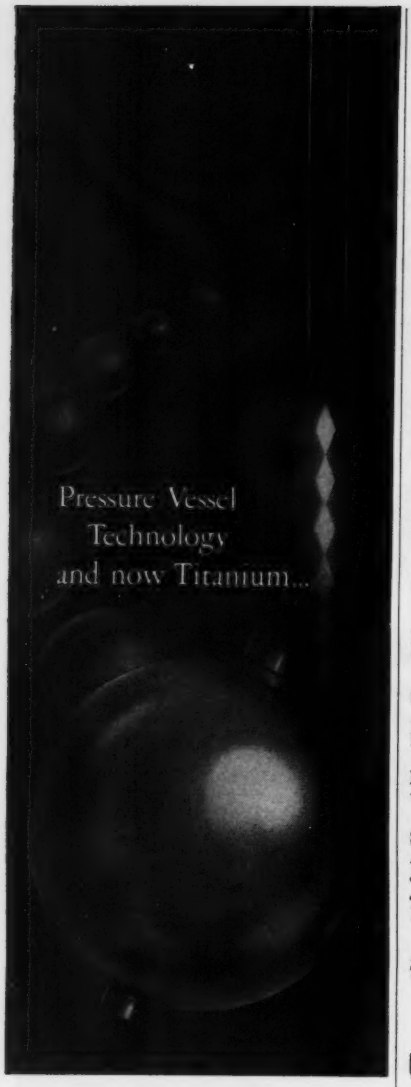

Spheres of titanium alloy represent the optimum configuration and material of maximum strength/weight for the storage of gases and liquids under extremes of pressure and temperature.

Rheem Aircraft, presently supplying pressure units to current ICBM programs, is directing its years of experience to the development and production of all types of vessels and propellant chambers.

RHEEM MANUFACTURING CO.
AIRCRAFT DIVISION
11711 woodruff avenue, downey, california

Rheem

Engineers: Join Rheem in challenging technical work.

Servomechanisms and Controls

Servo Analysis Charts, by Erwin Bieser and Samuel Adler, *Electronics*, vol. 30, Dec. 1, 1957, pp. 173–176.

Flight Vehicle Design and Testing

Dynamic Response of Beams and Plates to Rapid Heating, by B. A. Boley and A. D. Barber, *J. Appl. Mech.*, vol. 4, Sept. 1957, p. 413.

Some NACA Research on Effect of Transient Heating on Aircraft Structures, by J. E. Duberg, *Trans. ASME*, vol. 79, July 1957, pp. 1014–1018.

Achievement of High Heat Fluxes in a Wind Tunnel, by Antonio Ferri and Martin H. Bloom, *J. Aeron. Sci.*, vol. 24, Oct. 1957, pp. 772–773.

Some Structural Penalties Associated with Thermal Flight, by J. W. Mar and L. A. Schmit, *Trans. ASME*, July 1957, pp. 990–1004.

Space Flight

Man in Space Needed to Recapture Lead, by Evert Clark, *Aviation Week*, vol. 67, no. 20, Nov. 18, 1957, pp. 26–27.

What the Future Holds for the Earth Satellite, by Robert P. Haviland, *J. Astronautics*, vol. 4, no. 3, Autumn, 1957, p. 41.

Space Vehicles as Tools for Research in Relativity, by Fred Singer, *J. Astronautics*, vol. 4, no. 3, Autumn, 1957, p. 49.

Long Term Human Confinement in Space Equivalent Vehicles, by Charles A. Dempsey, Franklin D. VanWart, John H. Duddy and Jack K. Hockenberry, *J. Astronautics*, vol. 4, no. 3, Autumn, 1957, p. 52.

After the Sputniks, by Robert Saundby, *Aeroplane*, vol. 93, Nov. 22, 1957, pp. 783–784.

Astrophysics, Aerophysics

Atmospheric Temperature Observations to 100,000 Feet for Several Climatological Regions of the Northern Hemisphere, by H. B. Tolefson, *NACA TN* 4169, Nov. 1957, 26 pp.

Experimental Aspects of General Relativity Theory, by Louis Witten, *J. Astronautics*, vol. 4, no. 3, Autumn, 1957, p. 46.

The Ratio of Helium and Hydrogen Abundances in Planetary Nebulae, by John S. Mathis, *Astrophysical J.*, vol. 126, Nov. 1957, pp. 493–502.

High-dispersion Spectra of Mars, by C. C. Kiess, C. H. Corliss, Harriet K. Kiess and Edith L. R. Corliss, *Astrophysical J.*, vol. 126, Nov. 1957, pp. 579–584.

Nuclear Propulsion

The Application of Nuclear Power to Logistic Aircraft Systems, by Robert W. Middlewood and Robert B. Ormsby Jr., *SAE Prepr.* 206, Oct. 1957, 11 pp., 26 fig.

Progress Report on Nuclear Power, by Arthur C. Johnson, *SAE Prepr.*, Feb. 1957, 5 pp., 2 fig.

Corrosion and Wear Handbook for Water Cooled Reactors, by D. J. DePaul, *Atomic Energy Comm.*, TID 7006, March 1957, 293 pp.

Atomic Plane Acceleration, *Aviation Week*, vol. 67, no. 21, Nov. 25, 1957, pp. 28–29.

Readings in Atomic Energy, *SAE J.*, vol. 65, no. 12, Nov. 1957, pp. 82–83.

Testing Aircraft Nuclear Power Plants, by A. R. Crocker, *Aeron. Engng. Rev.*, vol. 16, no. 12, Dec. 1957, pp. 30–35.

Theory of Hydrogen Deuteride in Magnetic Fields, by Norman F. Ramsey and Henry R. Lewis, *Physical Rev.*, vol. 108, Dec. 1, 1957, pp. 1246–1250.

Motion of Charged Particles in a Force-free Magnetic Field, by Donat G. Wentzel, *Astrophysical J.*, vol. 126, Nov. 1957, pp. 559–564.

Bibliography

(*Continued from page 302*)

Astronautics 3: 1–3, 14, illus., Spring, 1956. The author illustrates the effects on the orbit due to errors in the injection condition, namely, cutoff, velocity increment above or below the circular orbit velocity, and that due to elevation angular errors. The necessary limits on injection velocity and angle are shown to give a resultant orbit within specific apogee and perigee bounds. Further, the errors in angle of inclination between orbit plane and equator are discussed.

Satellites. Aero. Eng. Rev. 15: 44–47, Sept. 1956. Some engineering aspects of the Vanguard project. A German translation appears in Physik Bl. 13: 73–82, 1957.

Article with same title in Navigation 5: 121–127, Sept. 1956.

Jones, L. M. and Bartman, F. L.

Satellite Drag and Air-Density Measurements. In Van Allen, J. A., ed., *Scientific Uses of Earth Satellites*, pp. 85–98, Ann Arbor, University of Michigan Press, 1956. Concerns calculation of air density from the measured drag of a satellite.

Kaplan, Joseph

Rocket and Satellite Studies During the IGY. Aero. Eng. Rev. 15: 64–67, Apr. 1956. A summary account of the various stages leading to the development by the United States of the earth satellite program and a description of present plans and organization.

United States Programme for the International Geophysical Year. Nature 178: 665–667, Sept. 20, 1956. The chairman of the U. S. National Committee for the IGY, National Academy of Sciences, describes the over-all scope of U. S. research program during 1957–1958, as well as the plans for upper atmosphere research.

Katz, Ludwig

Geomagnetic Information Potentially Available from a Satellite. In Van Allen, J. A., ed. *Scientific Uses of Earth Satellites*, pp. 247–252, Ann Arbor, University of Michigan Press, 1956. The mass-spectrometer action at the earth's field on charged cosmic-ray particles could be determined from a satellite and an effective dipole field; its eccentricity could also be determined.

King-Hele, D. G.

The Descent of an Earth-Satellite Through the Upper Atmosphere. Brit. Interplan. Soc. J. 15: 314–323, Dec. 1956. A discussion of the re-entry problem. The point is made that when a satellite encounters air resistance it is speeded up, instead of slowed down as might have been expected.

Klass, P. J.

Vanguard to Use Eight Control Systems. Missile Eng. 1: 24–25, Dec. 1956. Description of control systems to provide pitch, yaw and roll stabilization during ascent of Vanguard vehicle.

GIANT CAPACITOR SYSTEM POWERS ADVANCED EXPERIMENTS ON ELECTRICAL PROPULSION

A report to Engineers and Scientists from Lockheed Missile Systems—where expanding missile programs insure more promising careers

■

Lockheed experiments on electrical power sources for space craft are using electrical energy stored in a giant capacitor system, one of the largest in the aircraft industry. This propulsion research—based on electrohydrodynamics—is an example of the advanced work being conducted in Division laboratories near Stanford University in the electrical, chemical and nuclear fields.

The giant capacitor bank is capable of a 5 million kilowatt jolt of electricity, used to fire Lockheed's new "hotshot" wind tunnel to 18,000 degrees Fahrenheit with speeds up to 15,000 miles an hour.

Research in such sophisticated areas by Division scientists has earned Lockheed leadership in missiles. Nose cone reentry studies, for example, have helped speed delivery dates on Polaris, Lockheed's submarine fleet ballistic missile.

With expansion on our IRBM, Earth Satellite, and other advanced programs, new positions have opened for engineers and scientists... positions that call for the utmost in creative ability.

These areas include: **Propulsion, Aerodynamics-Thermodynamics, Guidance, Electronics, Flight Controls, Structures, Design.**

If you are qualified, you are invited to write Research and Development Staff, Palo Alto 20, California for further information.

Lockheed

MISSILE SYSTEMS

A DIVISION OF LOCKHEED AIRCRAFT CORPORATION

SUNNYVALE • PALO ALTO • VAN NUYS
SANTA CRUZ • CALIFORNIA
CAPE CANAVERAL, FLORIDA
ALAMOGORDO, NEW MEXICO

Discussing characteristics of the capacitor system are research scientist Dr. Edward Fisher of the Propulsion Staff, right, and Dr. Terry E. Turner, Hot Shot Tunnel Group Leader. The two groups are engaged in a joint effort on advanced propulsion experiments.

NOW IN VOLUME PRODUCTION AT C.A.E.

. . . the TC-106 (USAF TYPE MA-1A). PORTABLE STARTING UNIT for LARGE JET AIRCRAFT

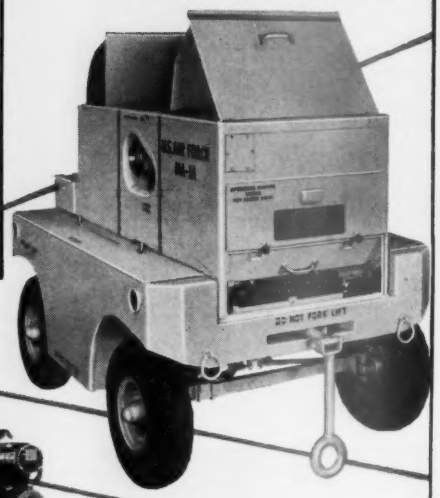

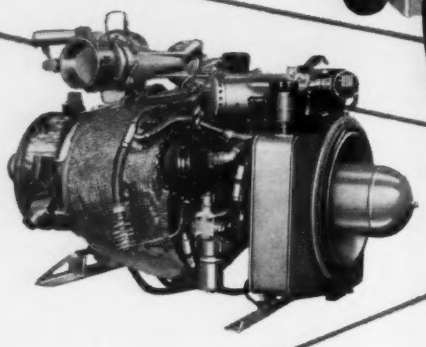

MODEL 141 TURBO-COMPRESSOR ENGINE

Typical of the fine results of Continental development is the TC-106 portable starting unit for large jet aircraft. This advanced new model, with a high performance turbine compressor as its heart, weighs one-third less than its predecessor, yet has 17 per cent higher output, and in addition, other important qualities: greater mobility, less noise, and a completely automatic control system. . . . It is now in volume production at the Continental Aviation and Engineering Toledo plant.

●

C.A.E. gas turbine models—the J69-T-9, the J69-T-2, and the J69-T-19A are being built for Cessna's T-37A twin jet trainer, Temco's TT-1 Navy jet trainer, the Beech jet Mentor trainer, and the Ryan Q-2A Fire Bee target drone.

CONTINENTAL AVIATION & ENGINEERING CORPORATION

12700 KERCHEVAL AVENUE, DETROIT 15, MICHIGAN

SUBSIDIARY OF CONTINENTAL MOTORS CORPORATION

LaGow, H. E.

Experiments for Measuring Temperature, Meteor Penetration, and Surface Erosion of a Satellite Vehicle. In Van Allen, J. A., ed. *Scientific Uses of Earth Satellites*, pp. 68–72, Ann Arbor, University of Michigan Press, 1956. Assesses importance of miniaturization in relation to environment including temperature extremes, surface erosion and surface penetration.

Lawrence, Lovell, Jr.

"Astro"—An Artificial Celestial Navigation System. In Franklin Institute. *Earth Satellites as Research Vehicles.* Proceedings of a Symposium, Philadelphia, Franklin Institute, April 18, 1956, pp. 89–99, Lancaster, Pa., Journal of the Franklin Institute, June 1956. (Monograph 2.) Discusses design, orbit, propagation of electromagnetic wave signals, and nuclear power source for "Astro"—an artificial satellite time-and-radio orbit.

Navigation by Satellites. Missiles and Rockets 1: 48–52, Oct. 1956. Indicates that an artificial satellite time-and-radio orbit celestial navigation system that is simple, yet reliable, may be feasible.

Ley, Willy

Rocket Fuel Research Paves Way for Space Flight. Indus. Labs. 7: 100–101, July 1956. Discussion of liquid and solid rocket fuels, advantages and disadvantages of each, and their applications to Project Vanguard.

Ludwig, G. H., and Van Allen, J. A.

Instrumentation for a Cosmic Ray Experiment for the Minimal Earth Satellite. J. Astronautics 3: 59, 60, 90, Autumn/Winter 1956. Discussion of a proposed experiment in which a single Geiger-Mueller counter would be used to study the geographical and temporal variations of the primary cosmic-ray intensity. The counter would incorporate a system for storing its output during the orbit of the satellite, and for a short-time read-out of this information.

Manchester, Harland

What Can We Expect of the Man-Made Moon? Reader's Dig. 69: 162–166, July 1956. Truths and untruths behind one of science's most ambitious ventures.

The Martin Co., Baltimore, Md.

Effect of the Earth's Oblateness and Atmosphere on a Satellite Orbit, by George Fosdick and Marvin Hewitt. 41 pp., Aug. 1956. (Rpt. ER-8262.) Presents results of investigations to determine the effects of the earth's oblateness and atmosphere on a satellite orbit.

Mazur, D. G.

Telemetering and Propagation Problems of Placing the Earth Satellite in Its Orbit. Inst. Radio Engrs. Proc. 44: 752–754, June 1956. Reviews the problems and general planning in connection with the earth satellite launching vehicles.

Mengel, J. T.

Tracking the Earth Satellite and Data Transmission by Radio. Inst. Radio Engrs. Proc. 44: 755–760, June 1956. Description of "Minitrack" which is to be used to track and send data from Vanguard.

Merrill, H. J.

Satellite Tracking by Electronic Optical Instrumentation. In Van Allen, J. A., ed. *Scientific Uses of Earth Satellites*, pp. 29–38, Ann Arbor, University of Michigan Press, 1956. Essential differences between satellite tracking and astronomical observations or missile tracking warrant improvements in optical instrumentation. These are associated with superior time constants, background elimination, utilization of the optimum spectral region, and the superior characteristics of the electronics in the servo tracking loop.

Missiles and Rockets

International Geophysical Year Earth Satel-

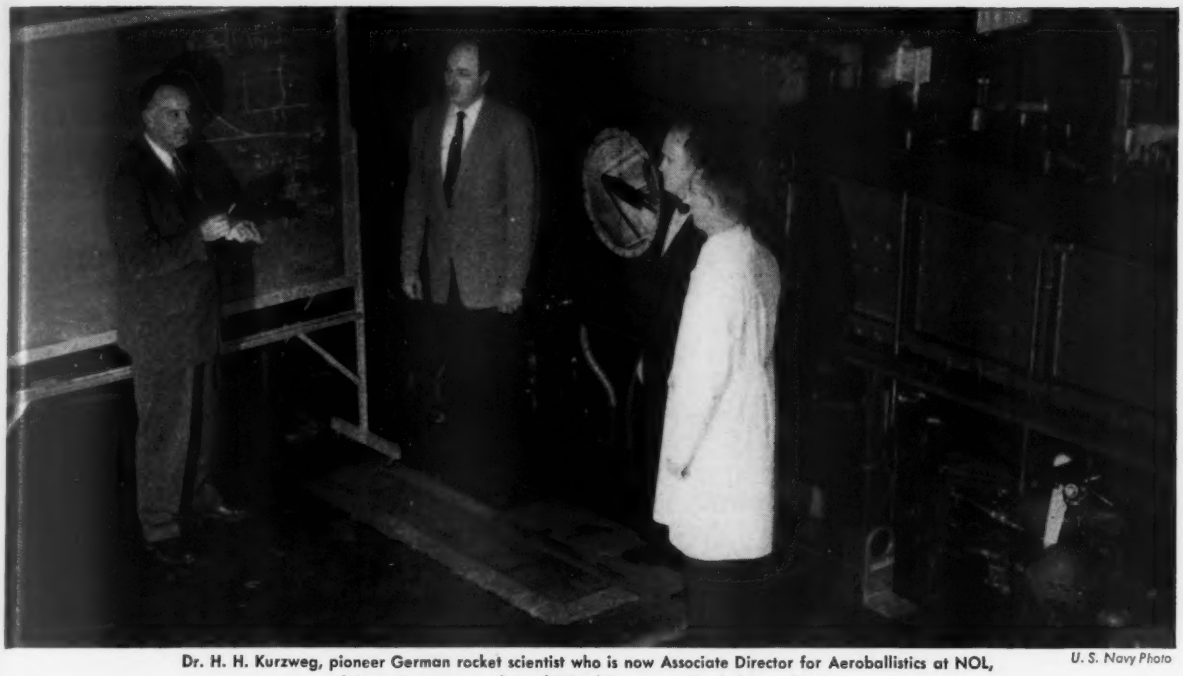

Dr. H. H. Kurzweg, pioneer German rocket scientist who is now Associate Director for Aeroballistics at NOL, interprets nose-cone data obtained in supersonic wind tunnel test.

U. S. Navy Photo

FROM UNDERSEAS TO OUTER SPACE—WEAPONS OF THE NAVAL ORDNANCE LABORATORY GUARD OUR FREEDOM

Basic and applied research—and the development of advanced weapons for underwater, surface and air warfare—are the vital missions of the U. S. Naval Ordnance Laboratory near Silver Spring, Md.

Established in 1918 as a small experimental group to design sea mines and fuzes, NOL has become one of the nation's most respected institutions for military research and development. Three thousand persons, including 1,000 scientists and engineers, work at its modern $50 million facility.

In its forty years, the Laboratory has made many notable contributions to science and technology, and to our national defense. In World War II, NOL-developed sea mines helped to strangle Japan's supply system. More recently, NOL's work on TARTAR, TERRIER and TALOS greatly speeded the development of these needed missiles. The atomic depth charge weapon BETTY, conceived and perfected by NOL in less than five years, now provides the U. S. Fleet a massive defense against modern enemy submarines.

Today, NOL's work embraces virtually the entire field of advanced weapons design. One highlight is the Laboratory's present key role in the development of POLARIS, the nuclear-capability missile that our submarines will soon be able to launch while submerged off enemy shores. This is one of many new weapons that NOL is developing or assisting with at present—weapons that are needed if the free world is to survive.

But in the long run, some of NOL's other work in basic and applied research may be of even more significance to mankind. For example, the advanced aeroballistics studies carried on at NOL, which already have solved some of the IRBM and ICBM problems, may help unlock the remaining doors to interplanetary space travel. Or NOL's work in advanced chemistry may provide entirely new and better types of metals, plastics and other substances. Or NOL's basic research in physics and mathematics may furnish a key to the internal structure of subatomic particles, and open up whole new worlds for science and mankind.

Thus the Naval Ordnance Laboratory aids our nation in two ways: by developing weapons that will insure the survival of freedom, and by finding new scientific knowledge that will enrich our lives.

B.7

This is one of a series of ads on the technical activities of the Department of Defense.

FORD INSTRUMENT CO.

DIVISION OF SPERRY RAND CORPORATION

31-10 Thomson Avenue, Long Island City 1, New York

Field Sales Offices: Beverly Hills, Calif.; Dayton, Ohio

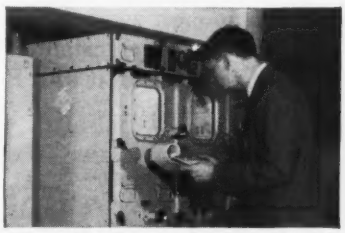

Engineer at Ford Instrument Co. checks out fire control computer developed and built by Ford for the U. S. Navy's Bureau of Ordnance.

DRENCHED *for Safety!*

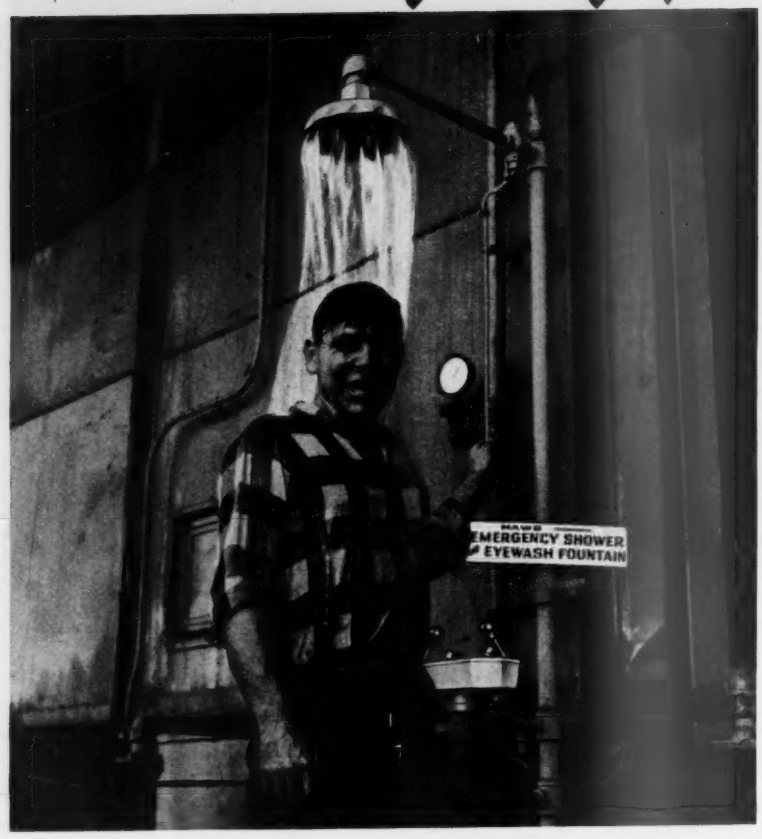

HAWS
EMERGENCY FACILITIES

This safety station is part of the comprehensive safety program maintained by the General Electric Company at its Appliance Park, Louisville, Kentucky. General Electric considers its safety record a prime achievement, and provides HAWS Emergency Facilities at critical locations throughout the production areas.

• Drench Showers • Eye-Face Wash Fountains

Not just a shower... a HAWS DRENCH SHOWER! A quick pull of the chain releases a solid sheet of water to rid body and clothing of dangerous chemicals and caustics. Safety in seconds—saving vital moments until medical aid arrives, perhaps avoiding serious injury. HAWS Eye-Wash Fountain, too, is ready to flood eyes from specially designed fountain heads. These are only two items from HAWS complete line of emergency facilities to meet every industrial need. Safety authorities stress the necessity of instant irrigation for eye or body contamination. Provide for it with HAWS equipment. Get the full facts now, by writing...

HAWS DRINKING FAUCET COMPANY

Leader in drinking water facilities since 1909

1443 FOURTH STREET • BERKELEY 10, CALIFORNIA

lite Vehicle Program. 1: 120–121, Nov. 1956. Complete organizational and functional charts for the United States IGY satellite program.

Newell, H. E., Jr.

The International Geophysical Year Earth Satellite Program. Franklin Institute. *Earth Satellites as Research Vehicles.* Proceedings of a Symposium, Philadelphia, Franklin Institute, Apr. 18, 1956, pp. 3–10, Lancaster, Pa., Journal of the Franklin Institute, June 1956. (Monograph 2.)

Article with same title in Sci. Mon. 83: 13–21, July 1956.

Odishaw, Hugh

The IGY Earth Satellite Program. Instr. Soc. Am. J. 3: 298–301, Sept. 1956. Objectives of the IGY and methods used to implement them. Includes description of proposed rocket and satellite operation and instrumentation.

Ovenden, M. W.

The Astronomical Uses of Small Artificial Satellites. Sci. Prog. 44: 472–479, July 1956. Summarizes possible astronomical uses of the IGY satellites.

Perkins, F. M.

Flight Mechanics of Ascending Satellite Vehicles. JET PROPULSION 26: 352–358, May 1956. Solution of the optimum vacuum stage thrust axis pitch program for a satellite using continuous thrust all the way from ground to orbit, with an explanation of trajectory optimization to minimize propellant consumptions for a vehicle using a power-off coast up to the orbit, and of analog and digital computor techniques for trajectory calculations. Includes discussion of types of orbits and trajectories.

Petersen, N. V.

Factors Affecting the Lifetime of Earth Satellites. Aero. Dig. 73: 74–76, 78, 80, 82, July 1956. Influence of gravitational field and atmospheric envelope of the earth are considered.

Lifetimes of Satellites in Near-Circular and Elliptic Orbits. JET PROPULSION 26: 341–351, diags., May 1956. The problem of determining the approximate lifetime or duration for simple satellite configurations as influenced by the gravitational field and atmospheric envelope of the earth is considered.

Pfister, Wolfgang

Study of Fine Structure and Irregularities of the Ionosphere and Rockets and Satellites. In Van Allen, J. A., ed. *Scientific Uses of Earth Satellites,* pp. 283–291, Ann Arbor, University of Michigan Press, 1956. Real advantage of the experiment will be that the changing aspect allows scientists to gain a three-dimensional picture of the configuration of the blob, while so far they are used to looking only at the two-dimensional diffraction pattern at the ground.

Porter, R. W.

Recovery of Data in Physical Form. In Franklin Institute. *Earth Satellites as Research Vehicles.* Proceedings of a Symposium, Philadelphia, Franklin Institute, Apr. 18, 1956, pp. 103–112, Lancaster, Pa., Journal of the Franklin Institute, June 1956. (Monograph 2.) The chairman of the Panel on Earth Satellites outlines the difficulties of recovering data, possible methods of attack, proposed design, trajectory computations and thermal considerations.

Rand Corp., Santa Monica, Calif.

Skin Temperature Variation During Reentry of Scientific Satellite, by D. J. Masson. 4 pp., Mar. 30, 1956. (Res. Memo 1693.) From the point of view of destruction by heat, the recovery of a satellite is considered possible.

Rosen, M. W.

Placing the Satellite in Its Orbit. Inst. Radio Engrs. Proc. 44: 748–751, June 1956.

STRAIGHT TALK TO ENGINEERS

from Donald W. Douglas, Jr.

President, Douglas Aircraft Co., Inc.

Here at Douglas we're involved in a greatly accelerated missile and space program. This requires one of the most intensive engineering and research efforts in our history.

The problems are great ones as we move into the new dimension of unmanned and manned space vehicles. They require specialists in almost every engineering field. But their solution will result in great benefits not only to our own nation but to all mankind.

If you're interested in tackling these problems with us... in giving your best in an all-out drive to solve them... we're interested in you!

Please write to Mr. C. C. La Vene
Douglas Aircraft Company, Box J-620
Santa Monica, California

AEROJET-GENERAL CORPORATION

TURBO-MACHINERY DIVISION

Offers Key Positions

for specialists, design engineers and test engineers with creative ability and broad experience in cycle and performance analysis, design, and development in following fields:

***TURBINES**

Propellant-powered, high-speed machines from one to several thousand horsepower, operating at high pressure ratios and temperatures.

***PUMPS**

Axial and radial flow pumps of high suction specific speed for mono-propellant and bi-propellant systems.

***GAS GENERATORS**

Mono-propellant and bi-propellant systems for wide ranges of design and operating conditions.

***ELECTRICAL**

Frequency, voltage, sequencing, and other electrical controls for turbo-machines, auxiliary power and magnetic amplifier systems, and related ground support equipment.

You are cordially invited to send a detailed resume to:

L. L. THOMPSON

AEROJET-GENERAL CORPORATION

Box 296-H

Azusa, California

A Subsidiary of The General Tire & Rubber Company

Description of Vanguard launching vehicle. Republished in J. Astronautics 3: 61–64, 82, illus., Autumn/Winter 1956.

Saelman, B.

Note on an Artificial Satellite. Am. J. Phys. 24: 630, Dec. 1956.

Sedwick, J. L., Jr.

Interpretations of Observed Perturbations on a Minimal Earth Satellite. In Van Allen, J. A., ed. *Scientific Uses of Earth Satellites*, pp. 44–48, Ann Arbor, University of Michigan Press, 1956. Gives a method for calculating the perturbing forces from observations of the orbit, considering air resistance and effects of the earth's oblateness.

Shternfel'd, A.

Iskusstvennye Sputniki Zemli (Artificial Earth Satellites). 180 pp., Moscow, State Publishing House of Technicotheoretical Literature, 1956. In Russian. Contains information about propellants for outer space rockets, satellites and ballistic missiles.

Sicinski, H. S., Spencer, N. W., and Boggess, R. L.

Pressure and Density Measurements Through Partial Pressures of Atmospheric Components at Minimum Satellite Altitudes. In Van Allen, J. A., ed. *Scientific Uses of Earth Satellites*, pp. 109–118, Ann Arbor, University of Michigan Press, 1956. Pressure and density measurements by means of a "Synchrometer."

Singer, S. F.

Application of an Artificial Satellite to the Measurement of the General Relativistic "Red Shift." Phys. Rev. 104: 11–14, Oct. 1, 1956. Some experimental schemes for the measurement of the clock shift are discussed.

The Artificial Earth Satellite. Discovery 17: 140–145, Apr. 1956. A description and plan of MOUSE are given.

The Artificial Earth Satellite—Past, Present and Future. Interavia 11: 956–959, illus., Dec. 1956. How satellite experiments may lead to a better scientific understanding of our environment which may have important consequences for our economy and way of life.

The Effect of Meteoric Particles on a Satellite. JET PROPULSION 26: 1071–1075, Dec. 1956. Discusses some physical models to allow calculations of the erosion rate of high velocity meteoric dust on space vehicles. Important indications are derived for the choice of material and construction of a satellite skin to minimize meteor effects. An erosion experiment for the Vanguard satellite is described.

Geophysical Research with Artificial Satellites. In Landsberg, H., ed. *Advances in Geophysics*, pp. 301–367, New York, Academic Press, 1956. A review of experiments which have been suggested for a satellite, a geophysical tool whose scope extends further than any other known technique.

Measurements of Interplanetary Dust. In Van Allen, J. A., ed. *Scientific Uses of Earth Satellites*, pp. 301–316, Ann Arbor, University of Michigan Press, 1956. Indicates that a study of interplanetary dust can give a great deal of new information on the electromagnetic conditions of interplanetary space.

Measurements of the Earth's Magnetic Field from a Satellite Vehicle. In Van Allen, J. A., ed. *Scientific Uses of Earth Satellites*, pp. 215–233, Ann Arbor, University of Michigan Press, 1956. Discusses the application of satellite observations to magnetic measurement on three different time scales.

Satellites for Physicists. Phys. Today 9: 21–23, diags., Apr. 1956. Points out the educational and missionary aspects of satellites as well as other possibilities with which the geophysicist and the astrophysicist are concerned.

Studies of a Minimum Orbital Unmanned Satellite of the Earth (MOUSE). Part II. Orbits and Lifetimes of Minimum Satellites.

MARTIN DENVER

has created an Applied Research Section for which the following specialists are required. Education requirements in all cases are a Ph.D. Experience should be heavy enough to permit independent research activity with a minimum of supervision:

- **Solid State Physicist** to work on electronic devices.
- **Nuclear Physicist** with experience in nuclear propulsion and general applications of nuclear power.
- **Applied Mathematician** with experience in computers, aerodynamics, trajectories, etc. Must be a senior man.
- **Magneto-Hydrodynamicist** to do developmental work in advanced propulsion systems.
- **Information Theory and Noise Analysis Engineer** experienced in mathematical analysis and theoretical electronics.
- **Engineer** experienced in advanced propulsion techniques such as ion motors, free radicals, etc.
- **Physicist** experienced in re-entry field, familiar with problems of radiation from high temperature gases, hypersonic flow, etc.

Qualified persons are urged to write, giving complete details of education, experience (including personal technical accomplishments) and salaries earned to:

DAVID POTTER H-10 DIV.
MARTIN-DENVER
P.O. BOX 179
DENVER 1, COLORADO

Astronautica Acta 2: 125–144, 1956. Purpose is, first, to describe the (elliptical) orbit of an artificial satellite in terms of the launching conditions (i.e., at burnout); in particular, to give perigee (minimum) and apogee (maximum) altitudes of the ellipse as a function of launching altitudes and of errors in launching velocity and angle. Second, to investigate the subsequent behavior of the orbit under the influence of the drag of the upper atmosphere.

Simas, V. R.

A Low-Noise Preamplifier for Satellite Tracking. QST 40: 42–43, 172, 174, 176, illus., Dec. 1956. Describes a preamplifier and converter fashioned for use in the Minitrack system for tracking the earth satellite.

Sixth Annual Congress of IAF

Abstracts of Papers. J. Astronautics 3: 15–16, 25, Spring 1956. Includes the following selected abstracts: Uses of Satellite Vehicles, by H. E. Canney and F. I. Ordway; The Visibility of an Earth Satellite, by R. Tousey (see also entry under Tousey); The Satelloid, by K. A. Ehricke; Some Problems on Rocket Development, by G. A. Partel; Estimated Lifetimes of Satellites from Near Circularity, by N. V. Petersen.

Sky and Telescope

Layout and Organization of a Moonwatch Station. 15:3–4(follows p. 552), Oct. 1956.

Spitzer, Lyman Jr.

Astrophysical Research with an Artificial Satellite. In Franklin Institute. *Earth Satellites as Research Vehicles.* Proceedings of a Symposium, Philadelphia, Franklin Institute, Apr. 18, 1956, pp. 69–74, Lancaster, Pa., Journal of the Franklin Institute, June 1956. (Monograph 2.) Lists and discusses, briefly, problems that could be investigated such as: Earth's atmosphere, planetary atmospheres, matter in space, and stellar atmospheres.

On the Determination of Air Density from a Satellite. In Van Allen, J. A., ed. *Scientific Uses of an Earth Satellite,* pp. 99–108, Ann Arbor, University of Michigan Press, 1956. Discusses various possible methods of evaluating the atmospheric density, including observation of the satellite's orbit, and measurement of the change of spatial orientation.

Stakutis, V. J., and Brennan, J. X.

Visibility from a Satellite at High Altitudes. In Van Allen, J. A., ed. *Scientific Uses of Earth Satellites,* pp. 137–146, Ann Arbor, University of Michigan Press, 1956. The simple design of two types of instrumentation for measuring luminous quantities is described to show their applicability to satellite installation.

Stedfield, R. L.

Engineering the Earth Satellite. Mach. Design 28: 82–86, Nov. 1, 1956. Description of the orbit, the launching rocket and of the Vanguard satellite itself and its instrumentation.

Steel

Metalworking Tackles Satellite. 139: 120–123, Oct. 15, 1956. Steps to be employed in manufacture of shell—building of aluminum magnesium skinned launching vehicle which will be a three-stage rocket about 72-ft long.

Steier, H. P.

Tracking the IGY Satellite. Missiles and Rockets 1: 76–77, Oct. 1956. Details of the transistorized subminiature transmitter called the Minitrack.

What Guides the Vanguard? Missiles and Rockets 1: 70–72, Nov. 1956. Minneapolis-Honeywell builds complex gyro reference system. Description and photos included.

Stroud, W. G. and Nordberg, W.

Meteorological Measurements from a Satellite Vehicle. In Van Allen, J. A., ed. *Scientific Uses of Earth Satellites,* pp. 119–132, Ann Arbor, University of Michigan Press,

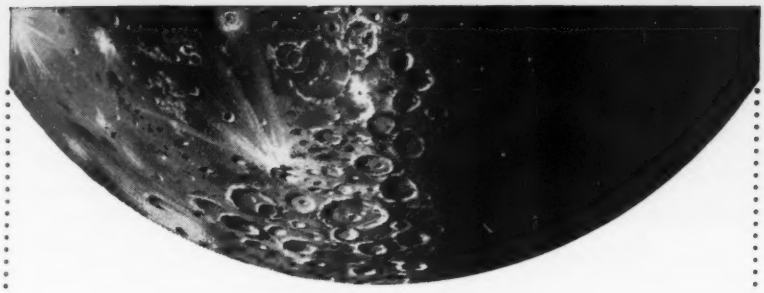

A quiz for Rocket Propulsion Engineers

(Time Limit: 10 years)

1. What is the maximum theoretical specific impulse obtainable for a rocket motor with zero combustion volume?
2. What is the basic mechanism involved in jet separation in nozzles, and how can the separation point be predicted as a function of nozzle divergence angle?
3. What is the effect on turbine blade design of a working gas which is still reacting and changing its composition?
4. What are the dynamic interrelations among the various components of a rocket engine, and what control systems will best solve the rocket engine control problems?
5. What is the flame holding mechanism in a rocket motor and how can fundamental understanding of such a mechanism be used to increase reaction ratio?
6. What types of fluid transport systems offer simplicity, efficiency, and light weight (other than the conventional turbopump)?
7. What are some workable methods of translating chemical energy into thrust – other than by the standard combustion at high pressure and then conversion to velocity?

If you would like to work in these areas and have an outstanding technical background, an inquiring mind, and the creative ability to visualize new solutions, possess a M.S. or Ph.D. degree in Physics, Chemistry, M.E., A.E., Ch.E., E.E., or a B.S. degree in the above with a thorough background in applied research, we have a place for you at Rocketdyne.

Please write to Mr. A. E. Jamieson, Engineering Personnel, 6633 Canoga Avenue, Canoga Park, California.

ROCKETDYNE

A DIVISION OF NORTH AMERICAN AVIATION, INC.

BUILDERS OF POWER FOR OUTER SPACE

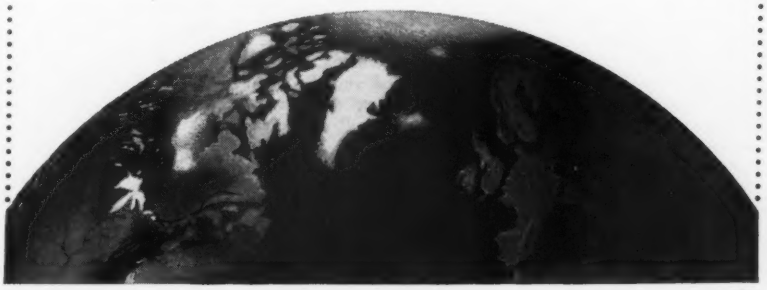

PRECISE CURRENT for your TESTING NEEDS!

VARIABLE FREQUENCY MOTOR GENERATOR SETS ADJUST 360 TO 440 CPS.

Generator mounted controls include reset buttons, limit switch. Motor and generator remain stationary. Variable drive pulley adjustment controlled by small motor. Remote control panels available

Units can be equipped with synchronous motor starter and magnetic amplifier, automatic voltage regulator.

KATO 400 CYCLE MOTOR GENERATOR SETS

NOW UP TO 250 KW!

KATO MOTOR GENERATOR SETS are available in frequencies, speeds and sizes for every specialized use . . . operating high cycle tools, testing components and electronic equipment.

INPUT 60 CYCLES

OUTPUT 400 CYCLES

WRITE FOR NEW FOLDER!

Builders of fine Electrical Machinery Since 1928

KATO Engineering Company

1498 First Ave., Mankato, Minn.

1956. Usefulness of observations is reviewed and various levels of information available from various levels of complexity of instrumentation are outlined. A specific instrumentation suitable for the initial IGY satellites is presented and basic aspects of operational problems outlined. It is shown that the necessary orientation information can be obtained from the albedo data.

Symposium on the U. S. Earth Satellite Program—Vanguard of Outer Space

Inst. Radio Engrs. Proc. 44: 741–767, illus., June 1956. See entries under Hagen, Rosen, Mazor, Mengel, Whipple and Van Allen for papers given at this symposium.

Tousey, R.

The Visibility of an Earth Satellite. Astronautica Acta 2: 101–112, 1956. Conditions for naked eye and telescopic visual observation of white 21-in.-diam earth satellite are calculated using known values of sky brightness, solar illumination and visual thresholds of eye. See also entry under Sixth Annual Congress.

U. S. National Committee for the International Geophysical Year

USNC-IGY Rocketry and Satellite Programs. 41 pp., Washington, National Academy of Sciences, National Research Council, 1956. Collection of five articles: The IGY Rocket and Satellite Program, by Joseph Kaplan; The U. S. IGY Rocketry Program, by H. E. Newell Jr.; Observations with Satellite-borne Apparatus, by J. A. Van Allen; Radio Tracking—Earth Satellite Program, by J. P. Hagen; The Optical Program, by F. L. Whipple.

Van Allen, J. A.

The Artificial Satellite as a Research Instrument. Sci. Am. 195: 41–47, Nov. 1956.

Cosmic-Ray Observations in Earth Satellites. In Van Allen, J. A., ed. *Scientific Uses of Earth Satellites,* pp. 171–187, diags., Ann Arbor, University of Michigan Press, 1956. A single Geiger tube or scintillator carried in a satellite will make possible the study of the cosmic-ray intensity above the atmosphere on comprehensive geographical and temporal bases for the first time.

Ed.: *Scientific Uses of Earth Satellites.* 316 pp., illus., Ann Arbor, University of Michigan Press, 1956. Includes thirty-three papers given at the Upper Atmosphere Rocket Research Panel at the University of Michigan on Jan. 26–27, 1956. Principal purpose of the book is, according to the editor's preface, to bring potential value of artificial satellites to the attention of the scientific community at large. See also entries under individual authors: Bennett, Berning, Chubb, Daniels, Davis, deBey, Dubin, Gast, Hartman, Heppner, Hinteregger, Hok, Hudson, Jones, Katz, LaGow, Merrill, Pfister, Sedwick, Sicinski, Singer, Spitzer, Stakutis, Stroud, Van Allen, Vestine, Ziegler and Zirker.

Scientific Value of the Earth Satellite Program. Inst. Radio Engrs. Proc. 44: 764–767, June 1956. Highest "flight-priority" in the Vanguard Project has been assigned to the following: (a) Monitoring of the intensity of the solar ultraviolet, (b) monitoring of cosmic ray intensity and the measurement of its latitude, longitude, and altitude dependence, (c) measurement of the size spectrum and the number density of interplanetary dust, and (d) measurement of the earth's optical albedo over large area.

Study of the Arrival of Auroral Radiations. In Van Allen, J. A., ed. *Scientific Uses of Earth Satellites,* pp. 188–193, diags., Ann

"MONOBALL"® Self-Aligning Bearings

CHARACTERISTICS

	ANALYSIS	RECOMMENDED USE
1	Stainless Steel Ball and Race	For types operating under high temperature (800-1200 degrees F.).
2	Chrome Alloy Steel Ball and Race	For types operating under high radial ultimate loads (3000-893,000 lbs.).
3	Bronze Race and Chrome Steel Ball	For types operating under normal loads with minimum friction requirements.

Thousands in use. Backed by years of service life. Wide variety of Plain Types in bore sizes 3/16" to 6" Dia. Rod end types in similar size range with externally or internally threaded shanks. Our Engineers welcome an opportunity of studying individual requirements and prescribing a type or types which will serve under your demanding conditions. Southwest can design special types to fit individual specifications. As a result of thorough study of different operating conditions, various steel alloys have been used to meet specific needs. Write for revised Engineering Manual describing complete line. Dept. JP-58.

SOUTHWEST PRODUCTS CO.

1705 SO. MOUNTAIN AVE., MONROVIA, CALIFORNIA

PHYSICISTS

Research and Development

Outstanding theoretical and experimental physicists needed for research programs in our Aerophysics group. Challenging research positions are availabe in the following fields:

Magneto-Fluid Dynamics
Shock and Detonation Wave Phenomena
Hypersonic Flow
Rarefied Gas Phenomena
Transport Phenomena
Plasma Physics

If you have an M.S. or Ph.D. degree and experience or interest in these fields, we offer you an opportunity to use your initiative and creative ability.

Excellent employee benefits including liberal vacation policy. Please send resume to:

E. P. Bloch

ARMOUR RESEARCH FOUNDATION
of Illinois Institute of Technology
10 West 35th Street
Chicago 16, Illinois

Arbor, University of Michigan Press, 1956. A satellite in a nearly pole-to-pole orbit is considered a splendid vehicle for plotting out auroral zone by direct observation.

Vestine, E. H.
Exploring the Atmosphere with a Satellite-Borne Magnetometer. In Van Allen, J. A., ed. *Scientific Uses of Earth Satellites*, pp. 198–214, diags., Ann Arbor, University of Michigan Press, 1956. Summary of explorations for consideration. Various electric current systems suggested for explaining the known geomagnetic variations at ground level are briefly described.

Webb, J. A.
Interplanetary Communications. J. Astronautics 3: 29–30, 36, illus., Summer 1956. Considers, in part, an earth satellite radio relay link.

Whipple, F. L.
Scientific Value of Artificial Satellites. Frank. Inst. J. 262: 95–109, Aug. 1956. History, present status and scientific value of artificial satellites launched as a part of the Vanguard Project during the IGY, 1957–1958.

Whipple, F. L., and Hynek, J. A.
Research Program Based on the Optical Tracking of Artificial Earth Satellites. Inst. Radio Engrs. Proc. 44: 760–764, June 1956. Problems and goals of satellite tracking, possible photographic techniques for observing a satellite, and the tracking system.

White, E. C., Foley, J., and Wilkins, R. G.
Power Supplies and Telemetry for an Instrumented Artificial Satellite. Part I. Orbital Consideration. Part II. Instrumentation and Telemetry. Part III. Availability of Power. Brit. Interplan. Soc. J. 15: 177–191, July-Aug. 1956.

Winterberg, F.
Relativistische Zeitdilatation Eines Kuenstlichen Satelliten (Relativistic Time Dilatation in an Artificial Satellite). Astronautica Acta 2: 25–29, 1956. In German. Applies the general theory of relativity to the problem of time measurement in a satellite.

Winternitz, P. F.
The Physical and Chemical Fundamentals of Satellite Flight: Part I and II. J. Astronautics 3: 43–47; 65, 68–70, 80, Spring, Autumn-Winter 1956. Physical principles of rocket operation, chemical principles, application to the design of rocket power plants for satellites, computation of circular and escape velocity, period of revolution of a satellite, lifetime.

Ziegler, H. K.
Components for Instrumentation of Satellites. In Van Allen, J. A., ed. *Scientific Uses of Earth Satellites*, pp. 55–67, Ann Arbor, University of Michigan Press, 1956. Environmental conditions are reviewed and special attention is given to comparison of power sources. Present and predictable availability of suitable chemical and solar batteries, electron tubes, transistors and frequency control devices is discussed.

Zirker, J. B., Whipple, F. L. and Davis, R. J.
Time Available for the Optical Observation of an Earth Satellite. In Van Allen, J. A., ed. *Scientific Uses of Earth Satellites*, pp. 23–28, Ann Arbor, University of Michigan Press, 1956. Light curves during a twilight observation are computed for specularly and diffusely reflecting spheres of 20-in. diam. The specular reflector is visible over a larger fraction of its path. The time available for observation of the specular reflector is computed for several cases. Sky brightness, geometry, and the earth's shadow are factors.

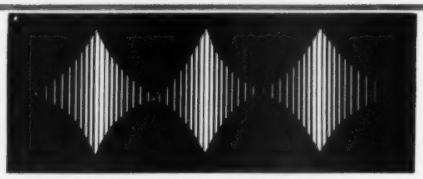

ENGINEER, ME

FLUTTER & VIBRATION ANALYST

Senior Position With General Electric

Several years experience in vibration analysis of turbo machinery assemblies—plus a strong background in fundamental concepts and applications in this field—are essential for this advanced assignment. M.S. desirable.

The work concerns the development of *nuclear power systems for aircraft* at General Electric. It deals specifically with high-temperature reactor core components.

Engineers who have contributed to the pioneering effort to achieve nuclear powered flight will find themselves in the forefront of their profession.

Is Nuclear Experience Necessary? No. In-plant courses and graduate study—on full tuition refund basis—provide essential nuclear theory and technology.

Publication of technical papers is encouraged

Location: Cincinnati, Ohio, known both as an engineering center and a fine place to live. Excellent housing available.

Please write in confidence, stating salary requirements to:
Mr. P. W. Christos

AIRCRAFT NUCLEAR PROPULSION DEPT.

GENERAL ELECTRIC

Div. 34-MQ P. O. Box 132 Cincinnati 15, Ohio

To the talented engineer & scientist

APL OFFERS GREATER FREEDOM OF ACTIVITY

APL has responsibility for the *technical direction* of much of the guided missile program of the Navy Bureau of Ordnance. As a result staff members participate in assignments of challenging scope that range from basic research to prototype testing of weapons and weapons systems.

A high degree of freedom of action enables APL staff members to give free rein to their talents and ideas. Thus, professional advancement and opportunities to accept program responsibility come rapidly. Promotion is rapid, too, because of our policy of placing professional technical men at all levels of supervision.

APL's past accomplishments include: the first ramjet engine, the Aerobee high altitude rocket, the supersonic Terrier, Tartar, and Talos missiles. Presently the Laboratory is engaged in solving complex and advanced problems leading to future weapons and weapons systems vital to the national security. Interested engineers and physicists are invited to address inquiries to:

Professional Staff Appointments

The Johns Hopkins University
Applied Physics Laboratory

8617 Georgia Avenue, Silver Spring, Md.

Launched!

The first volume of an important new work . .

AIRCRAFT AND MISSILE PROPULSION

Volume 1

Thermodynamics of Fluid Flow and Applications to Propulsion Engines

By M. J. ZUCROW
Purdue University

This is the initial volume of a three-volume work designed to give you a better understanding of the fundamental principles governing the functioning and operating characteristics of engines used to propel winged aircraft and missiles, both guided and unguided, at high speeds. Volume I discusses the thermodynamics of fluid flow and its application to propulsion engines.

These original features help you follow the subject matter with ease:

- **The nomenclature for a chapter precedes the chapter.**
- **All derivations are explained in detail.**
- **An unusually large number of illustrative problems are worked completely.**
- **Numerous exercise problems are included with their answers.**
- **Tables or figures needed for solving problems are provided.**
- **References at the end of each chapter guide you in further study.**

1958 538 pages Illus. $11.50

Mail this coupon for your ON-APPROVAL copy TODAY!

JOHN WILEY & SONS, Inc. JP-58
440 Fourth Ave., New York 16, N. Y.

Please send me a copy of AIRCRAFT AND MISSILE PROPULSION, Vol. I, to read and examine ON APPROVAL. Within 10 days I will return the book and owe nothing, or I will remit $11.50, plus postage.

Name.....

Address.....

City.....Zone....State.....

SAVE POSTAGE! Check here if you enclose payment, in which case we pay postage. Same return privilege, of course.

Index to Advertisers

AEROJET-GENERAL CORPORATION ..... Back Cover, 358
D'Arcy Advertising Co., Los Angeles, Calif.

APPLIED PHYSICS LABORATORY, THE JOHNS HOPKINS UNIVERSITY 361
M. Belmont ver Standig, Inc., Washington, D. C.

ARMOUR RESEARCH FOUNDATION OF ILLINOIS INSTITUTE OF TECHNOLOGY .. 360

AVCO MANUFACTURING CORPORATION, RESEARCH AND ADVANCED DEVELOPMENT DIVISION 296
Benton & Bowles, Inc., New York, N. Y.

COAST MANUFACTURING & SUPPLY COMPANY 297
Peter Hurst Advertising, Inc., San Francisco, Calif.

CONTINENTAL AVIATION & ENGINEERING CORPORATION 354
The Hopkins Agency, Detroit, Mich.

DIVERSEY ENGINEERING COMPANY 293
Roark & Colby Advertising, Chicago, Ill.

DOUGLAS AIRCRAFT COMPANY, INC. 357
J. Walter Thompson Company, Los Angeles, Calif.

EASTMAN KODAK COMPANY 343
The Rumrill Company, Inc., Rochester, N. Y.

FORD INSTRUMENT COMPANY, DIVISION OF SPERRY RAND CORPORATION 355
James Thomas Chirurg Co., New York, N. Y.

THE GARRETT CORPORATION, AiRESEARCH MANUFACTURING COMPANY 347
J. Walter Thompson Co., Los Angeles, Calif.

GENERAL ELECTRIC COMPANY
AIRCRAFT NUCLEAR PROPULSION 361
Deutsch & Shea, Inc., New York, N. Y.

HAWS DRINKING FAUCET COMPANY 356
Pacific Advertising Staff, Oakland, Calif.

JOHN WILEY & SONS, INC. 362
Norman D. Waters & Associates, New York, N. Y.

KATO ENGINEERING COMPANY 360
Frizzell Advertising Agency, Inc., Minneapolis, Minn.

LINDE COMPANY 298, 299
J. M. Mathes, Inc., New York, N. Y.

LOCKHEED AIRCRAFT COMPANY, MISSILE SYSTEMS DIVISION 353
Hal Stebbins, Inc., Los Angeles, Calif.

THE MARTIN COMPANY, DENVER DIVISION 358
E. M. Halvorson Co., Denver, Colo.

MORRIS BEAN & COMPANY 350
Odiorne Industrial Advertising, Inc., Yellow Springs, Ohio

NEWBROOK MACHINE CORPORATION 346
Melvin F. Hall Advertising Agency, Inc., Buffalo, N. Y.

NITROGEN DIVISION OF ALLIED CHEMICAL & DYE CORPORATION 351
G. M. Basford Company, New York, N. Y.

NORTH AMERICAN AVIATION, INC. 363
Batten, Barton, Durstine & Osborn, Inc., Los Angeles, Calif.

THE NORTON COMPANY 295
James Thomas Chirurg Co., Boston, Mass.

OLDSMOBILE DIVISION, GENERAL MOTORS CORPORATION 345
D. P. Brother & Company, Detroit, Mich.

PERKIN-ELMER CORPORATION 364
G. M. Basford Co., New York, N. Y.

THE RAMO-WOOLDRIDGE CORPORATION 300
The McCarty Company, Los Angeles, Calif.

REACTION MOTORS, INC. ..... Second Cover
The Aitkin-Kynett Co., Philadelphia, Pa.

RHEEM MANUFACTURING COMPANY 352
Getz & Sandborg, Inc., Beverly Hills, Calif.

ROCKETDYNE, A DIVISION OF NORTH AMERICAN AVIATION, INC. 359
Batten, Barton, Durstine & Osborn, Inc., Los Angeles, Calif.

SHELL OIL COMPANY 349
J. Walter Thompson Co., New York, N. Y.

SOUTHWEST PRODUCTS COMPANY 360
O. K. Fagan Advertising Agency, Los Angeles, Calif.

WESTVACO CHLOR-ALKALI DIVISION, FOOD MACHINERY AND CHEMICAL CORPORATION ..... Third Cover
James J. McMahon, Inc., New York, N. Y.

358
361
360
296
297
354
293
357
343
355
347

361
356
362
360
299
353
358
350
346
351
363
295
345
364
300
ver
352
359
349
360

ver

ULSION